The Dissertation Committee for Suzan Alharbi Certifies that this is the approved version of the following dissertation:

Preserved extracellular matrix in non-enzymatically detached cultured keratinocyte sheets bolsters the healing effects on grafted burn wounds

Committee:

Perenlei Enkhbaatar, MD, Ph.D., Mentor and Committee chair

Hiroyuki Sakurai, MD, Ph.D.

Hal Hawkins, MD, Ph.D.

Vsevolod Popov, Ph.D. DSc

Christopher Fry, Ph.D.

Dean, Graduate School

Preserved extracellular matrix in non-enzymatically detached cultured keratinocyte sheets bolsters the healing effects on grafted burn wounds

by

Suzan Alharbi, M.S.

Dissertation

Presented to the Faculty of the Graduate School of

The University of Texas Medical Branch

in Partial Fulfillment

of the Requirements

for the Degree of

Doctor of Philosophy

The University of Texas Medical Branch

November, 2019

Dedication

This work is dedicated to my husband, Abdulsattar Alyamani, whose love, support, and faith in me allowed me to finish this journey.

This work is dedicated to my kids, Saden and Sinan, for motivating me to become a better student, better scientist, and most importantly a better mother.

Acknowledgments

I would like to thank my mentor, Dr. Perlene Enkhbaatar, for helping me to grow as a scientist, as well as giving me the opportunity to present my work at national and international conferences. Without his guidance and supervision I would not have been able to reach to what I am today. I would also like to thank the many individuals in my laboratory who assisted and contributed a lot to this work. Additionally, thank you to my committee members who supported me throughout this process and who continue to help me improve my scientific and critical thinking. Also, I would like to thank John Salsbury and Clemmie White-Matthews for proofreading many of my writings and helping me to improve my writing skills. Special gratitude for Clark Anderson for his guidance and help regarding statistical analysis that has been used in this research. Additionally, I would like to thank Dr. Dominique Judith Wiener for her great assistance in analyzing and understanding many of the histopathological slides. Also, I would like to thank some faculty members who didn't hesitate for a second to open their doors and allows me to use either their equipment or materials, even if my research was totally not related to theirs. Thank you, Dr. Mark Emmett, Dr. Hal Hawkins, Dr. Helen Hellmich, Dr. Rakez Kayed, Dr. Ramkumar Menon, Dr. Maria Micci, Dr. William Russell, Dr. Thomas Smith, and Dr. Natalie Williams-Bouyer. Special thanks to Dr. Pomila Singh an Dr. Joan Nichols for their great guidance and help during many complications throughout my journey. Many thanks to King Abdulaziz University in Jeddah, Saudi Arabia for funding my school tuitions and part of my research expenses. For those who made this journey less hectic and been there for me when I needed a friend, thank you Amina El Ayadi, Anesh Prasai, Lauren Richardson, and Olga Zolochevska. Lastly, I would like to thank my family for their constant support and prayers.

Preserved extracellular matrix in non-enzymatically detached cultured keratinocyte sheets bolsters the healing effects on grafted burn wounds

Publication No._____

Suzan Alharbi, Ph.D.

The University of Texas Medical Branch, 2019
Supervisor: Perenlei Enkhbaatar, MD, Ph.D.

After escharotomy, full thickness large burn wounds are temporarily covered with cadaver skin because of the limited availability of autologous skin. However, cadaver skin is eventually rejected still requiring autologous skin grafting. To overcome this obstacle, cultured autologous keratinocyte sheets (KS) have been proposed to substitute the autologous skin; however, this technology has not been translated to clinical practice because of the poor quality of KS. Although the exact reason remains unknown, it is suggested that the use of enzyme for the KS detachment may have negatively impacted the overall quality of KSs. The current work is designed to address this pitfall, offering novel technology for detachment of cultured KS. Our studies demonstrate that non-enzymatic detachment of cultured KS, using temperature responsive dishes preserves extracellular matrix (ECM) (such as collagen IV and laminin 5) in KS by activating the MAPK pathway which plays an important role in cells survival and proliferation. We have shown that the cytoskeleton of keratinocytes in cultured sheets was disrupted with Dispase treatment resulting in sheet shrinkage. Importantly, we did not observe the same shrinkage if the cells were cultured in temperature-responsive dishes and detached by culture temperature reduction (T-KS). It also appears that integrity of T-KS is preserved after shear stress. Additionally, we have determined proliferation rates of KS in novel *in vitro* wound healing models that mimic burn wound harsh environments; the T-KS proliferation capacity was significantly higher in T-KS than the KS detached using Dispase treatment (D-KS) with or without coincubation with burn wound exudates collected from ovine third degree burn wounds. Our major finding is that T-KS overlaid onto third degree burns grafted with cadaver skin (which is rejected) resulted in better burn wound healing than D-KS. The advanced wound healing was evidenced with a greater epithelialization rate and well defined dermal-epidermal junction with continuous and better-defined lamina densa and significantly higher numbers of hemi-desmosomes. Additionally, the wounds were more mature with T-KS treatment which was evidenced by reversed keratinocyte growth factors to normal ranges after its transient increase. Furthermore, vascularization percentage was higher in wounds treated with T-KS compared to wounds covered with D-KS. Taken together, our findings point out the critical importance of non-enzymatic detachment of cultured KS and demonstrate that the effects of non-enzymatically detached KSs are superior to those of enzymatically detached sheets on ovine grafted burn wounds healing. We believe that the results of our present study will potentially enable the successful translation of KS to clinical practice for treating burn wounds.

TABLE OF CONTENTS

List of Tables xiv

List of Figures xv

List of Abbreviations xvii

CHAPTER 1 1

Background and significance 1

Epidemiology of burn injury 1

The structure and function of normal skin 1

Biology of wound healing 5

Clinical practice for burn wound care and challenges 7

Autologous keratinocyte sheets (KSs) 10

Temperature-responsive dishes (TRDs) 12

Preclinical usage of temperature-responsive dish for skin wound healing treatment 13

Clinically relevant ovine model of grafted burn wound healing 14

The relevance of the present study 16

Innovation 17

CHAPTER 2 22

Aim 1. Non-enzymatic effect of detaching cultured KSs and their effect on *in vitro* burn wound healing 22

Introduction 22

Materials and methods 23

Human keratinocytes (hKC) culture 23

Sheep keratinocytes (sKC) isolation and culture 24

Keratinocyte sheet formation 25

In vitro skin model 26

Western blotting 26

Keratinocyte sheet thickness 28

Mechanical cell dissociation assay 28
Shrinkage percentage 29
Burn wound exudate (BWE) collection 29
Wound healing scratch assay 29
In vitro burned skin wound healing model 30
Statistical analysis 31
Results: 31
Keratinocytes sheets characteristics 31
ECM preservation in T-KS and the activation of MAPK pathway 31
Preservation of intercellular adhesion in T-KS 32
Cytoskeleton disruption and sheet shrinkage with Dispase treatment 33
Impact of burn exudate on *in vitro* wound scratch assay 33
Proliferation KC sheet overlaid onto *in vitro* burn wound 34
Discussion 35

AIM 2: TO INVESTIGATE THE EFFICACY OF KERATINOCYTE SHEETS DETACHED BY TEMPERATURE GRADIENT IN THE OVINE GRAFTED SKIN BURN MODEL WITH SPECIAL EMPHASIS ON ENGRAFTMENT AND WOUND CLOSURE 49

CHAPTER 3 51

Aim 2.1: Establish ovine cadaver skin bank 51

Introduction 51
Material and Methods 52
Donor selection 52
Skin collection site preparation 53
Cadaver skin (allograft) collection 53
Processing and disinfection of cadaver skin (allografts) 54
Preservation of cadaver allografts 54
Thawing frozen cadaver skin and sample collection 55
Tissue preparation for histology and cadaver skin thickness measurement 56
Microbiological testing of cadaver skin 56
Evaluation cadaver skin viability 57
Cell proliferation assessment 58

Growth factors quantification 59
In vivo assessment of cadaver skin on burn wounds 60
Statistical analysis: 60
Results 61
Histological analysis and cadaver skin thickness 61
Microbiological evaluation of cadaver skin 61
Evaluation cadaver skin viability 61
Cell proliferation assessment 62
Growth Factor Quantification 62
Macroscopic and microscopic evaluation for grafted sheep cadaver skin 62
Discussion 63

CHAPTER 4 80

Aim 2.1: Examine wound healing efficacy of cultured KSs in healing of burn wounds grafted with cadaver skin 80

Introduction 80
Material and Methods 81
Experimental design 81
Ovine keratinocytes isolation and sheet formation 82
Applying KSs over cadaver skin grafted burn wounds 83
Determination of wound epithelialization percentage 83
Microscopic analysis of wound healing 83
Electron microscopy 84
Collagen density 85
Angiogenesis evaluation 86
Western blotting 86
Statistical analysis 87
Results 88
Burn injury, escharotomy, skin grafting and keratinocyte sheet grafts 88
Epithelialization percentage 89
Microscopic analysis of wound samples 89
Well defined dermal-epidermal junction in wounds treated with T-KS 89

Collagen density is comparable between the T-KSs and D-KSs-treated wounds....90
Angiogenesis tend to be higher in wounds treated with T-KS....91
KGF level tend to be lower in wounds treated with T-KS....91
Discussion....91
CHAPTER 5 108
Summary, conclusion and future directions....108
Summary: 108
Conclusion:....112
Future directions....112
Appendix 113
Curriculum Vita....129
References 137

List of Tables

Table 2.1: Antibodies used for the western blot ……..…….. 40

Table 3.1: Assessment criteria for evaluating skin samples taken after grafting cadaver skin ……... 79

List of Figures

Figure 1.1: The layers of the epidermis ……. 19

Figure 1.2: The dermal-epidermal junction (DEJ) ……..... 20

Figure 1.3: The properties of the temperature responsive dish ……. 21

Figure 2.1: Schematic of keratinocyte sheet detachment ……...……... 41

Figure 2.2: Schematic of *In vitro* skin model …… 42

Figure 2.3: Preservation of Intercellular Adhesion in T-KS…….…. 43

Figure 2.4: Cytoskeleton disruption and sheet shrinkage with Dispase treatment …… 44

Figure 2.5: Schematic of *In vitro* skin burn wound healing model ……..…. 45

Figure 2.6: Keratinocyte sheet thickness ……... 46

Figure 2.7: ECM preservation in T-KS and the activation of MAPK pathway …… 47

Figure 2.8: Using burn exudate in the *in vitro* burn wound healing model and acceleration of cell proliferation ……..……... 48

Figure 3.1: Schematic of clinical burn wound care ……... 69

Figure 3.2: Schematic of *in vivo* grafting of ovine cadaver skin onto 3rd degree excised burn wounds ……..……... 70

Figure 3.3: *In vivo* transplantation of cadaver skin over excised third degree burn wound ……..…….. 71

Figure 3.4: Histopathological evaluation of cadaver skin ……. 72

Figure 3.5: Evaluation of cadaver skin viability ……..... 73

Figure 3.6: Cell proliferation assessment …….. 74

Figure 3.7: TGF-β level in fresh or frozen cadaver skin for 10 or 40 days ……... 75

Figure 3.8: Cadaver skin rejection …… 76

Figure 3.9: Histological evaluation for skin samples collected after 7, 14 and 20 day of autograft, fresh allograft, and frozen allograft ……. 77

Figure 3.10: Histopathological evaluation of skin samples collected after autograft, fresh allograft, frozen allograft ……..... 78

Figure 4.1: Schematic of keratinocyte sheet overlaid onto burn wounds grafted with cadaver skin ……..…… 101

Figure 4.2: Epithelialization percentage after keratinocyte sheet autograft ……..... 102

Figure 4.3: Histopathological evaluation of wounds at 14 days after treatment with keratinocyte sheets ……..... 103

Figure 4.4: Well defined dermal-epidermal junction in wounds treated with T-KS ….... 105

Figure 4.5: Evaluation for collagen and vascularization in wounds after KSs grafting. ...106

Figure 4.6: KGF level in wounds treated with different types of KSs ……..… 107

Supplement Figure 2.1: Primary keratinocyte culture ……..…… 113

Supplement Figure 2.2: Scratch assay testing the optimal culture condition for the *in vitro* burn wound healing model …… 114

Supplement Figure 2.3: Scratch assay testing the optimal dose and collection time of burn exudate used in the model ……..…… 115

Supplement Figure 3.1: Cadaver skin (allograft) collection …… 116

Supplement Figure 3.2: Processing, disinfection and preserving of cadaver skin ……... 117

Supplement Figure 3.3: Thawing frozen cadaver skin and sample collection ……. 118

Supplement Figure 3.4: Method used to measure cadaver skin thickness ……... 119

Supplement Figure 3.5: Method used for MTT assay to asses cadaver skin viability …...120

Supplement Figure 4.1: Skin burn wound induction and escharotomy procedure …..….121

Supplement Figure 4.2: Applying KSs over cadaver skin grafted burn wounds ……..... 122

Supplement Figure 4.3: Use of nitrocellulose carrier membrane for applying KSs over cadaver skin grafted burn wounds ….…… 123

Supplement Figure 4.4: The method used to measure epithelialization percentage and epidermis thickness ….……..…… 124

Supplement Figure 4.5: Method used to determine wound ulceration and separation between epidermis and dermis ….……..…… 125

Supplement Figure 4.6: Method used for TEM analysis of wounds samples 14 days after KSs grafting ….……..…… 126

Supplement Figure 4.7: Method used for measuring collagen and vascularization percentage in wound samples 14 days after KSs grafting …….. 127

Supplement Figure 4.8: TEM micrographs of keratinocyte sheets before grafting to burn wounds …….. 128

List of Abbreviations

α-tubulin	Alpha-tubulin
3-D	Three-dimensional
ABA	American Burn Association
BM	Basement membrane
BrdU	Bromodeoxyuridine
BSC	Biological safety cabinets
BWE	Burn wound exudate
Ca^{+2}	Calcium
CKM	Complete keratinocyte medium
CP	Closure percentage
D-KS	Keratinocyte sheet cultured in regular dish and detached by Dispase treatment
DEJ	Dermal-epidermal junction
dH_2O	Distilled water
DMEM	Dulbecco's modified Eagle's medium
ECM	Extracellular Matrix
ERK	Extracellular signal-regulated kinase
FBS	Fetal bovine serum
GAG	Glycosaminoglycans
hDFb	Human dermal fibroblasts
hDMEC	Human dermal microvascular endothelial cells
hKC	Human keratinocytes
HLA-DR	Human Leukocyte Antigen – antigen D Related
KGF	Keratinocyte growth factor
KS	Keratinocyte Sheets
LCST	Lower critical solution temperature
MAP	Mitogen-activated protein
MMPs	Matrix metalloproteinases
MT	Masson Trichrome
MTT	3-(4,5-Dimethylthiazol-2-yl)-2,5-diphenyl-tetrazolium bromide
NBR	National Burn Repository
NHEK	Normal human epidermal keratinocyte
NV	Neovascularization
OD	Optical density
PDGF	Platelet-derived growth factor
PG	Proteoglycans
PIPAAm	Poly-N-isoproprylacrylamide
RD	Regular dish
SCID	Severe combined immunodeficiency disease
sKC	Sheep keratinocytes
SP	Shrinkage percentage

T-KS	Keratinocyte sheet cultured in temperature-responsive dishes and detached by culture temperature reduction
T/D-KS	Keratinocyte sheet detached by temperature reduction and treated with Dispase
TBSA	Total body surface area
TEM	Transmission electron microscopy
TGF-β	Transforming growth factor β
TRDs	Temperature-responsive dishes
UV	Ultraviolet
Vac.	Vacuolization

CHAPTER 1

Background and significance

EPIDEMIOLOGY OF BURN INJURY

In the United States, over 2 million people suffer from cutaneous burns each year [1]. Based on the 2016 National Burn Repository (NBR) and American Burn Association (ABA) report from 2006 to 2015, pediatric patients aged 1 to 15 years represent 30% of total burn patients, while adults aged 20 to 59 years represent 54% of burn cases [2]. The overall mortality rate in the past 10-year reporting period is 3.3% and increases with the larger burn size. Patients with burn wounds >65 -70% TBSA have more than a 50% fatality rate [2].

Treatment of burn patients can impose a huge financial burden. The average total healthcare expenses per burn patient in high-income countries is $88,218 [3]. A higher TBSA is associated with increased care and treatment costs. Based on the 2016 NBR report, cost for patients with 0–9.9% and 60-69.9% TBSA is $47,557 (n=53,165) and $798,355 (n=355), respectively [2].

THE STRUCTURE AND FUNCTION OF NORMAL SKIN

Normal skin provides diverse functions: permeability barrier, protection from pathogens, thermoregulation, sensation, ultraviolet (UV) protection, and wound repair and regeneration [4]. The skin is composed from three main components--epidermis, dermis, and hypodermis [4].

Epidermis: Epidermis is a stratified and cornified epithelium that is continually renewed [4]. It is attached to the dermis by the basement membrane zone, which is called a dermal-epidermal junction [4]. Epidermis consists mostly of keratinocytes, but also has other cell types, such as melanocytes (pigment-synthesizing dendritic cells), Langerhans cells (antigen-presenting cells) and Merkel cells (mechanoreceptors) [4]. Epidermis, as other epithelial cells, also contains keratin, an intermediate filament and a component of cell cytoskeleton [4]. Keratin's expression depends on the cell location, differentiation stage, developmental phase, and disease state [5, 6]. The keratinocytes in the epidermis are organized into 4 layers, as shown in Figure 1 [4].

The first layer of skin epidermis is the basal layer (Fig. 1.1). The basal layer has a columnar-shaped primary and mitotically active keratinocytes attached to the epidermal basement [4]. These basal layer cells are gradually differentiated to other layers of epidermis. Basal layer cells are attached to the basement membrane zone with keratin filaments (K5 and K14) and hemi-desmosomes [4], while the cells are attached to each other via desmosomes.

The second layer of skin epidermis is the spinous layer (Fig. 1.1), wherein keratinocytes become flatter with rounded nucleus [4]. Spinous cells synthesize keratin filaments K1 and K10 that are organized around the nucleus and inserted into peripheral desmosomes [4]. Spinous cells have abundant desmosomes in spine-like structures, that provide strong intercellular adhesion and resistance to mechanical stress [7].

The third layer in the epidermis is the granular layer (Fig. 1.1), where several structural components are generated to form epidermis barrier [4]. The KSs in this layer is

distinguished by the presence of keratohyalin granules that contain profilaggrin, keratin filaments, and loricrin [4].

The final and outermost layer of the epidermis is stratum corneum (Fig. 1.1), where the KSs undergo programmed destruction of all components except keratin filaments and filaggrin matrix [8], thus becoming corneocytes. The stratum corneum functions as an epidermal barrier and provides mechanical protection from various environmental factors and prevents water loss [4, 9, 10].

Dermis: The dermis consists of many cellular and non-cellular components that support nerves and vascular network [4]. Several cell types located in the dermis include fibroblasts, macrophages, mast cells, and immune cells [4]. Fibroblasts are responsible for synthesizing and degrading extracellular matrix (ECM) [4], and play an important role in wound healing [4]. Monocytes and macrophages form the phagocytic system in the skin and are also involved in wound healing [4]. Mast cells, specialized secretory cells, are responsible for hypersensitivity reaction observed in the skin [4].

The ECM consist of fibrous proteins and non-fibrous molecules so called ground substances. Collagen, elastin, and fibronectin are fibrous proteins that provide a three-dimensional supporting scaffold for cells and blood vessels [11-13]. The ground substance of the ECM contains glycoproteins, proteoglycans (PG) and glycosaminoglycans (GAG) [14]. Due to strong hydrophilic characteristics, the ground substance surrounds the fibrous proteins like a jelly-like substance, which provides hydration to the skin and increases local concentrations of growth factors [11]. The ECM proteins are balanced by the activity of matrix metalloproteinases (MMPs) and tissue inhibitors of metalloproteinases (TIMPs) [11]. MMPs are mainly secreted by keratinocytes, fibroblasts, endothelial cells, and several

immune cells [15]. TIMPs are secreted by keratinocytes and fibroblasts [16]. Timely degradation of ECM, by the balance between MMPs and TIMPs, is an important feature of morphogenesis, cell migration and tissue repair/remodeling [11, 17].

Dermal-epidermal junction: The dermal-epidermal junction (DEJ) connects epidermis to dermis in the skin and provides resistance against shearing forces [18-20]. The DEJ is a complex structure which plays an important role in cell adhesion, organization of cytoskeleton, differentiation, polarization, migration, and apoptosis [21-23]. DEJ is composed of three major components: (1) the hemidesmosome-anchoring filament complex, (2) the basement membrane, and (3) the anchoring fibrils [18] (Fig. 1.2). The hemidesmosome-anchoring filament complex starts at the basal cells of the epidermis and extends to the lamina densa in the basement membrane through the lamina lucida [18, 19]. Hemidesmosomes are electron dense plates at the basal region of basal cells. They interact by intracellular architecture and keratin intermediate filaments [18] (Fig. 1.2).

The basement membrane (BM) consists of three distinctive areas: lamina lucida, lamina densa, and fibroreticular lamina [18, 19]. Lamina lucida is a superficial electron-lucent area that is beneath the basal cells, while lamina densa is a thick dark staining band [18, 19]. The major components of lamina densa are collagen IV, nidogens, perlecan, and laminins 5 [21, 22] (Fig. 1.2).

Collagen fibers in dermis (Collagen I or III) are connected to lamina densa by anchoring fibrils, such as collagen VII [19, 24, 25]. On the other hand, elastic fibers are connected to basal densa by fibrillin microfibrils [19, 26]. Fibroreticular lamina is located beneath lamina densa and contains abundant fibronectin [19] (Fig. 1.2).

Hypodermis: The hypodermis consists mainly of adipose tissue, and provides energy and skin protection [4]. Adipocytes form the majority of hypodermis cells [27, 28], and they are organized into lobules that are separated by septa of fibrous connective tissue [4]. Within this septa, nerves and vessels are located to supply the skin [4].

BIOLOGY OF WOUND HEALING

Wound healing occurs through three overlapping phases: inflammation, proliferation and remodeling [29]. After injury, blood and lymph vessels flush the wound to remove any pathogens or antigens [30]. A coagulation cascade helps to form a blood clot made of fibrin matrix, fibronectin, vitronectin, and thrombospondins [31]. Platelets attract leukocytes to the injury site by releasing chemotactic factors [32].

The first stage--the inflammatory phase: neutrophils are recruited to the wound site to degrade and phagocytize necrotic tissue and secrete proteases that kill local bacteria for about 2-5 days [33]. These actions serve as chemoattractants for other immune cells to invade the wound [34]. After approximately three days, in response to specific chemoattractants (e.g., transforming growth factor β [TGF-β]), monocytes infiltrate to the wound site to become activated macrophages [33]. Macrophages aid neutrophils in eliminating microorganisms and cell debris [33], and secrete growth factors, chemokines and cytokines that initiate the next phase of wound healing (proliferative phase) [35].

The second phase--the proliferative phase: lasts for 3-10 days after the injury. The focus in this phase is to cover wound-forming granulation tissue and restore the vascular network [30, 32, 33, 36]. To cover the wound surface, reepithelization begins from the edges of the wound, with the help of stem cells from hair follicles and sweat glands if they were preserved [37-41]. Enzymatic digestion of intercellular desmosomes facilitates

keratinocyte migration along the preformed fibrin blood clots and granulation tissues [42-44]. This process proceeds until the migrating cells touch each other, leading to the reorganization of cytoskeleton and basement membrane proteins [42, 45].

Restoring the missing vascular system is essential for providing nutrients and gas exchange for newly formed tissue [33]. The wound environment is hypoxic due to low oxygen supply, that induces angiogenesis [46]. The activated endothelial cells secrete proteolytic enzymes to digest the basal lamina, which allows the proliferation and sprouting of the endothelial cells into the wound [33]. Proliferating cells release MMPs that digest surrounding tissue, allowing further proliferation and sprouting [33].

The tissue granulation is initiated to replace fibrin-fibronectin clot formed by platelets [30, 32, 35, 39, 47-49]. Granulation tissue is characterized by the presence of fibroblasts, granulocytes and macrophages [33]. Macrophages are responsible for secreting growth factors that affect fibroblast activity and angiogenesis [50]. The fibroblasts are the dominating cells at this stage, and they start producing extensive amounts of loosely organized collagen type III, fibronectin, glycosaminoglycans, proteoglycans, and hyaluronic acid [33]. The formation of the ECM by fibroblasts is essential for cell adhesion, movement and differentiation [51, 52]. The remodeling phase ends by differentiation of fibroblasts to myofibroblasts, and is eventually terminated by apoptosis [53]. This termination will adjust the balance between synthesis and degradation of the ECM [54, 55].

The third phase--remodeling phase starts about 21 days after injury and can last up to 1 year or longer [33]. During remodeling, massive changes occur within the ECM, including synthesis and breakdown of collagen by MMPs and TIMPs [56]. Collagen III, formed during the proliferative phase is degraded by MMPs, derived from macrophages,

epidermal cells, and endothelial cells, and fibroblasts [57]. Collagen III is replaced by collagen I, that is stronger and more oriented [58]. Myofibroblasts facilitate wound contraction, which decreases scar formation [58, 59]. At this stage of wound healing, angiogenesis and metabolism decrease and are finally terminated. Several skin components, such as hair follicles and sweat glands do not recover if the injury is deep [33].

CLINICAL PRACTICE FOR BURN WOUND CARE AND CHALLENGES

Burn wound care depends on the depth of the burn injury. There are three types of burn injuries classified [60]. First degree burns: where the keratinized layers that protect and serve as a wall between the host and the environment is stripped away requiring minimal to no treatment because of rapid healing occurrence [60, 61]. In the second degree of burn, all epidermal layers and some dermal layers are affected. The wound heals through re-epithelialization from the edge of the wound and migratory cells from the remaining of dermal structure [60, 61]. Finally, the third-degree burn called as full thickness burn affects all structures in the epidermis and dermis. Epithelialization is limited from the edge of the wounds as all dermal adnexa are destroyed [60]. Therefore, timely management of burn patients with > 50% TBSA includes early excision of burned skin and wound closure within 24-48h after injury, which has resulted in significant survival improvements [62-65]. Early excision performed by removal of dry scab (eschar) eliminates heat-denatured proteins caused by burn injury. Heat-denatured proteins may play a role in uncontrolled inflammatory response, and provide a rich source of nutrition for microorganisms [66, 67]. Early burned skin excision is associated with a decrease in blood loss, infection, length of hospital stays and mortality, and helps to increase graft uptake [64, 68-70]. Delayed wound

closure leads to formation of hypertrophic scarring [66]. Cubison et al. reported that delayed wound closure (longer than 21 days) contributes to higher incidence of hypertrophic scarring in pediatric patients [71].

The ideal standard for wound closure is an autograft, that uses skin from the patient's uninjured site(s), because it eliminates immunogenic conflicts, thus preventing the rejection of graft [72, 73]. However, the main two drawbacks of using autologous split thickness skin grafts are pain and shortage of donor skin. The pain from the donor site is a major complaint in early days after skin collection, and requires the use of additional analgesics [66, 74]. With the large burns, donor skin is quickly exhausted [62, 63], necessitating temporary wound coverage using various sources to prevent fluid loss and microbial contamination, which increases the mortality of patients [72, 75]. Types of temporary wound covers include allografts, xenografts, artificial skin substitutes, and cultured keratinocytes, with- or without bioengineered skin substitutes [66].

Allografts, a skin harvested from living human donors or cadavers, promote re-epithelization from the edge of wounds, prepares wound beds for autograft, and increases healing rate [76]. Although cadaver skin is frequently used [77], it is eventually rejected due to immune reaction caused by the release of HLA-DR (Human Leukocyte Antigen – antigen D Related) expressed by the Langerhans cells [78].

To overcome these obstacles, tissue engineering combined with cell biology and medicine has created three-dimensional tissues to replace damaged skin [79]. Tissue engineering for skin provides innovative treatments for burn wounds, and is of particular interest when autologous donor skin is limited [80]. There are several skin substitutes and dermal analogs available for replacement of epidermis and dermis [66, 72, 81-86].

Commercial dermal substitutes are mainly acellular materials derived from human (Alloderm and GraftJacket) tissues or from non-human sources e.g., Integra, Biobrane and Pelnac or biodegradable materials, such as polyglycolic acid, collagen gel, fibrin gel, and gelatin [72, 87-89]. However, several drawbacks are associated with using acellular scaffolds, because of the pathological state of fibrosis, low cell density of re-constructed tissues, lack of micro capillaries, necrosis, and strong inflammatory responses to degraded scaffolds [89].

Cellular therapy for burn wound healing started in 1975, when protocols for isolating and culturing keratinocytes were established [79]. Autologous keratinocytes have been shown to be topically applied to the wounds as single cells (available within one week of culture) or as sheets (available after 3 weeks) [75, 90]. When cultured keratinocytes reach confluency, the proliferative basal cells can be separated from nutrients by upper differentiated cells that attach together with desmosomal junctions. Thus, longer culture, leading to formation of more cell layers, results in poor acceptance of the graft due to starvation of basal cells. Sub-confluent keratinocytes (after 5-7 days in culture) can be applied to wounds as aerosol (spray) [91], cell suspension (medium or with fibrin gel) [92], or cultured on membranes [93, 94].

In 1986, Gao et al. first reported successful use of autologous keratinocytes in two patients [95]. The keratinocyte graft was well accepted and wounds was epithelialized within 30-40 days in these patients [95]. Later, another clinical study reported the use of cultured autologous keratinocytes over meshed porcine xenograft in five patients (two with burn wounds, two with traumatic wounds, and one with a varicose ulcer) [96]. The epithelialization rate was 62% after 10 days and the histological analysis witnessed

differentiated keratinocytes and normal basement membrane formation [96]. However, cell spillage from the wound and uneven cell delivery was noted when cells were applied as a suspension [97]. To overcome the latter problems, cells have been mixed with matrix material to provide better cell adherence to wounds [96]. For this purpose, fibrin gel has been successfully used with mixture of allograft in two clinical trials [98, 99], but due to small patient numbers and lack of a control group, the results remain inconclusive. Fibrin net has also been used to apply autologous keratinocytes in suspension to the wound, which resulted in complete wound healing within 3 weeks in 80% of patients, but chronic skin defects persisted in some patients [100]. The technique for harvesting subconfluent keratinocytes required either mechanical or enzymatic treatment, which negatively affected the anchoring fibrils leading to poor graft attachment [101]. In addition, many studies with different disease models have shown poor engraftment and survival of cell suspensions in host tissues [102, 103].

In contrast, using cultured cells as sheets have many advantages over using cell suspension or biodegradable scaffolds [89]. Cell density and intracellular functions are preserved when cells are used as sheets [89]. Additionally, if the ECM is preserved along with the cell sheets, then it can be transplanted to the wound site without any need for sutures [89]. Cell sheets can be transplanted into wounds without any scaffolds, which will eliminate the inflammatory reaction to biodegraded scaffold materials [89].

AUTOLOGOUS KERATINOCYTE SHEETS (KSS)

The fact that HLA-DR are not consistently expressed in *in vitro* cultured keratinocytes [104] has led to the use of allograft keratinocytes for wound healing in clinical trials [78]. However, further studies showed that keratinocytes express HLA-DR

in response to gamma interferon [105]. Reducing immunogenicity of cultured allogeneic KSs helps in short-term tolerance in the case of partial thickness burns, but does not help in cases of full thickness wounds [106]. It is, therefore, important to provide autologous source of KSs for burn wound cover. Previously, O'Connor and others have reported efficacy of autologous KSs in burn wounds [107, 108]. For the isolation and culture of keratinocytes, a small skin biopsy (3 cm^2) can be obtained with initial wound debridement. Cells can be expanded *in vitro* over 3-4 weeks more than 5000-fold that is enough to cover the whole-body surface of an adult [66, 96]. KSs are formed of a thick layer of multiple layers of keratinocytes [109, 110].

However, clinical results with KS grafts have been disappointing with incidences of blistering, formation of hyperkeratosis, and scar contracture [63, 109, 111] that precluded the use of KSs. This was related to disruption of integrins, a family of cell surface proteins, that mediate graft attachment. The profile of integrins changes when cell growth is arrested and cells start differentiating [112, 113] in culture upon achieving confluency [114]. KSs are usually detached from culture dishes by an enzyme called Dispase [115]. Dispase type II is a natural protease from Bacillus polymyxa that is used for separating epidermis from dermis for isolation of keratinocytes or for detaching confluent cultured KSs from culture dishes [116]. However, Dispase disrupts ECM, adhesive proteins and surface integrins [117-119]. Dispase cleaves fibronectin and collagen IV, while laminin, collagen V, collagen VII are resistant to this enzyme [116]. Break down of the indicated proteins leads to upregulation of urokinase-type plasminogen activator and its receptor (CD87), which degrades ECM [120, 121], and cellular cytoskeleton [122]. Additionally, Dispase disrupts actin and intermediate filaments (keratin), which

significantly alters the structure of KSs [122]. These undesirable effects of Dispase result in poor attachment of the sheets to the burn wounds [118, 123]. Histological evaluation of wounds treated with KSs (which had been detached with Dispase) show a delayed rete ridge formation and maturation of basement membrane [96, 124, 125]. Poor graft acceptance leads to blistering with minor shearing forces which persists a few months [108]. To overcome the Dispase-related limitations, a new technology using temperature-responsive culture dishes has been introduced. This technology allows for non-enzymatic detachment of cell sheets.

TEMPERATURE-RESPONSIVE DISHES (TRDS)

Temperature-responsive dishes are covered with thermo-responsive polymer, poly-N-isoproprylacrylamide (PNIPAAm) [126]. PNIPAAm has an intelligent characteristic that changes the lower critical solution temperature (LCST) below or above 32°C [126]. The dishes coated with PNIPAAm have similar thermo-responsive features as the polymer [126-128]. At 37ºC, the dish surface is hydrophobic and allows cells to attach to the dish; in contrast a decrease in surface temperature below 32ºC changes it to a hydrophilic state (which rapidly hydrates the culture dish surface) [117, 127, 129], resulting in detachment of cells without use of any enzymes [117] (Fig. 1.3).

As mentioned, enzymatic (i.e. Dispase) treatment for cell detachment cleaves various membrane-associated proteins, cell surface proteins, and ECM, thus altering cellular function [130-132]. Cells detached from temperature-responsive dishes maintain better cell–cell interactions and preserve ECM proteins [126, 133, 134]. Preserving the extracellular proteins is essential for cell sheets to adhere and graft to host tissue [134, 135]. Several attempts have been made to incorporate bioactive molecules, such as cell adhesive

peptide, antibody and growth factors to PNIPAAm layer to improve the efficiency of the temperature-responsive surface for cell culture [136-138]. A few cell types have been successfully cultured on temperature-responsive dishes to form cellular sheets, like corneal epithelial cells [139], oral mucosal epithelial cells [140], renal epithelial cells [141], keratinocytes [117], periodontal ligament cells [142, 143], chondrocytes [144], middle ear mucosal cells [145], pancreatic islet cells [146], hepatocytes [147], thyroid cells [148], cardiac myocytes [149], and mesenchymal stem cells [150].

Cell sheets can be transplanted to tissue without any need for suturing [89]. Clinically, corneal epithelial cell sheets have been used for patients with thermal or chemical burns and certain eye diseases [140]. Autologous oral mucosal cell sheets have been used to repair corneal damage as a safe and effective treatment [140, 151]. Ohki et al. have used the oral mucosal cell sheet to replace esophageal mucosa after esophageal ulcerations [152]. In the case of dilated cardiomyopathy, myoblast sheets have been transplanted in patients to improve cardiac performance [153]. Iwata et al. have used periodontal ligament cell sheets for treating periodontal disease as they induce bone regeneration, cementum formation and well-oriented collagen fibers [154].

PRECLINICAL USAGE OF TEMPERATURE-RESPONSIVE DISH FOR SKIN WOUND HEALING TREATMENT

In an *in vitro* setting, Yamato et al. reported efficacy KSs cultured in temperature-responsive dishes [117]. The authors demonstrated that this approach preserved the desmosomes between the cells, while the desmosomes were destroyed in KSs detached by Dispase. Moreover, D-KS displayed disruption of E-cadherin and laminin 5 [117]. In another study, three cells types (human keratinocytes (hKC), dermal microvascular

endothelial cells (hDMEC) and dermal fibroblasts (hDFb) were used for sheet formation and implanted on murine full-thickness wounds. Homotypic and heterotypic three-dimensional (3-D) cell sheets constructs were developed to target wound re-vascularization and re-epithelialization. Both hKC and hDMEC significantly contributed to re-epithelialization by promoting rapid wound closure and early epithelial coverage [133]. In a rodent skin defect model, Osada et al. studied survival and morphology of keratinocyte sheets harvested by temperature reduction (T-KS) vs. sheets detached by Dispase treatment (D-KS) [118]. The T-KS better preserved keratin structure and expressed collagen IV and laminin 5 compared to in D-KS [118].

CLINICALLY RELEVANT OVINE MODEL OF GRAFTED BURN WOUND HEALING

Several small (mice, rats and rabbits) and large animal (swine) models have been used for burn wound healing studies. Rodents models used to understand quickly the mechanisms of wound healing [155]. However, wound healing in mice and rats, occurs primarily through wound contraction [156-158], while human wounds heal primarily through re-epithelialization and granulation [35, 159]. Further, compared to humans, mice do not form hypertrophic and keloid scarring[157]. Pig skin structures and wound healing patterns are similar to that in humans. Pigs and human wound healing occur through same physiological phases [160]. Investigators have used the pig model to uncover mechanism of hypertrophic and keloid scar formation in burn patients [161]. Despite the advantages of using pigs as an animal model for burn wound studies, there are several limitations e.g., difficulties in continuous care and handling of wounds without sedating the animal, including special dressing requirements, mechanical damage to grafts due to rubbing the

wounds against the cage wall, or rolling over on the wounds. These limitations are associated with both intensive labor and high cost [156].

Sheep have become one of the major animal models for burn wound healing [162]. Adult female sheep are usually used as they are docile and quiet [162]. During studies, sheep are placed in individual metabolic cages, where they stay content as long as they have food and water and the presence of accompanying sheep [162]. The size of the sheep (~40kg) allows the placement of various vascular catheters (e.g., Swan-Ganz, arterial and venous catheters) by which hemodynamic variables, such as cardiac output, heart rate, systemic and pulmonary arterial pressures, central venous pressure, and core body temperature are monitored. These variables can be continuously monitored in a conscious state for an extended time period up to a few weeks [163]. Importantly, the sheep's wound healing process is similar to human wound healing including all 3 phases [164]. In an ovine punch wound, on the day 1 of healing, there is obvious acute inflammation, while at day 7 the wound is filled with granulation tissues that have deep and fine collagen fibers [164]. At day 14 the wound is covered with new cells due to reepithelization, lacking hair follicles [164]. The collagen in the connective tissue changes to parallel bundles of collagen fibers [164]. Additionally, sheep allow continuous care to wounds without any sedation. The novel ovine model of grafted burn wounds developed at our laboratory has been presented at major critical care meetings, such as the American Burn Association conference with good acceptance and recognition. The model has been published in burn specialty journals and used in our laboratory as a model for many studies, such as cutaneous flame burn injury [165, 166], smoke inhalation injury [167, 168], combined cutaneous flame burn and smoke inhalation injury [169, 170], septic shock [171], hemorrhagic shock [172], and toxic

gas inhalation injury. To my knowledge, there is no study using T-KS from TRDs for treating third degree burn wounds in clinically relevant large animal models that closely mimics all aspects of burn wound care and healing, which will be investigated for the first time in this proposal.

THE RELEVANCE OF THE PRESENT STUDY

Use of split-thickness skin autografts is considered as the "gold standard" for burn wound closure. In severely burned patients, the availability of donor skin is limited. With the advancement in cell culture techniques, cultured autologous keratinocyte sheets (KSs) have been proposed for treatment of burn wounds. However, their clinical outcome has been discouraging because of certain complications and poor results. Conventionally, KSs are detached from culture dishes using enzyme Dispase, that degrades the quality of these sheets. **Therefore, we hypothesize that preserved extracellular matrix in non-enzymatically detached cultured keratinocyte sheets bolsters the healing effects on grafted burn wounds.** To test this hypothesis, a novel technology was employed for culturing KSs in especial dishes that are responsive to temperature changes. The temperature gradient changes the surface of culture dishes from a hydrophobic to hydrophilic state allowing cell detachment from the culture dish surface without using any enzymes. To achieve this goal, the efficacy of KSs detached either by temperature reduction or Dispase was compared in both *in vitro* and *in vivo* settings.

Specific Aim 1: To demonstrate that non-enzymatic detachment of cultured KSs improves their overall quality and effectively accelerates wound healing in *in vitro* setting.

Specific Aim 2: To investigate the efficacy of KSs detached by temperature gradient in an ovine grafted skin burn model with especial emphasis on engraftment and wound closure.

The studies are highly translational and offer a novel treatment approach, using autologous KSs for patients with large full thickness burns.

INNOVATION

We are proposing a novel method for burn wound coverage using KSs detached without the use of harmful enzymatic treatment. The method will bridge the gap towards using autologous KSs for successful management of burn wounds. This research is conceptually innovative demonstrating better quality of T-KS vs. D-KS and its effectiveness as a graft for burn wound healing.

To my knowledge, this study first uses autologous KSs cultured in temperature-responsive dishes and detached by a non-enzymatic method using temperature gradients for coverage of burn wounds grafted with cadaver skin.

The concept that non-enzymatic detachment of cultured keratinocytes from the culture dishes preserves extracellular matrix (ECM) is novel. A novel hypothesis that preserved ECM will lead to more firm conjunction of epidermis (grafted KSs) and dermis (wound bed) with specific focus on desmosomes (intercellular junction), hemidesmosomes (epidermis-dermis junction) and major components of skin e.g., laminin 5, collagen IV will be tested.

This study, for the first time, demonstrates cellular behavioral changes e.g., viability, proliferation capacity in harsh burn wound environments using *in vitro* models for burn wound and elucidates underlying mechanistic aspects.

Finally, the ovine model of grafted burn wound is novel. This model closely mimics clinical practice reflecting all aspects of burn wound pathophysiology as well as current standards of burn wound care, thus making the model highly translational.

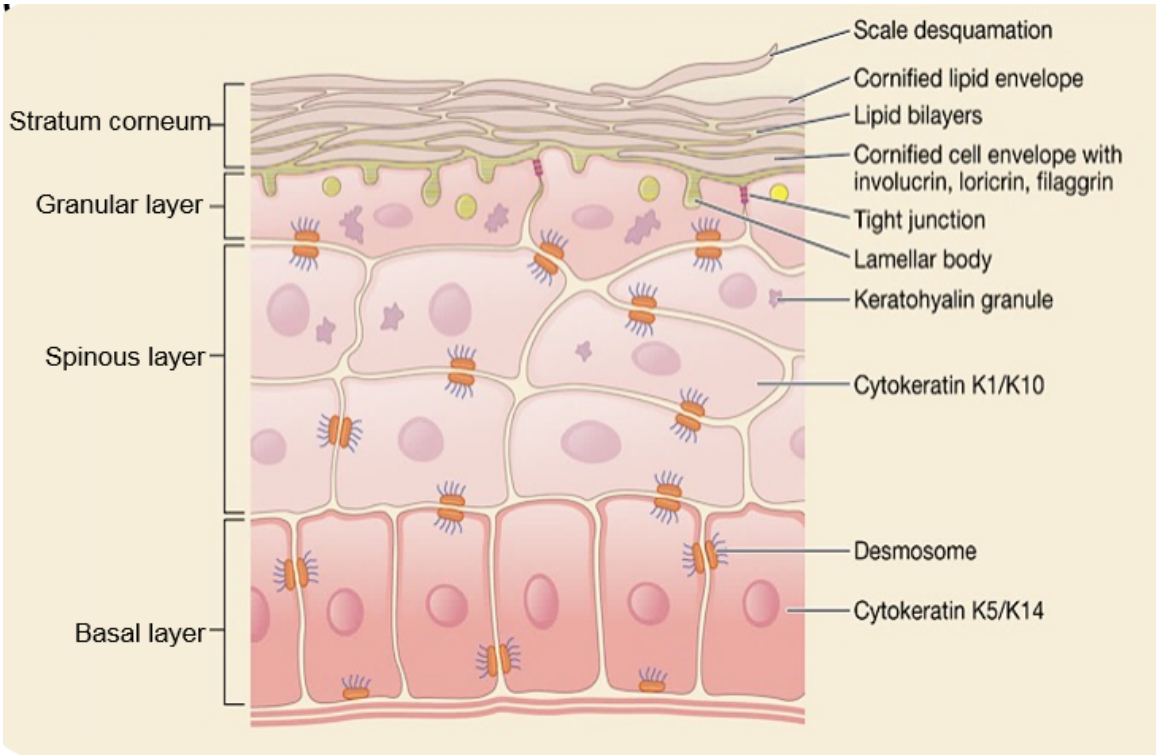

Figure 1.1: The layers of the epidermis [173].

Basal cell layer is the deepest layer of epidermis that differentiates to spinous cells then to granular cells and finally to stratum conrneum.

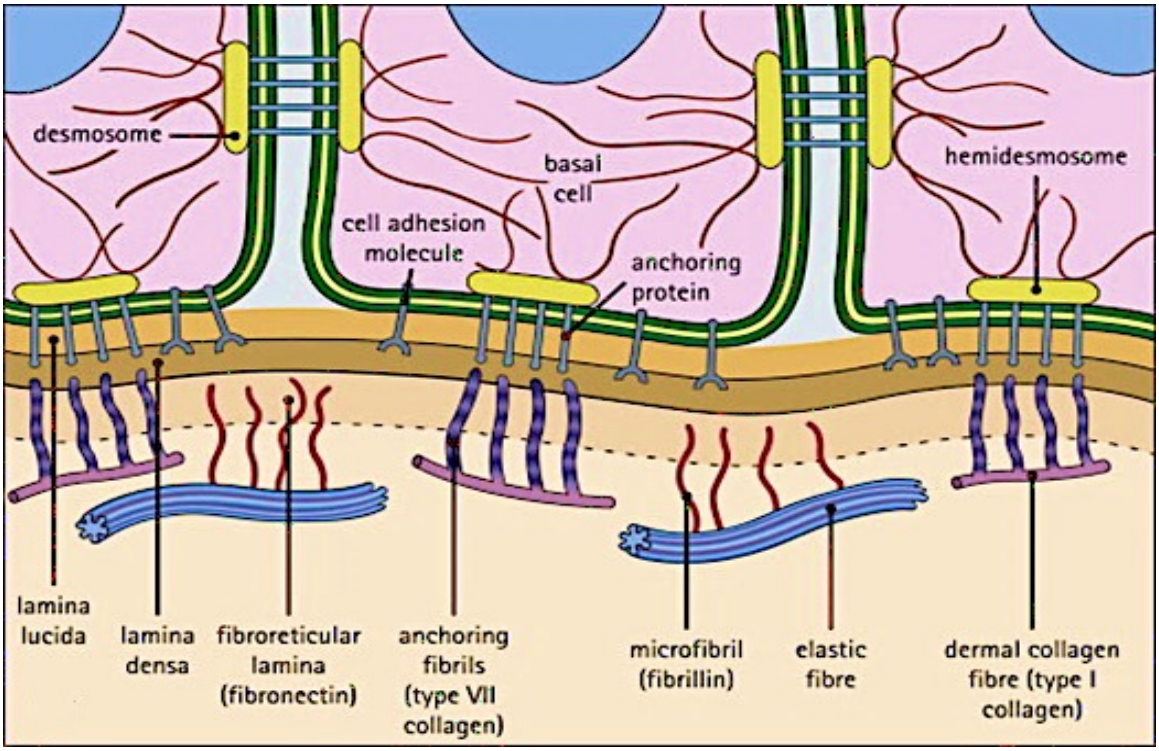

Figure 1.2: The dermal-epidermal junction (DEJ) [19].

Hemidesmosome-anchoring filament complex assist in anchoring the basal keratinocytes to the underlining basement membrane (lamina lucida, lamina densa, and fibroreticular lamina) that is connected to dermis proteins with anchoring fibrils and microfibrils.

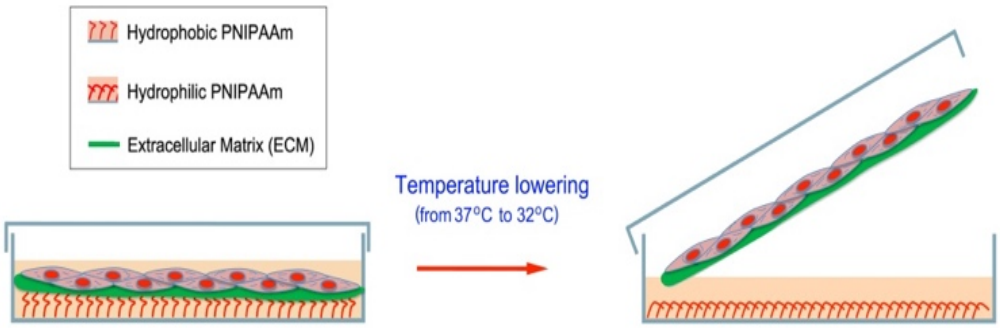

Figure 1.3: The properties of the temperature responsive dish [129].

Cells grown onto temperature-responsive dishes coated with poly-N-isopropylacrylamide (PNIPAAm) can be detached by temperature reduction to 32°C. At 37°C, the surface is hydrophobic allowing cells staying attached and proliferating to confluence. When the temperature is reduced, PNIPAAm becomes hydrophilic, and the cell sheet is detached with preserved extracellular matrix (ECM).

CHAPTER 2

Aim 1. Non-enzymatic effect of detaching cultured KSs and their effect on *in vitro* burn wound healing

INTRODUCTION

Burns are one of the devastating injuries that affects its patients physically and emotionally. Burn wounds require extensive wound care and surgeries [174]. Timely covering of burn wounds and rapid epithelialization after burn excision is crucial to restore skin function, prevent scarring, and inflammation occurrence [174]. Dealing with patients with large burn size and limited skin donor sites led to the discovery of autologous expansion of their skin keratinocytes [115, 175]. Using cultured keratinocytes autografts as confluently grown cell sheets for treating burn wounds was first reported in 1981 [107]. However, there was a certain concern on the efficacy that prevented their broad use in clinical practice. The reports on use of autologous keratinocytes documented that the uptake rate is varied between 15-85%. These studies related the reason for such poor acceptance to the use of enzyme (Dispase) for detachment of the sheets [96, 118].

Well established ECM play a major role in cellular programing for growth, differentiation and apoptosis [176]. Integrins is the major cell adhesion to the ECM in which transmit signals from the ECM to the cells [177, 178]. The survival of epithelial cells due to their interaction with the ECM can be regulated with the extracellular signal-regulated kinase (ERK) family of mitogen-activated protein kinases (MAP kinases). Once ERK is activated by integrin-mediated signals, cell survival genes will be transcribed due to the translocation of ERK to the nucleus after its phosphorylation [179]. However, the

critical role of preserved ECM in cell sheet acceptance after grafting onto wound bed is not fully investigated.

In this study, we want to understand the differences between cell sheets detached from temperature-responsive dishes without using enzyme and cell sheets detached from standard culture dishes using enzymatic treatment. In addition, we created skin and burn wound healing *in vitro* models transplanted with both types of cultured keratinocyte sheets to evaluate their cellular pathways activation and proliferation. Normal human epidermal keratinocyte (NHEK) cells were used to increase the translational aspect of this study. Also, ovine primary isolated keratinocytes were used in this study to facilitate creating *in vitro* wound healing model supplemented with ovine burn wound exudate.

MATERIALS AND METHODS

Human keratinocytes (hKC) culture

Adult primary normal human epithelial keratinocytes (NHEK) was purchased from Lonza (Cat # 00192627). The NHEK cells were initially cultured on regular plastic flasks (BioLite; Thermo Scientific) in serum-free conditions in Lonza's KGM-Gold media that is supplemented with bovine pituitary extract with cell density at 3500 cells/cm^2. KGM-Gold media contains low Calcium (Ca^{+2}) which prevents cells to go through differentiation. The cells were cultured in a 37°C incubator with 5% CO_2, with the media being changed every 2 days until approximately 80% confluent. The NHEK's were then lifted with Trypsin/EDTA (Lonza), which was neutralized by adding Trypsin Neutralizing Solution (Lonza), before cells were centrifuged at 200 × g for 5 minutes and frozen for further sheet formation. Cell subcultures were passaged no more than twice before using it for sheet experiments. The same NHEK primary cell line patch was used to perform all experiments.

Sheep keratinocytes (sKC) isolation and culture

For sKC isolation, partial thickness skin samples were harvested from dorsum (unburned area) of adult sheep using a dermatome fixed at 0.07 inches (7x8 cm^2). Keratinocytes were isolated by methods described elsewhere with minor modifications [118]. Skin pieces were minced and digested for four rounds in 0.25% trypsin at 37°C with shaking for 30 min each round. The cell suspension was filtered using a 70 µm cell strainer and complete keratinocyte medium (CKM) containing 5% FBS was added to stop further trypsin action. The cells from each round was centrifuged at 200 g for 5 min and the pellets were suspended in CKM with high Ca^{+2} as published previously [118] and seeded into a flask prepared with a feeder layer. CKM is composed of Dulbecco's modified Eagle's medium-high glucose (DMEM; Gibco) and Ham's F-12 (Gibco) were mixed at a 3:1 (v/v) ratio. The medium was supplemented with 100 IU/ml penicillin, 100 µg/ml streptomycin (Gibco) and fetal bovine serum (FBS, Corning) at a concentration of 5%. The following supplements were also added to the medium: 2 nM triiodothyronine, 5 µg/ml transferrin, 0.4 µg/ml hydrocortisone (MP Biomedical), 10 ng/ml recombinant human epidermal growth factor, 5 µg/ml insulin (Gibco), 1 nM cholera toxin (Millipore). The feeder layer is a 3T3 cells which are a mouse embryonic fibroblast cell line that is essential for the keratinocyte proliferation and differentiation. The feeder layer was treated with Mitomycin C (4 µg/ml for 2h, Stem Cell Technologies) in order to inhibit their proliferation. The medium that is optimal for culture and treating 3T3 cells is DMEM high glucose supplemented with 10% FBS and 100 IU/ml penicillin, 100 µg/ml streptomycin. Treated 3T3 cells were seeded at $3x10^4/cm^2$ density and allowed their attachment for at least 2 hrs before adding the keratinocytes. The keratinocyte culture dishes were incubated at 37°C in

a humidified atmosphere of 5% CO2. Characterization of keratinocytes was validated by microscopic assessment of cells shapes and morphology to ensure that keratinocytes grow as colonies with polygonal shape. The culture routinely screened for possible contamination with fibroblasts. Other cells like Merkel cells and Langerhans cells do not survive in culture and melanocytes do not proliferate unless special culture conditions are used. Once the cells are 80 - 90% confluent, cells were treated with 0.25% trypsin (Gibco) for cells detachment. For cell expansion, keratinocytes are re-seeded ($3x10^4/cm^2$) in regular flasks prepared with a Mitomycin-C treated 3T3 feeder layer. Experimental repeats were performed using 3 or more different cell isolations.

Keratinocyte sheet formation

For sheet formation, human or sheep keratinocytes from the second and third passage respectively were seeded into 35 mm regular culture dish (RD) (Corning) or temperature responsive dish (TRD; provided by CellSeed, Tokyo, Japan) with $4x10^4$ cells/cm^2. The cells were cultured on a mitotically inactivated feeder layer (3T3 cells) in CKM at 37 °C in the presence of 5% CO_2. After 10 days, the cells cultured in RD were harvested as a cell sheet detached by Dispase treatment (2.4U/ml) for 55 and 35 min at 37 °C for human and sheep cell keratinocyte sheets respectively. These sheets were labeled as keratinocyte sheet detached by Dispase (D-KS). On the other hand, the cells grown in TRD were harvested as a cell sheet detached by lowering the temperature to 20 °C (room temperature) for about 1h. The Keratinocyte sheet detached by temperature reduction is abbreviated as (T-KS). A nitrocellulose membrane was used to peel off the sheets from both types of culture dishes. To demonstrate that ECM mediates superior effects of T-KS vs D-KS, T-KS was treated with Dispase anticipating that this will remove ECM in these

sheets. The Keratinocyte sheet detached by temperature reduction and treated with Dispase is abbreviated as (T/D-KS) (Fig. 2.1).

In vitro skin model

To model the skin, collagen gel mix was formed by combining ($3x10^4/cm^2$) mitotically inactivated treated 3T3 fibroblasts and 3mg/ml of bovine collagen type I (Gibco). Collagen type I was prepared based on the manufacturer gelling procedure with modification that 3T3 medium mixed with 3T3 cells was used instead of the sterile distilled water (dH_2O). The mixture was aliquoted into 35 mm cultured dishes (2 ml/dish) and placed at 37°C for gel formation, which mimics the dermal structure of the skin. After collagen-fibroblast matrix formation, cultured and detached human keratinocyte sheets (T-KS, D-KS or T/D-KS) were cut in half and grafted on top of the matrix. A silicon disk (30 x 30 x 1 mm; ~ 0.8 g) was used to press down the cell sheet to facilitate cell adhesion to the collagen-fibroblast matrix. After incubation at 37°C for 1h without medium, the silicone disk was removed and 2 mL of CKM was added to the culture dish. The adherent cell sheets were cultured for another day, and samples collected for Western blotting at 0 h (the other half of the sheet before grafting), 2h, 8h, 24h after grafting the sheet. A schematic of these procedures is shown in Fig. 2.2.

Western blotting

Human keratinocyte sheets (T-KS, D-KS and TD-KS) gathered from 3 different experiments were extracted in 200 µl RIPA protein extraction reagent (Thermo Scientific). The samples were homogenized (Bullet Blender, Next Advance) with 2 zirconium oxide beads 2.0 mm for 1 min. After 1 min cooling on ice, the samples were again homogenized

for 1 min followed by gentle shaking for 15 min at 4°C. Digested samples were centrifuged at 14000 g for 15 min at 4°C. The supernatants were recovered and stored at -80°C for analysis using Western blot. To estimate the amount of protein the supernatant was tested by using a BCA Test (Pierce) which was performed according to the manufacturer's instructions. Collagen IV and laminin 5 were measured as a representative for ECM proteins, actin and alpha-tubulin (α-tubulin) were measured as representatives for cytoskeleton proteins. The sheet samples collected from the *in vitro* skin model were used to measure the level of MAPK phosphorylation. The GAPDH was used as a loading control. Protein samples were mixed with NuPAGE LDS sample buffer and NuPAGE sample reducing agent (Invetrogen) for reduced condition and heated for 10 min at 70°C for denatured condition, and then separated through NuPAGE™ 4-12% Bis-Tris Protein Gels (Invitrogen). After electrophoresis, proteins were transferred to PVDF membranes by using an iBlot Dry Blotting system (Invitrogen). Membranes were blocked for 1 hr, rinsed and incubated with primary antibody in blocking buffer at 4°C overnight. Primary antibody was then removed by washing in TBS-T thrice and labelled by incubating with HRP-labelled secondary antibodies for 1 hr at room temperature. Membrane was washed thrice in TBS-T and visualized using Pierce ECL Western Blotting Substrate (Thermo Scientific) and the emitted light is captured on CCD camera using G Box imaging system (Syngene) with GeneSnap Software (Syngene, Version 7.09). Results were calculated by imageJ software and expressed as ratio to GAPDH protein as the loading control. Table 2.1 summarizes the antibodies with their suppliers, catalog numbers, dilutions, amount of proteins, running conditions, and blocking solutions.

Keratinocyte sheet thickness

Cultured sheep keratinocyte sheets (T-KS, D-KS and TD-KS) were carefully transferred to 10% formalin to be processed for FFPE (Formalin-Fixed Paraffin-Embedded). Histological sections were carried at 4-micron thickness then sections were stained with Hematoxylin and Eosin. Sections were observed by light microscope (Olympus BX51) and images was taken using 4x magnification using Stereo Investigator software (Micro Bright Field Inc., Version 2018.2.1). The sheet thickness was semi-quantified using ImageJ software (NIH, Bethesda, MD, USA) (version 1.52g) using a line grid with 722500 μm^2 area per point; whenever the grid touches the sheet section a perpendicular line to the sheet was measured.

Mechanical cell dissociation assay

A shear test used to assess KSs tensile strength, reflecting cell-cell adhesive strength. The method was adapted from a well-established protocol [180]. Sheep T-KS, D-KS and T/D-KS were detached from 35 mm culture dishes and carefully washed twice with PBS and transferred to 15 mL tubes containing 5 mL of PBS. Tubes with the cell sheets were vortexed for 20 cycles at 2000 rpm with 5 second intervals. Sheet fragments were filtered through 70 μm strainer (Fisherbrand) and the number of detached cells was counted in the filtrate using Countess II Automated Cell Counter (Invitrogen). The advanced counting algorithms of the Countess Automated Cell Counter can clearly identify cell boundaries within clumps of cells, resulting in accurate cell counts (Fig. 2.3A).

Shrinkage percentage

Still images of KSs before and after detachment without medium or PBS were photographed, and the size analysis of the cell sheets was performed by measuring still images with ImageJ. Shrinkage percentage (SP) was calculated as SP= [(Sheet size before harvesting – Sheet size after harvesting) / Sheet surface size before harvesting] x 100 (Fig. 2.4 C).

Burn wound exudate (BWE) collection

To mimic a harsh burn wound environment *in vitro*, burn exudates were collected from ovine burn wounds that was added to culture medium in the *in vitro* burned skin wound healing model. For burn wound exudate collection, a third-degree burn (5 x 5 cm) was induced in the sheep dorsum and after 24 hrs the wounds were excised and covered with an ostomy drain pouch to collect burn exudate for 24, 48 and 72 hrs separately. Burn exudates were centrifuged at 1500 rpm for 15 min at 12°C, then followed by the filtration with a 0.22 μm filter. To estimate the amount of the proteins, the exudate was tested by using a BCA Test (Pierce) which was performed according to the manufacturer's instructions. Samples were aliquoted and stored at -80°C for further use. Burn exudate was collected from burn wounds that was initiated in sheep that were allocated for another study.

Wound healing scratch assay

Sheep keratinocytes were seeded in 3 x 10^4 cells/cm^2 on polystyrene 6 well plate (Corning) prepared with a feeder layer. Once the cells were confluent (~2 days), a scratch was drawn in a confluent monolayer of sKC with a plastic disposable pipette tip. To find

the optimal culture conditions, after washing, the cells were exposed to keratinocyte medium with or without FBS supplemented with different collection time points of BWE (24, 48 or 72h) at 50 μg/ml. In separate experiments, the optimal dose of burn exudate was tested by exposing the cells to different concentrations of BWE (0, 50 or 100 μg/ml) from different collection time points of BWE (24, 48 or 72h) in CKM with FBS. Phase contrast pictures were taken directly after drawing the scratch and after 6 and 12-h exposure using an inverted light microscope (Olympus CKX41) with camera (Olympus DP73) and cell imaging software (CellSense Standard 1.11) (4 images/condition/time point). Wound sizes were determined using ImageJ software with the MRI wound healing tool macro (http://dev.mri.cnrs.fr/projects/imagej-macros/wiki/Wound_Healing_Tool). The closure percentage (CP) was determined by CP= [(Open area at 0h - Open area at time point t = 6 h or t = 12 h) / Open area at 0h] x 100.

In vitro burned skin wound healing model

The burned skin wound healing model was modified from the *in vitro* skin model. After removing the silicon disk, that was used to weigh down half of the grafted cell sheet (T-KS, D-KS and T-KS) to facilitate cell adhesion to the collagen matrix, a 2 mL of CKM was added to the culture dish with and without burn exudate 50μg/ml from 48h collection time (determined based on the results from the wound healing scratch assay). Medium was changed daily and cell proliferation or migration from the edge of the sheets, was monitored daily for 3 days. A pictorial record from day 3 was analyzed using ImageJ software (NIH, Bethesda, MD, USA). To normalize the proliferation quantification, the outgrowth area from the edge of the sheet was divided by the length of that sheet edge. A schematic of this model is shown in Fig. 2.5.

Statistical analysis

All data were analyzed using Prism GraphPad version 8.1.0 (GraphPad software, Inc.). All quantitative data were expressed as means ± standard error of the mean. Comparisons between sheet types (T-KS, D-KS, and T/D-KS) were made using the Kruskal Wallis with the Dunn's test for pairwise comparisons. Comparisons between grafted sheets at different time points were made using Two-way ANOVA RM with Sidak's multiple comparison test. Comparisons between D-KS and T-KS were made using Unpaired t test with Welch's correction. Quantitative variations were considered significant when the P value was < 0.05.

RESULTS:

Keratinocytes sheets characteristics

Human and sheep keratinocytes were successfully cultured for 10 days as a cell sheet in both RD and TRD (Sup. Fig 2.1). The sheep keratinocyte sheets were confirmed to be multilayered (2-4 layer) using light microscope (Fig. 2.6 A&B). The thickness of the cell sheets cultured on TRD was 18.17 ± 0.9177 μm and vs. 11.68 ± 1.216 μm for the sheets cultured on RD. There was a significant difference on the sheet thickness between the two types of sheets (Fig. 2.3 C).

ECM preservation in T-KS and the activation of MAPK pathway

In order to clarify the noninvasiveness of the temperature reduction method, multilayered keratinocytes sheets were recovered (T-KS, D-KS, T/D-KS) and the recovered keratinocytes were subjected to immunoblotting with anti–collagen IV antibody (Fig. 2.7 A) or anti–laminin 5 antibody (Fig. 2.7 B). Collagen IV with

1063, 0.02916 ± 0.01950 and 0.01856 ± 0.01293 for T-KS, D-KS and T/D-KS, respectively. After Dispase treatment, laminin 5β3 chain (molecular weight-140 kD), was faintly detected in both D-KS and T/D-KS. In contrast, a higher amount of laminin 5β3 was detected in the sheets recovered by temperature reduction treatment (Fig. 2.7 B). The Laminin 5 expressions after normalization with GAPDH were 1.071 ± 0.2366, 0.07280 ± 0.03906 and 0.1072 ± 0.05736 for T-KS, D-KS and T/D-KS, respectively. We then examined the activation of survival signals due to preserving these ECM proteins on cell sheets after engraftment. The samples of cells sheets (T-KS, D-KS) were collected before and after grafting onto the *in vitro* skin model for 2h, 8h, and 24h. Two hrs after grafting onto the *in vitro* skin wound model, we detected phosphorylated MAPK in KC sheets that were detached from TR or RD dishes. Interestingly, phosphorylated MAPK was detected in both types of cell sheets (T-KS and D-KS) before being grafted on the substrates. However, the ratio of phospho-MAPK protein to total-MAPK was always lower in the sheet detached by Dispase treatment compared with that detached by temperature reduction (Fig. 2.7 C).

Preservation of intercellular adhesion in T-KS

To test whether enzymatic treatment altered intercellular adhesive strength, we performed a mechanical dissociation assay using all types of keratinocyte sheets (T-KS, D-KS, T/D-KS). The results showed that the D-KS was fragmented to multiple pieces, while T-KS was still intact. The number of disassociated cells were significantly higher (6-fold increase) in D-KS compared to T-KS (12308 ± 1626 for T-KS vs. 55882 ± 8162 for D-KS). Interestingly, the treatment of T-KS sheets with Dispase (T/D-KS) significantly increased the number of disassociated cells (78945 ± 15678) (Fig. 2.3 B, C).

Cytoskeleton disruption and sheet shrinkage with Dispase treatment

The effect of enzymatic or temperature reduction treatment for detaching keratinocyte sheets on cell cytoskeleton was investigated by measuring a representative of cytoskeleton proteins in keratinocyte sheets using Western blotting with anti–actin antibody (Fig. 2.4 A) or anti–α-tubulin antibody (Fig. 2.4 B). Dispase treatment significantly reduced actin molecular weight (normal weight is 42 kD). In contrast, a significantly higher amount of actin was detected in the sheets recovered by temperature reduction treatment compared to D-KS and T/D-KS (Fig. 2.4 A). On the other hand, α-tubulin (molecular weight 50 kD in normal condition) was detected with the intact molecular size in cell sheet lysates obtained by the temperature reduction treatment. However, it was undetectable in the sheets that were treated with Dispase or sheets detached by temperature reduction but treated with Dispase treatment (Fig. 2.4 B). Next, we have measured the sizes of all types of sheets (T-KS, D-KS, T/D-KS) before and after detachment. The size of the T-KS was almost intact—it was reduced by only 5.087% ± 1.937 after detachment compared to pre-detachment size. However, the D-KS and T/D-KS sheets' sizes were reduced by 33.77% ± 4.676 and 54.06 ± 4.973, respectively after detachment using Dispase ($p<0.05$ vs. T-KS).

Impact of burn exudate on *in vitro* wound scratch assay

To test the hypothesis that burn wound exudate (BWE) may negatively affect grafted keratinocyte sheets, we have investigated the effects of burn wound exudates on keratinocyte proliferation and migration using *in vitro* wound healing scratch assay. After the scratch, cells were incubated with different concentrations of BWE collected at different time points after induction of burn in sheep. We have also cultured these cells

with or without FBS to reveal the possible medium impact effects of BWE on keratinocytes proliferation in the scratch assay. Closure percentage was increased after BWE treatment in medium without FBS compared to control (no FBS, no BWE). Interestingly, the closure percentage cultured in medium added with BWE & FBS was decreased compared to control (+FBS, no BWE). The decrease was more pronounced with the BWE collected after 48h after burn. (Fig. 2.8 A) (Sup. Fig. 2.2). Next, we wanted to test effects of different concentrations of the BWE on the keratinocyte proliferation. Two concentrations of BWE were tested (50 and 100 μg/ml). The most decrease in closure percentage was observed in medium treated with 50 μg/ml (33.24 ± 15.85%) BWE collected at 48 hrs compared to control (41.21 ± 17.77%). There was significant reduction compared to the control on closure percentage using 100 μg/ml of BWE but was not consistent with specific time collected BWE. Burn exudate taken at 48h significantly reduced the closure after 6h of wound scratch initiation, while BWE collected at 72h had significant closure percentage after 12 hrs of wound scratch initiation. (Fig. 2.8 B) (Sup. Fig. 2.3). Therefore, we have chosen to use culture medium with FBS and 50 μg/ml of burn serum (collected at 48 hrs postburn) for future studies.

Proliferation KC sheet overlaid onto *in vitro* burn wound

Within 1 day of grafting keratinocyte sheets, a number of keratinocytes could be seen protruding from the edge of all types of sheets (T-KS, D-KS, and T/D-KS). In order to asses cell proliferation from the edge of the sheet, the area of outgrowth was measured and compared between different types of keratinocyte sheets (T-KS, D-KS, and T/D-KS). T-KS had a significantly higher rate of proliferation with or without burn exudate treatment

compared to all the other groups (D-KS and T/D-KS) with 704.1 ± 65.84 and 983.6 ± 84.10, respectively.

DISCUSSION

The results from this study demonstrate the importance of preserving the ECM in keratinocyte sheets. The ECM preservation was achieved by culturing the cells on temperature responsive dishes, which enables them to detach the sheets without using any enzyme(s). These results enabled potential use of cultured autologous keratinocytes in a clinical practice for covering large burn wounds.

Osada et al. [118] and Matsumine et al. [181], reported no difference in the sheet thickness or cellular density between T-KS and D-KS. However, our microscopic results showed that there is a significant difference in sheet thickness between cell sheets cultured in TRD and those cultured in RD. This suggests that either the culture surface or detaching method had a significant impact on sheet thickness after detachment.

Previous studies showed the importance of ECM (Laminin 5 and collagen IV) for cell attachment to coated culture surfaces [182, 183], proliferation [184, 185] and survival [185]. Stenn et al. [116] showed the cleavage activity of Dispase on different purified basement membrane components. The authors reported that Dispase cleaves fibronectin, collagen IV, but not laminin, collagen V, albumin, and transferrin. Lim et al. investigated the effect of Dispase on an amniotic membrane which degrades membrane associated proteins like fibronectin, elastin, thrombospondin, collagen IV, collagen VII and laminin [186]. In our study, after detaching the sheets, the level of collagen IV and laminin 5 was preserved on T-KS. However, the concentration of these proteins was remarkably reduced

with Dispase treatment (D-KS & T/D-KS). These data are consistent with immunostaining data for keratinocyte sheets reported by Osada et al. [118] and Lim et al. [186].

Matsubayashi et al. reported that the activation of ERK MAP kinase (ERK1/2) spreads in cells in accordance to cell movement using their *in vitro* wound healing model, [181]. The survival signal (MAPK pathway) for the keratinocytes cultured over different ECM matrix was activated due to the interaction of ECM with cell integrins [187, 188]. However, the question whether preserving ECM to cell sheets activates the same signals after the cell sheet has been grafted, remained unanswered. Therefore, we measured the phosphorylation of MAPK before and after grafting the cell sheets over the *in vitro* skin model. We detected different levels of phosphorylated MAPK in KC sheets that were detached from the culture dishes under all conditions (T-KS and D-KS) and even in the non-adhesive cell sheets before being grafted on the substrates. However, the ratio of phospho-MAPK to total-MAPK was lower in the sheet detached by Dispase treatment compared with that detached by temperature reduction. Previously, the role of MAPK pathway on the cells survival, proliferation and migration was clarified [187-190], which may indicate the importance of preserving the ECM for the cell sheet survival and proliferation after being grafted over the *in vitro* burn wound healing model.

The effects of EGF on the keratinocyte sheet's intercellular adhesive strength that has been detached by Dispase treatment has been investigated [180]. In this study we adapted the same method that had been used for assessing the effect of the enzymatic treatment vs the temperature reduction method on the intercellular adhesive strength. We also based our experiments on previous results published showing E-cadherin disruption by Dispase, since E-cadherin is required in cell–cell junctions with barrier function [117].

Our results showed fragmented cell sheets after vortexing with the D-KS along with increased numbers of cells detached compared to T-KS. The results from the T-KS sheets was totally diminished after Dispase treatment in T/D-KS sheets confirming that the weakened adhesion was a result of Dispase treatment.

The three major parts of cellular cytoskeleton is: actin, microtubules and intermediate filaments [191]. The role of the cytoskeleton in cell adhesion, ECM interaction, proliferation and signaling had been extensively investigated [133, 192, 193]. Actin filament are linked to focal adhesion points and it is well studied as it plays an important role in mechanotransductive signaling [194]. Microtubules (α & β-Tubulins) are supporting actin's function and they also play an important role in cell division and protein trafficking [195]. Wei et al. [122] showed that Dispase lifting disrupts the cytoskeleton, therefore, altering cytoskeletal distribution. Our data showed significant impact on the level of cytoskeleton proteins (actin & α-tubulin) by detaching the sheet using Dispase treatment. On the other hand, these proteins were protected by using the temperature reduction method of sheet detachment. Our data regarding Dispase detachment was consistent with the finding by Wei et al. [122]. Cell sheets contraction after detachment is correlated with increase in cell-cell adhesion [196]. Our data showed that D-KS and T/D-KS sheet's shrinkage percentage was significantly increased after Dispase treatment compared to T-KS. These results suggest cell-cell adhesion was stronger in sheets detached without using enzyme. Preserving the cultured sheet size is of particular importance in the efficient coverage of wounds.

Different *in vitro* wound healing models have been established with different varieties and complexity, starting with simple wound healing scratch assay [197] ending

with tissue engineered wound construct [198] along with ex-vivo wound healing models [199, 200]. In our *in vitro* model, we aimed to closely mimic the burn wound environment. For this purpose, we have developed for the first time a 3D burn wound model to test the efficacy of keratinocyte sheets. The closer burn wound environment was achieved by adding burn wound exudate collected from 3rd degree burn wounds at different time points in sheep.

Burn exudate is considered as a relevant source to monitor burn wound healing [201]. Several studies showed that the data collected from analyzing burn exudate accurately reflected wound pathophysiology compared to the data collected from blood or serum samples [202]. Different techniques have been used over the years to collect the burn exudate, such as aseptic aspiration from intact blisters [203, 204], elution from dressing covering burn wounds [205], aspiration beneath temporary dressing [206], using negative pressure [201] or a patch device that can collect fluid from a wound site [207]. In this study, we collected drained burn exudate in an ostomy bag for 3 days separately.

Pan et al. [203] showed that early stages of burn exudate (within 3 days post injury) promotes endothelial cells proliferation, migration and vascularization. Also, the effect of burn exudate that was collected within 48 hrs following burn injury on fibroblast was investigated. Their data showed that exposed fibroblasts seeded into collagen lattices to burn blister fluid increase the contraction more than control cell lines not exposed to this fluid [204]. Also fibroblasts proliferation was significantly increased after incubating with burn exudate for 72 hrs [208]. Our data showed that burn exudate have positive or negative effect depends on the culture conditions. Burn exudate consists of negative and positive components which can be masked by adding FBS to the culture medium. Therefore,

culturing the cells without FBS, stimulated cell proliferation. On the other hand, adding FBS for the culture medium masks all the beneficial benefit of burn exudate and maintained a negative effect. We also demonstrated the dose dependent effects of burn exudate on the cell's proliferation in the *in vitro* wound healing model. To assess how the sheets will behave after being grafted over burn wounds, the sheets were grafted over an *in vitro* burn wound healing model. Cells started to protrude from the edge of the sheet within one day of grafting sheets over the model. This data correlated with the *in vivo* wound healing report of cells starting to migrate from the edge of the wound within 16 ± 24hrs after injury [209].

Kainulainen et al. [210] showed in blister and full thickness mucosal wounds that laminin 5 is upregulated within hours of injury at the leading front of migrating epithelial cells and promotes rapid migration over the wounded surface. Laminin 5 is the first of basement membrane components to appear after injury, which was shown to be proceeded with different laminin types and collagen type IV and VII [211-213]. Also, Collagen IV and collagen VII play important role in wound healing as they both co-distributed in the wound area in human skin lesions with no significant differences in the location or appearance time of these collagen types [214]. Taking all these data together, it is supporting our findings that preserving ECM to the cell sheets in T-KS accelerated cell proliferation after being grafted over the *in vitro* burn wound healing model.

In summary, this study clearly demonstrates the difference between T-KS and D-KS in regard to overall quality i.e., sheet thickness, integrity, ECM, and cytoskeleton, and negative impact of Dispase on these important variables for wound healing.

Antigen	Dilution	Loading	Running condition	Blocking	Supplier	Catalog number
Collagen IV	1:500	50 µg	Reduced	5% Milk	Abcam	ab6586
Actin	1:25000					ab49900
Laminin 5	1:500	25 µg	Denatured			ab14509
α-Tubulin	1:1000					ab15246
GAPDH	1:2500					Ab9485
MAPK	1:1000	20µg	Reduced and denatured	5% BSA	Cell Signaling	4695S
p-MAPK			Reduced and denatured			4377S
GAPDH					Abcam	ab9482

Table 2.1: Antibodies used for the western blot.

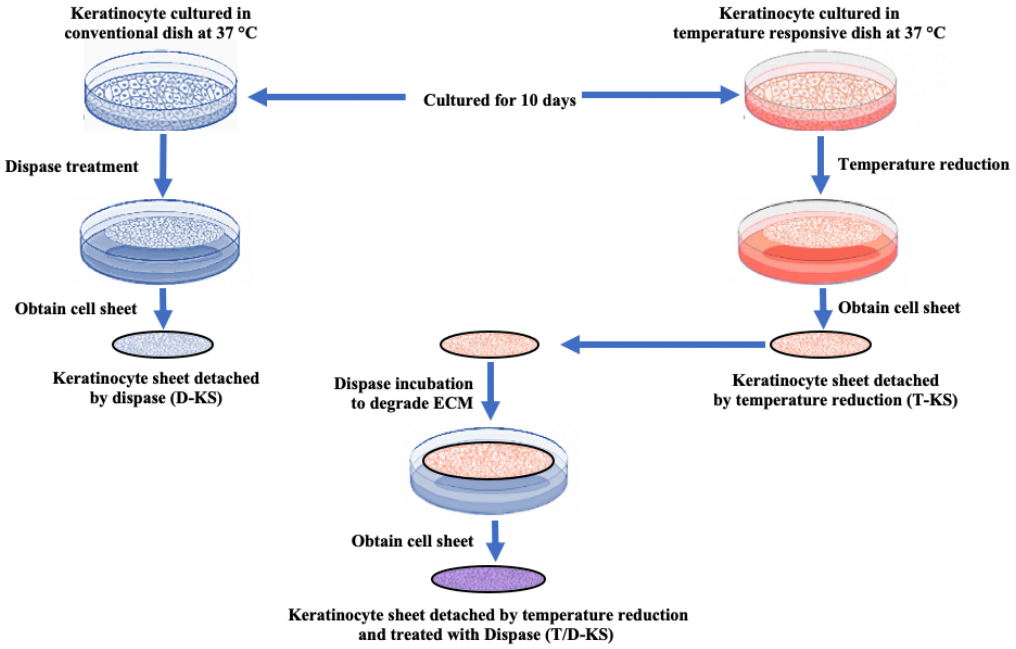

Figure 2.1: Schematic of keratinocyte sheet detachment.

Keratinocytes were seeded into RD or TRD and cultured on a mitotically inactivated feeder layer (3T3 cells). After 10 days, the cells cultured in RD were harvested as a cell sheet detached by Dispase treatment (2.4U/ml) at 37 °C (D-KS). On the other hand, the cells grown in TRD were harvested as a cell sheet detached by lowering the temperature to 20 °C (room temperature) for about 1h (T-KS). To demonstrate that ECM mediates superior effects of T-KS vs D-KS, T-KS was treated with Dispase anticipating that this will degrade ECM in these sheets (T/D-KS).

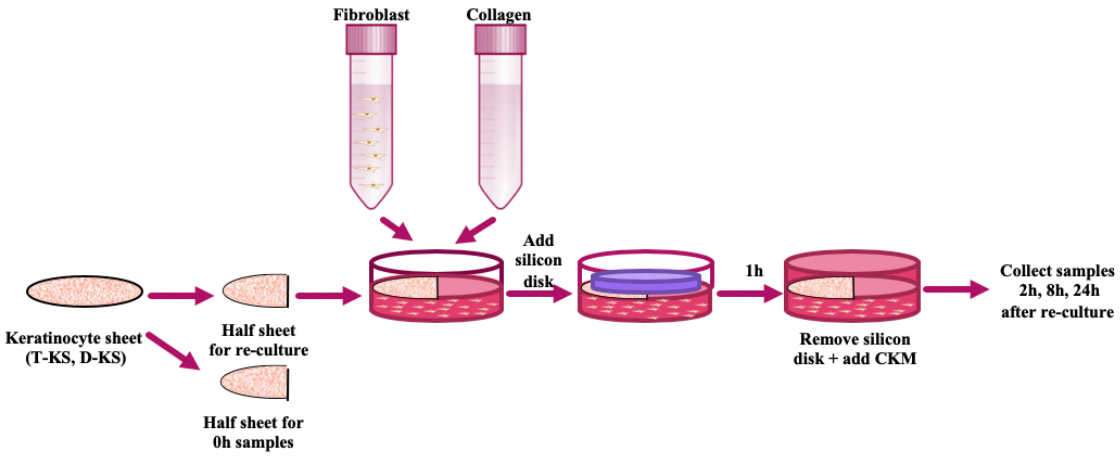

Figure 2.2: Schematic of *In vitro* skin model.

Collagen gel mix was formed by combining mitotically inactivated treated 3T3 fibroblasts with bovine collagen type I. The mixture was aliquoted into 35 mm cultured dishes and placed at 37°C for gel formation, which mimics the dermal structure of the skin. After collagen-fibroblast matrix formation, cultured and detached human keratinocyte sheets (T-KS, D-KS or T/D-KS) were cut in half and grafted on top of the matrix. A silicon disk was used to press down the cell sheet to facilitate cell adhesion to the collagen-fibroblast matrix. After incubation at 37°C for 1 h without medium, the silicone disk was removed and CKM was added. Samples were collected for Western blotting at 0 h (the other half of the sheet before grafting), 2h, 8h, 24h after grafting the sheet.

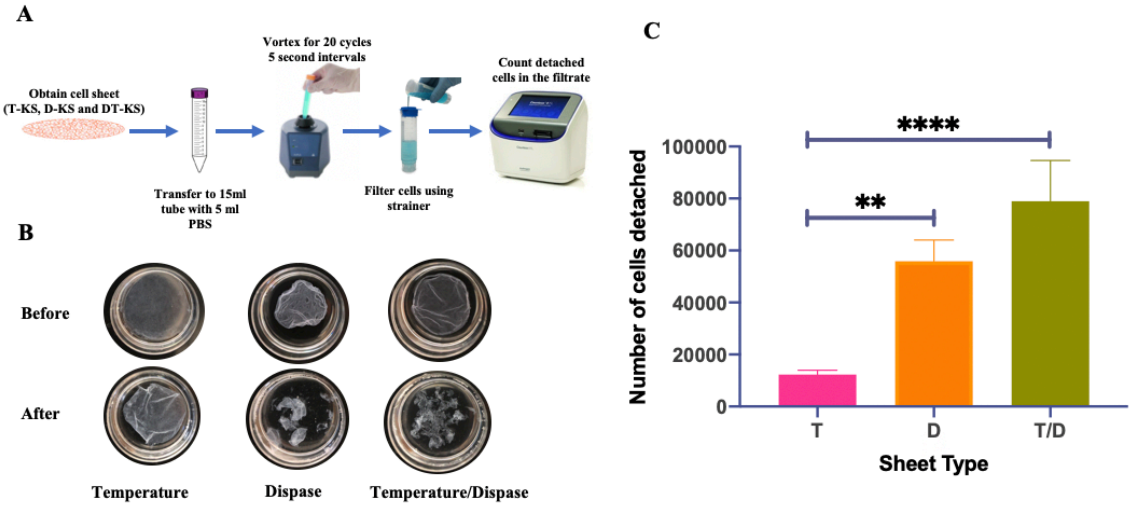

Figure 2.3: Preservation of Intercellular Adhesion in T-KS**.**

A) schematic of mechanical cell dissociation assay, sheep T-KS, D-KS and T/D-KS were detached from culture dishes and carefully washed twice with PBS and transferred to 15 mL tubes containing 5 mL of PBS. Tubes with cell sheets were vortexed and sheet fragments were filtered through strainer and the number of detached cells was counted in the filtrate. B) Representative images of cell sheets before and after mechanical cell dissociation assay showing D-KS and T/D-KS were fragmented to multiple pieces, while T-KS was still intact (N=3). C) The number of free disassociated cells after mechanical cell dissociation assay were significantly higher in D-KS and T/D-KS compared to T-KS. Error bars represent Mean±SEM (Kruskal-Wallis test with Dunn's multiple comparisons test, N=3) (**P<0.002, ****P<0.0001).

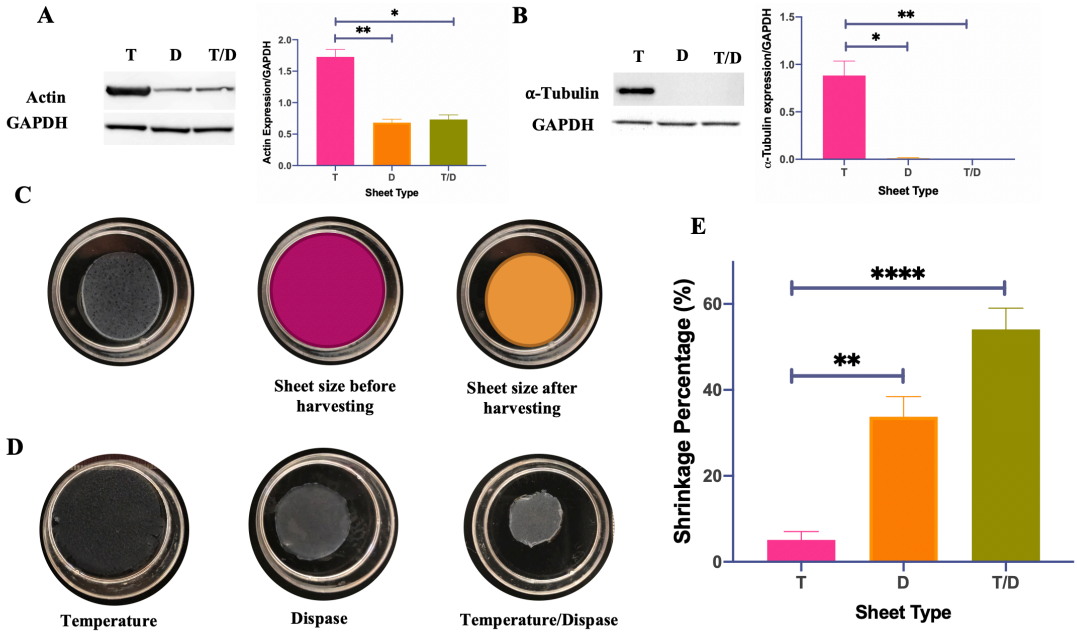

Figure 2.4: Cytoskeleton disruption and sheet shrinkage with Dispase treatment.

Measured cytoskeleton proteins in keratinocyte sheets using Western blotting with A) anti–actin antibody or B) anti–α-tubulin antibody, a significantly higher amount of actin and α-tubulin was detected in the sheets recovered by temperature reduction treatment compared to D-KS and T/D-KS. GAPDH was used as loading control. Error bars represent Mean±SEM (Kruskal-Wallis test with Dunn's multiple comparisons test, N=3) (*P<0.03, **P<0.002). C) Method used for measuring shrinkage percentage (SP), still images of KSs before and after detachment were photographed, and the size analysis of the cell sheets was calculated as SP= [(Sheet size before harvesting – Sheet size after harvesting) / Sheet surface size before harvesting] x 100. D) Representative images of sheet sizes for T-KS, D-KS and T/D-KS. E) Shrinkage percentage of cell sheets, the size of the T-KS was almost intact after detachment compared to pre-detachment size. However, the D-KS and T/D-KS sheets' sizes were significantly reduced after detachment using Dispase. Error bars represent Mean±SEM (Kruskal-Wallis test with Dunn's multiple comparisons test, N=4) (**P<0.002, ****P<0.0001).

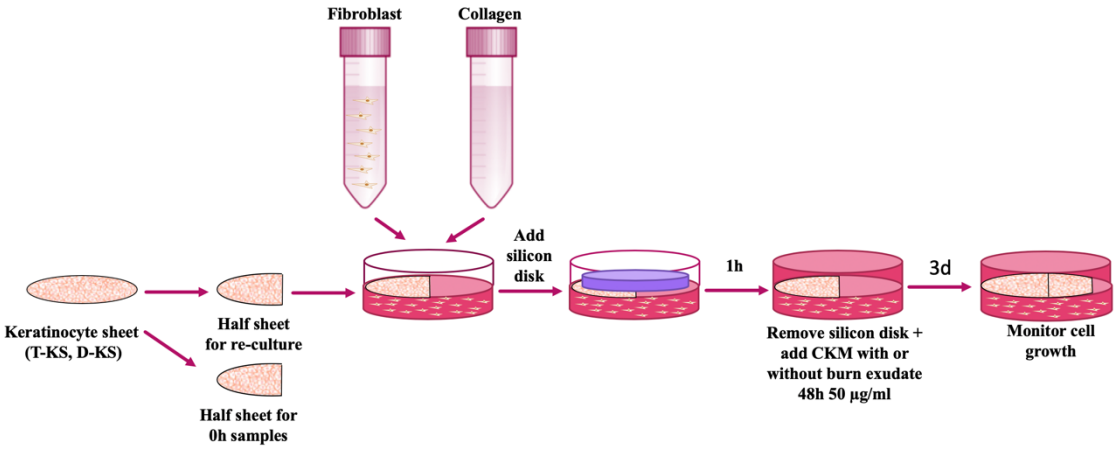

Figure 2.5: Schematic of *In vitro* skin burn wound healing model.

Burned skin wound healing model was modified from the *in vitro* skin model. After removing the silicon disk, CKM was added to the culture dish with and without burn exudate 50µg/ml from 48h collection time. Cells proliferation or migration from the edge of the sheets, was monitored daily for 3 days.

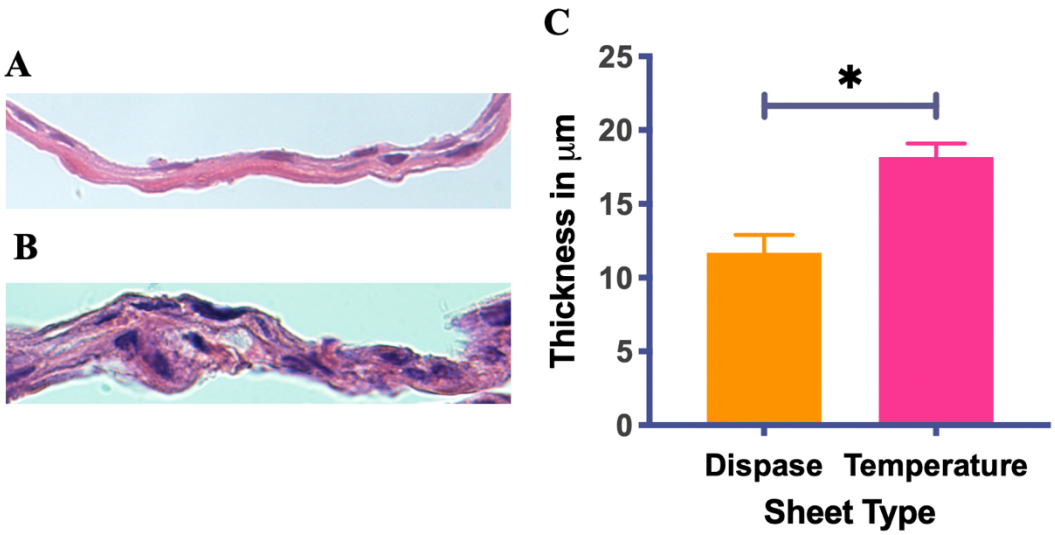

Figure 2.6: Keratinocyte sheet thickness.

Cultured sheep keratinocyte sheets A) T-KS and B) D-KS) were transferred to 10% formalin to be processed for FFPE. Histological sections were stained with Hematoxylin and Eosin. Images were cropped from 40x magnification image. C) The sheet thickness was semi-quantified using ImageJ software using line grid, there was a significant difference on the sheet thickness between the two types of sheets. Error bars represent Mean±SEM (Two-Tailed Paired t test, N=4) (*P<0.03).

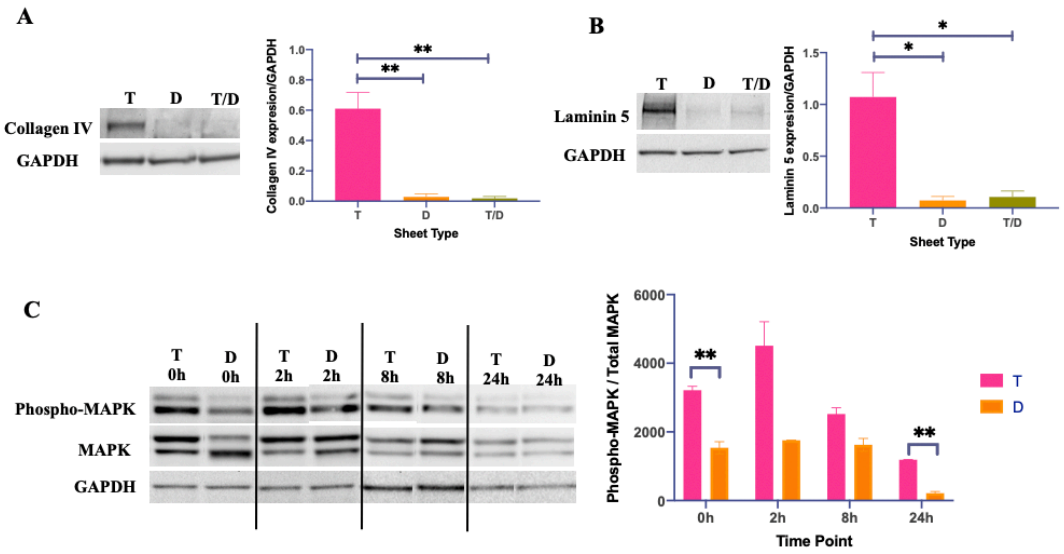

Figure 2.7: ECM preservation in T-KS and the activation of MAPK pathway.

Western blot analysis of A) anti–collagen IV antibody or B) anti–laminin 5 to recovered multilayered keratinocytes sheets (T-KS, D-KS, T/D-KS), both proteins were detected at the intact molecular size in cell lysates obtained by temperature reduction. However, with Dispase treatment (for D-KS and T/D-KS), the band was faintly detected. GAPDH acted as loading control. Error bars represent Mean±SEM (Kruskal-Wallis test with Dunn's multiple comparisons test, N=3) (*P<0.03, **P<0.002). C) Western blot analysis for phosphorylated MAPK in T-KC and D-KS before and after grafting onto the *in vitro* skin model for 2h, 8h, and 24h. The phosphorylated MAPK in KC sheets that were detached from TR or RD. Interestingly, phosphorylated MAPK was even detected in the both types of cell sheets (T-KS and D-KS) before being grafted on the substrates. However, the ratio of phospho-MAPK protein was always lower in the sheet detached by Dispase treatment compared with that detached by temperature reduction and significantly at 0h and 24h after grafting. GAPDH was used as loading control. Error bars represent Mean±SEM (Two-way ANOVA RM with Bonferroni's multiple comparison test, N=2) (*P<0.03, **P<0.002).

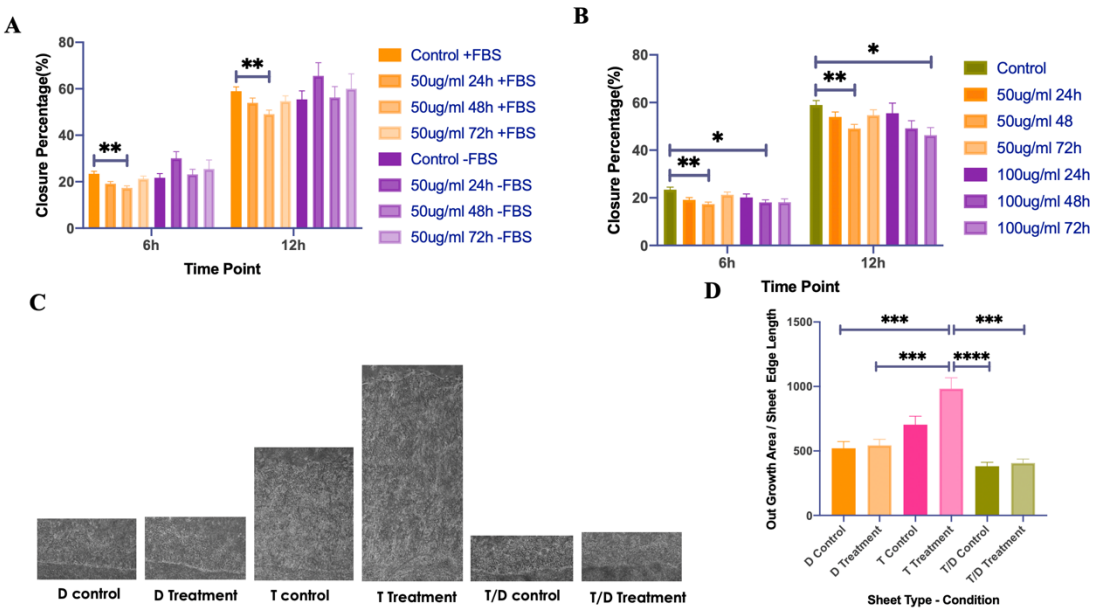

Figure 2.8: Using burn exudate in the *in vitro* burn wound healing model and acceleration of cell proliferation.

Sheep keratinocytes were seeded in 6 well plate prepared with feeder layer. Once the cells were confluent, a scratch was drawn in a confluent monolayer of sKC with a plastic disposable pipette tip. A) Cells were exposed to keratinocyte medium with or without FBS supplemented with different collection time points of BWE (24, 48 or 72h) at 50 µg/ml. The closure percentage cultured in medium added with BWE & FBS was decreased compared to control (+FBS, no BWE). The decrease was more pronounced with the burn exudate collected after 48 hrs after burn. Error bars represent Mean±SEM (Two-way ANOVA RM with Tukey's multiple comparison test, N=4) (**P<0.002). B) The cells were exposed to different concentrations of BWE (0, 50 or 100 µg/ml) from different collection time points of BWE (24, 48 or 72h) in CKM with FBS. The most decrease in closure percentage was observed in medium treated with 50 µg/ml BWE collected at 48 hrs compared to control. Error bars represent Mean±SEM (Two-way ANOVA RM with Tukey's multiple comparison test, N=4) (*P<0.03, **P<0.002). C) A pictorial record from day 3 after grafting cell sheet (T-KS, D-KS and T-KS) onto *in vitro* burn wound healing. D) The outgrowth from the edge of the cell sheet was quantified and normalized, the outgrowth area from the edge of the sheet was divided by the length of that sheet edge. T-KS had significantly higher rate of proliferation with or without burn exudate treatment compared to all the other groups (D-KS and T/D-KS). Error bars represent Mean±SEM (T Kruskal-Wallis test with Dunn's multiple comparisons test, N=at least 4) (***P<0.0002, (****P<0.0001).

AIM 2: TO INVESTIGATE THE EFFICACY OF KERATINOCYTE SHEETS DETACHED BY TEMPERATURE GRADIENT IN THE OVINE GRAFTED SKIN BURN MODEL WITH SPECIAL EMPHASIS ON ENGRAFTMENT AND WOUND CLOSURE

In this aim, the efficacy of T-KSs vs. D-KSs in healing of ovine burn wounds grafted with ovine cadaver skin were compared. To achieve these goals, we proposed the following sub aims:

Aim 2.1. Establish sheep cadaver skin bank (Chapter 3):

Effective and timely covering of the wounds is essential as it is correlated with a reduced scar formation, reduced mortality rate and improved physical performance [66, 71, 215]. In hospitals, cadaver skin is frequently used as a temporary cover (Fig. 3.1). To more closely mimic clinical practice, we have established the sheep cadaver skin bank. This was essential for temporary covering of burn wounds until the autologous KSs became available. To my knowledge, this study was the first to establish the ovine cadaver skin preparation method, and there is no study evaluating grafted burn wounds in sheep using cadaver skin.

Aim 2.2 Examine wound healing efficacy of cultured KSs in healing of burn wounds grafted with cadaver skin (Chapter 4):

To my knowledge, this is the first study examining the efficacy of T-KSs in a clinically relevant large animal model of grafted burn wound. There are only few previous studies reporting effectiveness of temperature gradient-detached KSs on full thickness wounds in rodent models. In these studies, the authors studied the healing of non-burn wounds without skin grafting [118, 133]. In the present study, we have tested efficacy of T-KSs in an ovine model of wound healing. Our well-characterized ovine model closely

mimics all aspects of clinical burn wound care, including early excision of burned tissues, allograft with cadaver skin, debridement of grafted cadaver skin epidermis after 3 weeks, and intermittent wound dressing changes [216]. Therefore, I believe that this study is highly translational to clinical practice.

CHAPTER 3

Aim 2.1: Establish ovine cadaver skin bank

INTRODUCTION

Timely covering the excised burn wounds is critical for prevention of infection, fluid loss and excess scar tissue formation to improve physical performance and survival of burn patients [66, 71, 215, 217]. When there is a limited source of autografts due to large burns, cadaver skin is frequently used in clinical practice as a temporary cover [216, 218, 219] (Fig 3.1). Cadaver skin helps in wound bed maturation by accelerating granulation and secreting necessary factors for wound healing [217, 220, 221]. It is used as a temporary cover (until enough donor skin sites become available [222]), because of immune conflicts that lead to its total rejection [220, 223].

Different methods are used for preparing cadaver skin. The most common method used is cryopreserving in DMSO or glycerol [224-226]. Also, storage at 4°C has been used for short time storage [225, 227-230]. Glyceropreservation with high concentration of glycerol is used to have non-viable allografts [230-234] . The allograft cryopreserved or stored at 4°C is viable. However, the viability rapidly decreased when stored at 4°C for long time. The viability of the allograft is important as it serves as dermis and further supports autologous graft acceptance and wound maturation [222]. Therefore, cryopreserving of allograft skin is essential.

Several animal models have been used to investigate immunological mechanisms of allograft rejection for development of new therapies to suppress immune responses [235-242]. Although some success has been achieved, there are a lot of unsatisfying problems

related to wound contractures in murine models [243, 244]. Porcine model is used for grafted wound healing studies [245]. However, pigs are challenging in handling and caring of wounds. Also, these animals require special dressing and grafts could be damaged because of rubbing the wound on the cage walls. All these limitations are associated with both intense labor and high cost [156]. There is need for a reliable and clinically relevant animal model to assess novel therapies to improve the healing process.

The aim of this study was to establish an ovine cadaver skin bank using a cryopreserving method. We will evaluate the method for cost and time-efficiency. We will test the prepared skin for viability before and after transplanting on ovine burn wounds. The ovine burn model we propose to use is reproducible, easy to maintain, and allows direct testing of new therapies or drugs.

To my knowledge, this study will be the first to describe the method for ovine cadaver skin preparation, and there is no study evaluating grafted burn wounds using cadaver skin in sheep. For this purpose, we followed and modified the same method used for collecting, processing, and cryopreserving human cadaver skin. Skin viability was tested by the MTT assay. Micro and macroscopic examination of the grafted wounds were performed to evaluate close resemblance to human wound healing aspects, including efficient coverage, intensity, and timing the rejection of grafted cadaver skin.

MATERIAL AND METHODS

Donor selection

Adult female ewes were selected for skin collection. Any sheep used for burn or sepsis studies were excluded. The skin collection was done in the necropsy room at the end of the study after other tissue samples were taken.

Skin collection site preparation

Skin collection site preparation and collection were done by two people: operator and assistant with an appropriate PPE. The cadaver sheep were placed on a table with the skin collection side up. The wool was trimmed using a clipper (KM2 Speed, WAHL), then the skin was washed with disinfectant solution (Antimicrobial foam solution with 4% CHG, BD E-Z Scrub). Utilizing disinfectant lather as a lubricant and a fresh disposable razor, residue wool was shaved. After complete shaving, the skin was washed generously with sterile water then with 70% ethanol. For further sterilization, the Skin Recovery Pack, containing 3 sterile prep foil trays, was used. Laparotomy sponges were soaked in Hibiclens (4% CHG, Molnlycke Health Care) (first tray) and the collection site was scrubbed in a circular motion. The disinfectant was allowed to remain on the body for at least 10 minutes. Then, with the sterile surgical gloves, the collection site was wiped with a sponge soaked in 70% alcohol (second tray) to remove disinfectant solution. These manipulations completed a primary disinfection procedure and the skin was ready for collection.

Cadaver skin (allograft) collection

The collection site was guarded with sterile drapes to prevent possible contamination from adjacent areas. Sterile 0.9% NaCl solution (Baxter) was injected sub-dermally using 60 ml syringe with a 16G needle to separate the skin from subcutaneous tissue (Sup. Fig. 3.1A). Using aseptic techniques, the skin collection was started on the posterior dorsum toward the anterior side (Sup. Fig. 3.1B, C) using a dermatome set to 3-inch width and 0.02-inch thickness. Tissue recovery was avoided from areas with abrasions or puncture wounds. Skin strips were placed in foil trays (third tray) with rinse solution (0.9% NaCl sterile solution) (Sup. Fig. 3.1D), the skin was transferred to sterile jar setting on wet ice containing RPMI

medium without antibiotics. Jars were labeled with sheep identification number, type of study, and collection date then stored at 4°C until process time.

Processing and disinfection of cadaver skin (allografts)

Under biological safety cabinets (BSC) and with appropriate protective clothing, a sterile surface was created to process and disinfect the cadaver skin. Three sterile foil container and sterile jars for the tissue were placed in the BSC (Sup. Fig. 3.2A). Collected cadaver skin was poured into the first sterile foil container. Using surgical gloves, skin was placed on a sterile cutting board and skin edges were trimmed and cut into pieces of size ranging from (1.5X2 inches) to (3 x 4 inches) by using scalpel (Sup. Fig. 3.2B). Skin pieces were then transferred to second sterile foil container filled with the Dakins Solution (Sodium hypochlorite 0.025%). Tissues were moved gently around and left to be soaked in solution for 2 min. Using forceps, tissues were gently picked up and Dakins Solution allowed to drain, then transferred into another sterile foil container and rinsed with 0.9 % Sodium Chloride. Tissues were aseptically removed from the 0.9% Sodium Chloride rinse solution and placed into sterile jar. An ample amount of RPMI media was poured in to cover the tissue and the jar was secured with lid. The jar was labeled (Sheep ID#, date of processing) and was placed in the refrigerator (+4°C) as fresh cadaver skin (collected, processed and disinfected but not cryopreserved).

Preservation of cadaver allografts

After the first round of disinfection, samples were processed and packaged within 24hrs for storage in frozen condition. For this purpose, the skin samples had undergone a

second round of disinfection in the exact same way that was done during first disinfection procedure described in section Processing and Disinfection of Cadaver Skin.

After the second disinfection procedure, the skin was placed in the sterile foil container with freezing medium (RPMI 1640 with 15% sterile glycerin "Sigma") and was soaked in about 10 min. Prepared skin was placed, dermal side up, on doubled 4 inches wide gauze (COVIDEN, Dermacea). Two to three pieces of skin were placed in one set of gauze with 1-inch distance, making sure that the length of gauze exceeds the actual length of skin (about 2 inches). The gauze with skin was rolled and returned to the freezing medium until packaging of all skin pieces was completed (Sup. Fig. 3.2D). Packaged tissues were removed from the bowl and excess medium from tissue was pressed out. The tissue was placed in 50 ml tubes labeled with sheep information, number of skin pieces, size of each piece and date of freezing. The tubes containing freezing skin were transferred to Styrofoam box with 2 inches thick wall and stored in -80°C until use. At this stage the skin was labeled as frozen cadaver skin (collected, processed, disinfected, and cryopreserved).

Thawing frozen cadaver skin and sample collection

The tubes with frozen cadaver skin was taken from -80°C and placed in 37°C water bath for 1 min. Then the rolled (in gauze) skin was removed from the tube under aseptic techniques (Sup. Fig. 3.3A) and thawed in bath with 37°C sterile 0.9% sodium chloride (Sup. Fig. 3.3B). The skin was washed from frozen medium twice in warm 0.9% sodium chloride. For the sample collection, skin was placed on a sterile cutting board with epidermis side up and samples were taken using a 10 mm punch biopsy (Acuderm) for different *in vitro* analyses (Sup. Fig. 3.3C).

Tissue preparation for histology and cadaver skin thickness measurement

To determine whether freezing affected the cadaver skin structure, three random skin samples (from 4 different skin collecting procedures) were taken from fresh and frozen cadaver skins for 10 and 40 days. Then the samples were fixed in 10% natural buffered formalin. Samples were processed according to standard protocols and embedded on the long axis for cross sectioning all the anatomical layers of the skin. Five-micron-thick sections were prepared for Hematoxylin & Eosin staining (Sup. Fig. 3.4A). Slides were observed by light microscope (Olympus BX51) and images were taken with 4x magnification. Images were analyzed using ImageJ software (version 1.52g) using a line grid with 722500 μm^2 area per point; whenever the grid touches the section a perpendicular line to the epidermis was measured (Sup. Fig. 3.4B). Also, epidermal vacuolization was determined using score system: 0 indicates no vacuolization; 1 indicates small areas of vacuolization (<10%); 2 indicates large areas of vacuolization (>10%; >50%); 3 indicates diffuse vacuolization (>50%).

Microbiological testing of cadaver skin

Microbiological screening was performed in random 3 samples (1 cm^2) from 3 different skin collection taken at 2 different stages: 1) after initial skin harvesting that had primary disinfection; and 2) after secondary disinfection. The skin samples were collected in a 120 ml sterile specimen container (Medegen Medical Product) containing sterile 0.9% sodium chloride and transported, on crushed ice, to the microbiology laboratory. Then under laminar air flow cabinet, the samples were transferred to BBL Enriched Thioglycollate medium tube (Becton, Dickinson and Company Sparks) and cultured at 37°C for 14 days were then screened for any microbial growth.

In microbiology laboratory, skin samples were transferred to Thioglycollate broth tube and cultured at 37°C for 14 days. After that, tubes were examined daily for visual evidence of growth (turbidity). In cases where microbial growth is detected, gram staining was performed, and samples were processed de pending on the culture condition i.e., aerobic or anaerobic culture.

Evaluation cadaver skin viability

The viability test was conducted to verify method used for preserving the cadaver skin. Several methods are used for assessing cadaver skin viability in skin banks and one of the most reliable and reproducible method is using MTT assay. The method is based on the reduction of water-soluble tetrazolium salts to insoluble formazan purple pigments by mitochondrial dehydrogenase. Six punch biopsies (10 mm) were taken from the fresh and frozen cadaver skin for 10 and 40 days. Samples were placed in 24 well plate and incubated in RPMI 1640 and MTT (3-(4,5-Dimethylthiazol-2-yl)-2,5-diphenyl- tetrazolium bromide, Sigma) 1mg/ml for three hours at 37°C, 5% CO_2 (Sup. Fig. 3.5A). After washing twice with PBS, the formed formazan (Sup. Fig. 3.5B) in the tissue was dissolved in 300 µl isopropanol/skin biopsy at room temperature for 1 hour (Sup. Fig. 3.5C). A 25µl of the dissolved formazan in isopropanol was diluted 4X in 96 well plate (3 wells/sample) and the optical density (OD) was quantified in a spectrophotometer (OD_{560}) (Sup. Fig. 3.5D). Negative controls were made by boiling the samples in distilled water for 30 min in the microwave. The viability percentage of the samples was expressed using the following formula: [(OD sample day 10 or 40 - OD negative control) ÷ (OD sample day 0 - OD negative control)] x100. Sample weight was not considered as the variation between the samples size was minimal and most of the activity is related to the epidermal layer. In order

to visualize which cells in the skin were mainly reducing MTT salts, we performed a histological examination in frozen skin samples after the MTT test. Frozen sections (thickness 6 μm) were cut and placed directly on a glass slide. The slides were air-dried for 2 hrs and then observed by light microscopy.

Cell proliferation assessment

To evaluate whether keratinocytes proliferate in fresh and frozen cadaver skin, skin samples were placed in 24 well plate and incubated with 50 μM of bromodeoxyuridine (BrdU, Sigma–Aldrich) in RPMI 1640 (HyClone) at 37°C, 5% CO_2 for 24 h before fixation and processing for paraffin embedding. The distribution of BrdU-positive cells in cadaver skin was detected by immunohistochemical method. The sections were deparaffinized and rehydrated and the antigens were retrieved using a steamer with Antigen Retrieval Citra Plus Solution (Biogenex Laboratories) for 20 minutes. DNA denaturation was processed by incubating the sections in 2N HCL for 60 minutes at 37°C then neutralized in 0.1M Borate buffer for 10 minutes. Then the sections were incubated in a blocking solution containing 10% normal goat serum in TBS-T for 1 hour at room temperature. The samples were immunostained with primary rat anti-BrdU antibody conjugated with FITC (ab74545, Abcam, 1:200) diluted with 1% BSA and 1% NGS in TBS-T overnight in the dark at 4°C. The next day, slides were washed, and cover slipped with DAPI mounting medium (Vector Laboratory, Vectashield). Slides were viewed under a florescent microscope and evaluations were performed blindly by counting the total number of BrdU positive cells on the epidermis (surface epidermis or invaginated epidermis in the dermis around hair follicles) then divided over the total section area. The percentage of BrdU+ cells was

calculated by considering day 0 as a 100% and then calculate the percentage of day 10 and 40 as follows:

The percentage of BrdU+ cells= (Number of positive cells/μm2 at day 10 or 40 ÷ Number of positive cells/μm2 at day 0) X 100

Growth factors quantification

Biopsies (10 mm) from fresh and frozen cadaver skin for 10 or 40 days, each gathered from 3 different skin collection, were cut into small pieces and extracted in 200 μl T-PER tissue protein extraction reagent (Thermo Scientific). The samples were extracted in a tissue homogenizer (Pro Scientific Bio-Gen PRO200 Homogenizer) for 30 seconds 3 times with 1 min cooling on ice, followed by gentle shaking for 22 hours at -4°C. Digested samples were centrifuged at 12000 g for 15 min at 4°C. The supernatants were recovered and stored at -80°C for analysis using Western blot. Transforming growth factor beta (TGF-β) was measured as a representative for the level of the growth factors on the fresh or frozen cadaver skin. Protein samples (50 μg) were mixed with NuPAGE LDS sample buffer and NuPAGE sample reducing agent (Invetrogen) and heated for 10 min at 70°C, and then separated through NuPAGE™ 4-12% Bis-Tris Protein Gels (Invitrogen). After electrophoresis, proteins were transferred to PVDF membranes by using an iBlot Dry Blotting system (Invitrogen). Membranes were blocked in 3% BSA in TBS-T (1 hr), rinsed and incubated with mouse anti-TGFβ1 primary antibody (diluted at 1:500) in blocking buffer at 4°C overnight. Primary antibody was then removed by washing in TBS-T thrice and labelled by incubating with HRP-labelled secondary antibodies (1:1000) against mouse for 1 hr at room temperature. Membrane was washed thrice in TBS-T and visualized using

Pierce ECL Western Blotting Substrate (Thermo Scientific) and exposed to the emitted light is captured on CCD camera using G Box imaging system (Syngene) with GeneSnap Software (Syngene, Version 7.09). Results were calculated by imageJ software and expressed as ratios to β-actin protein as the loading control.

***In vivo* assessment of cadaver skin on burn wounds**

The experiment timeline is detailed in (Fig. 3.2). Briefly, third degree burn wounds on three locations was induced on the sheep dorsum, that was excised the next day. After excision, wounds were allocated randomly to one of the following groups: 1) covered with fresh allograft cadaver skin, 2) covered with frozen allograft cadaver skin that frozen for an average of 17 months, or 3) covered with autograft skin (Fig 3.3). Skin punch biopsies at 10mm were collected after 7, 14, and 20 days of grafting. Skin samples were fixed, processed, and stained with H&E. Skin biopsies were assessed based on the criteria shown in (Table 3.1). Also, a pictorial record was taken at day 7, 14, and 20 after grafting to assess graft rejection rate.

Statistical analysis:

All data were analyzed using Prism GraphPad version 8.1.0 (GraphPad software, Inc.). All quantitative data were expressed as means ± standard error of the mean. Comparisons between groups (fresh cadaver skin and frozen for 10 or 40 days) were made using the Kruskal Wallis with the Dunn post hoc test for pairwise comparisons. Comparisons between different grafts at different time points were made using two-way ANOVA RM with Sidak's multiple comparison test. Quantitative variations were considered significant when the P value was ≤ 0.05.

RESULTS

Histological analysis and cadaver skin thickness

Histological observation of fresh and 10 or 40 day cryopreserved skin samples showed no sign of gross damage, dermal cavitation or stratum corneum fragmentation (Fig. 3.4A-C). There was an incremental epidermal vacuolation noted with increasing freezing period (Fig. 3.4D, E). The disruption of collagen fibers was consistent in all samples, including fresh skin. There was no significant difference in the thickness between fresh cadaver skin or cadaver skin frozen for 10 or 40 days (Fig. 3.4F). The dermal-epidermal junction was generally, on the whole, intact.

Microbiological evaluation of cadaver skin

No bacterial growth was detected in skin samples (fresh, and frozen for 10 and 40 days) cultured in broth for 14 days.

Evaluation cadaver skin viability

Fresh skin viability was considered as 100% for normalization of viability of cryopreserved skins for 10 or 40 days. The viability of frozen cadaver skin gradually declined over time. After 10 days of freezing, the viability percentage varied from 59.32% to 94.20% (average of 72.17±7.61%), while it was 53.43–86.23 % after 40 days of freezing (average of 67.87±6.88%) (Fig. 3.5A). The viability was reduced by 28 % in 10-day frozen skin compared to fresh skin viability, while there was only 4% difference between 10-day and 40-day frozen skins. Histological examination performed after the MTT test showed pigmentation in the epidermal and dermal layer, thus confirming the contribution of keratinocytes and fibroblasts in the MTT viability assay (Fig. 3.5B).

Cell proliferation assessment

Skin samples were incubated in medium containing BrdU for 24 hrs prior to fixation to test the proliferative capacity of keratinocytes and the number of positive keratinocytes per μm was counted (Fig. 3.6A-C). Proliferation capacity significantly decreased after 40 days of freezing compared to fresh and cadaver skin frozen for 10 days. No differences were found between fresh cadaver skin and frozen cadaver skin for 10 days (Fig. 3.6D).

Growth Factor Quantification

To examine the protein levels of growth factors in fresh and frozen cadaver skin, we performed Western blot analysis for TGF-β1 in the protein isolated from fresh cadaver skin or frozen for 10 and 40 days. The TGF-B1 levels were comparable in all types of skin samples, suggesting that the level of TGF-β1 was not affected by the freezing for extended time period (Fig. 3.7).

Macroscopic and microscopic evaluation for grafted sheep cadaver skin

Macroscopic evaluation revealed normal autograft color during the study time period with no signs of rejection. The allografts turned to a pink whitish color at 7 days and started to be rejected at day 10. There was a slight delay for frozen cadaver skin rejection compared to frozen skin. However, after 3 weeks, both the fresh and frozen cadaver skin were completely rejected, enabling subsequent grafting (Figure 3.8). The wound overlaid with autograft healed completely.

Histological sections were performed in skin biopsies taken at day 7 (Figure 3.9 A, D, G), day 14 (Figure 3.9B, E, H) and day 20 (Figure 3.9C, F, I) after transplanting of

autograft, fresh or frozen allografts to excised wounds after 3rd degree burns. Fresh or frozen cadaver skin showed some signs of rejection with presence of vacuoles (arrow) on the epidermis after 7 days of grafting. At day 14, the epidermis was mostly rejected, and the dermis was highly vascularized (circle). After 20 days, 100% epidermis rejection was observed in both types of grafted skins. While there were no signs of rejection found in autografted skin at all indicated time points.

Histopathological evaluation for ulceration, inflammation, hemorrhage and neovascularization was compared in wounds covered with fresh or frozen cadaver skin vs. autografted wounds (Fig. 3.10). Primary histopathological analysis showed that ulceration, inflammation, and hemorrhage scores were significantly higher in wounds covered with fresh cadaver skin at days 14 and 20 compared to control. Neovascularization rate was significantly higher in wounds grafted with fresh cadaver skin compared to the autograft on day 14, while ulceration was significantly higher at day 20 on wounds grafted with frozen cadaver skin compared to autograft.

DISCUSSION

Wound closure is the ultimate goal for treating burn patients. The use of autograft is an ideal option for successful achievement of the goal. However, the availability of autografts often does not match the need. Therefore, the need for finding an alternative method is enormous. Using cadaver skin allograft was first tested in burn wounds in 1881 [246]. Since then, the grafting techniques including skin harvesting, treating, storing, and evaluating preserved skin were improved. Currently, skin allograft is used as a standard method for temporary covering of burn wounds. With increased demands for allografts, skin banks were established at several institutions [246].

Castagnoli *et al*. showed that specimens preserved at 4 °C showed a similar pattern at days 3, 5 and 7 with no signs of tissue damage. However, the tissue architecture was seen to be modified at day 15 with separation between epidermis and dermis and vacuolated cells [247]. Our histological analysis of cadaver skin before being grafted confirmed the validity of the cryopreservation methods: there were no signs of histological alterations due to freezing, such as epidermal-dermal junction separation, dermal cavitation or fragmentation of collagen fibers, and slight increase in epidermal vacuolation. Our data are consistent with previously published work by Castagnoli *et al*. [247]. To note, Wood et al. showed that different preservation methods (i.e., Glycerol, cryopreserved without DMSO or cryopreserved with DMSO) resulted in damage to the tissue structure compared to fresh skin (processed but not frozen) [248]. However, in our studies ovine cadaver skin thickness didn't seem to be affected with the freezing method and this was supported by previous published data [248].

Sheep possess a mixed population of bacteria and fungi that live primarily in their skin [249]. Unfortunately, collected viable skin cannot be sterilized, which increases the risk of disease transmission when grafted onto the excised burn wounds [250]. With no proper disinfection, non-pathogen bacteria can grow during the storage period to reach massive population densities that can damage the skin [250]. Therefore, it is important to eliminate microbial population even before skin harvesting. Britton-Byrd et al. analyzed 735 donated skin cultured for 7 days and reported that only one had positive cultures post 3 days [251]. Consequently, they concluded that 3 days of microbiologic cultures are as safe as 7 days of cultures [251]. On the other hand, Pirnay et al. observed that 64% of these culture positives only appeared post 8 days of incubation [252]. In this work, we adopted

the method of microbiological screening for cryopreserved skin allografts for 14 days in enrichment broth cultures of freshly collected skin as well as processed samples just before freezing. Our results showed negative cultures after collection and after processing which indicated that our disinfection method was acceptable.

There is still an ongoing debate on the significance of cell viability in allografts. Some practitioners prefer a non-viable skin because of longer storage and low cost. Non-viable cadaver skin can be stored at room temperature versus storage in liquid nitrogen for cryopreserved cadaver skin. However, Cryopreserved viable skin allograft is accepted to be superior to other dermal substitutes, and higher viability is associated with better wound bed preparation and final graft acceptance [224, 226, 247, 253, 254]. We have performed MTT assay to evaluate the quality of ovine cadaver skin prepared and stored at our laboratory. Our data indicated moderate decrease in viability of frozen skin overtime. An interesting finding was that there was no difference (4%) between viability in skins frozen 10 and 40 days, suggesting that longer storage in frozen conditions (-80°C) does not negatively affect viability of preserved skins. The percentage cell viability maintained after 10 and 40 days of cryopreservation of sheep cadaver skin appears to be in agreement with published data from human skin banks. Franchini et al. showed that the average of cadaver skin viability percentage after 10 days of cryopreserving using DMSO was 45.09 ± 20.11% [226], while Cleland at al. documented 18 and 26% viability compared to freshly isolated skin [254]. To note the viability of frozen ovine cadaver skins in our laboratory was 72.17±7.61% and 67.87±6.88% at 10 and 40 days respectively, where we immediately processed the skin with a short pre-freezing time. Previous studies reported that prompt

processing and less pre-freezing period positively affects cell survival in preserved skins [247, 255-257].

Several studies showed human allograft preserved in anhydric sodium chloride was accepted after been grafted in mice with severe combined immunodeficiency disease (SCID). In these studies, the authors also reported intensive incorporation of BrdU and presence of proliferative cell nuclear antigen in basal keratinocytes [258, 259]. On the other hand, Boekema et al. previously found that the capability to proliferate using BrdU incorporation in the basal layer did not differ between different storage media (saline, DMEM/F12 or RPMI) in a skin sample stored for 3 days at 4 °C [260]. In our study we employed this technique to identify the capacity of cadaver skin cells to proliferate before and after cryopreservation. Proliferation capacity significantly decreased after 40 days of freezing compared to fresh and cadaver skin frozen for 10 days. No differences were found between fresh cadaver skin and frozen cadaver skin for 10 days.

Cadaver skin not only works as a temporary cover, but also secrets the necessary factors for wound healing. TGF-β is among other potent angiogenic factors in wound healing [261]. TGF-β regulates cell migration, capillary tubule formation, and ECM deposition [261, 262]. In the current study, TGF-β were found to be statistically comparable between fresh and frozen cadaver skin for 10 and 40 days. There is no significant increase of TGF level, which can be explained by the sample processing occurring on the distinguished time points. However, samples were frozen until the Western blot run where all samples were loaded in the gel at the same time. The freezing time for fresh cadaver skin samples after proteins isolating was longer than the frozen time

for frozen cadaver skin for 40 days. Preserving TGF-β level on preserved cadaver skin promises a better wound healing after applying cadaver skin.

In vivo, viable human skin allograft are revascularized after their grafting and then rejected between 2 and 4 weeks later [263]. Our results indicated that graft rejection occurred the soonest with fresh skin allografts, followed by cryopreserved allografts. Our results agree with those in the literature with delay in rejection rate in cryopreserved skin allograft compared to fresh skin allograft [263]. However, previous data showed that despite the significant difference in the rejection rate between fresh and frozen skin allograft, there was no significant difference in the healing delay found between these two groups [263]. Our macroscopic evaluation at day 7 did not reveal any differences, while histological analysis revealed significant differences in epidermal vacuolization, which was consistent to results described in the literature [264, 265]. The rejection seen in fresh skin allografts can be attributed to a direct mechanism involving the transfer of donor dendritic cells to the recipient [263, 266]. Langerhans cells became impaired as a result of the cryopreservation process, which may explain the delayed rejection seen in the cryopreserved skin [267]. Several studies have been reported to the successful use of immunosuppressor therapy for treating large burn patients [65, 268, 269]. However, in clinical practice long-term immunosuppressor therapy cannot be induced in severely burned patients. Therefore, having less immunogenic skin with cryopreservation is critical to reduce the time and the number of allografts in severely burned patients.

This study is associated with some limitations, such as use of cadaver skin frozen with an average frozen time of 17 months. We have demonstrated the viability of cadaver skin does not significantly affected by freezing time and method. Additionally, the cadaver

skin used in clinical practice are stored frozen for a few years. Further research is needed comparing efficacy of fresh or frozen (for various time period) cadaver skin vs. various dermal substitutes wound bed preparation for subsequent autografting.

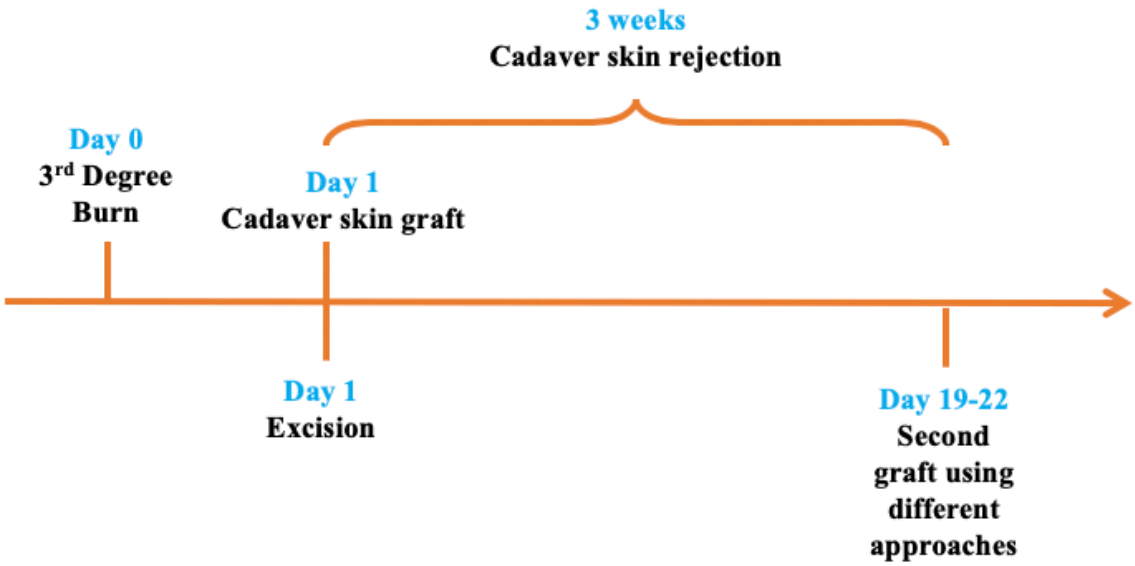

Figure 3.1: Schematic of clinical burn wound care.

After 3rd degree burn, timely covering the excised burn wounds is critical. When there is a limited source of autografts due to large burns, cadaver skin is frequently used in clinical practice as a temporary cover until enough donor skin sites become available. Cadaver skin is eventually rejected within 3 weeks because of immune conflicts.

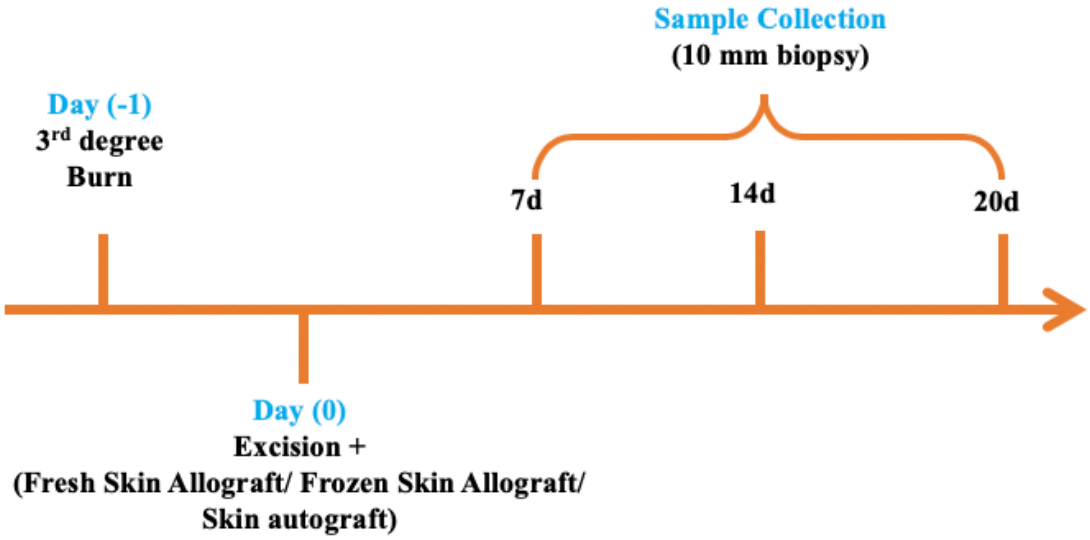

Figure 3.2: Schematic of *in vivo* grafting of ovine cadaver skin onto 3rd degree excised burn wounds.

Third degree burn wounds were induced on the sheep dorsum, that was excised next day and wounds were allocated randomly to one of the following groups: 1) covered with fresh allograft cadaver skin, 2) covered with frozen allograft cadaver skin, and 3) covered with autograft skin. Skin punch biopsies at 10mm were collected after 7, 14, and 20 days of grafting for histological evaluation.

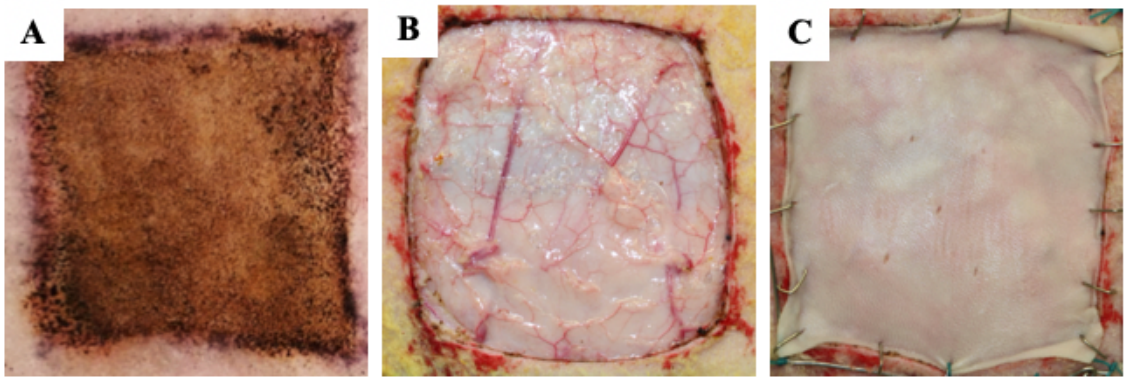

Figure 3.3: *In vivo* transplantation of cadaver skin over excised third degree burn wound.

A) A third degree burn wound (5 cm^2). B) Excised burn wound after removing all the dead and necrotic tissue. C) Grafted cadaver skin and stabilized using a surgical stapler.

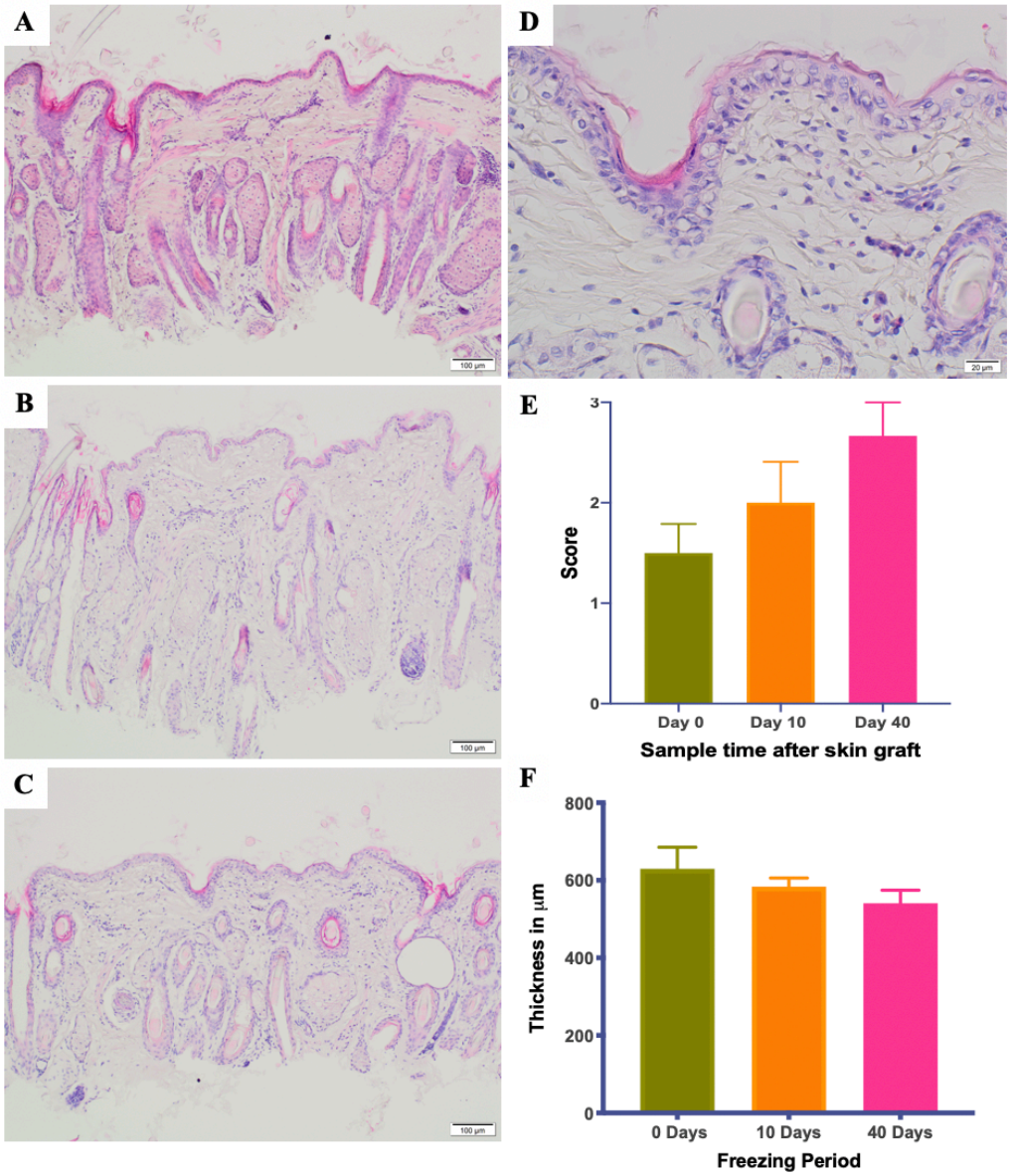

Figure 3.4: Histopathological evaluation of cadaver skin.

H&E staining for cadaver skin A) fresh, B) frozen for 10 days or C) frozen for 40 days. Histological observation showed no sign of gross damage, dermal cavitation or stratum corneum fragmentation. Scale bar 100 µm. D) There was an incremental epidermal vacuolation noted with increasing freezing period. Scale bar 20 µm. E) The epidermal vacuolization was determined using score system: 0 indicates no vacuolization; 1 indicates small areas of vacuolization (<10%); 2 indicates large areas of vacuolization (>10%; >50%); 3 indicates diffuse vacuolization (>50%). Error bars represent Mean±SEM (Kruskal-Wallis test with Dunn's multiple comparisons test, N=3). F) Cadaver skin thickness. There was no significant difference in the thickness between fresh cadaver skin or cadaver skin frozen for 10 or 40 days. Error bars represent Mean±SEM (Kruskal-Wallis test with Dunn's multiple comparisons test, N=4).

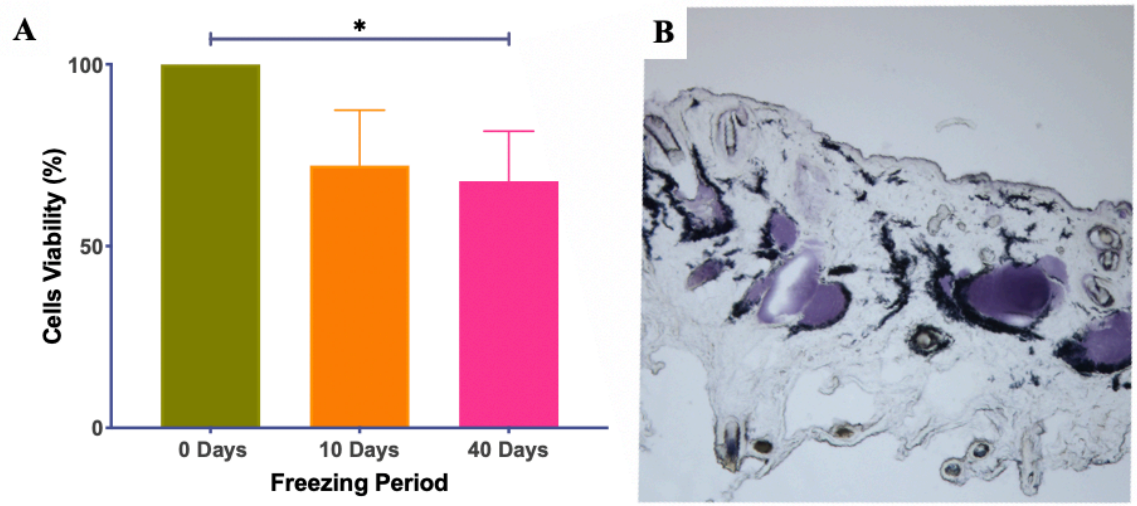

Figure 3.5: Evaluation of cadaver skin viability.

A) Viability of fresh and cryopreserved skins for 10 or 40 days. Fresh skin viability was considered as 100% for normalization. The viability of frozen cadaver skin gradually declined over time. Error bars represent Mean±SEM (Kruskal-Wallis test with Dunn's multiple comparisons test, N=3) (*P<0.03). B) Histological examination in frozen skin samples after the MTT test. Frozen sections were cut and placed directly on a glass slide and observed by light microscopy. Pigmentation in the epidermal and dermal layer was observed in keratinocytes and fibroblasts.

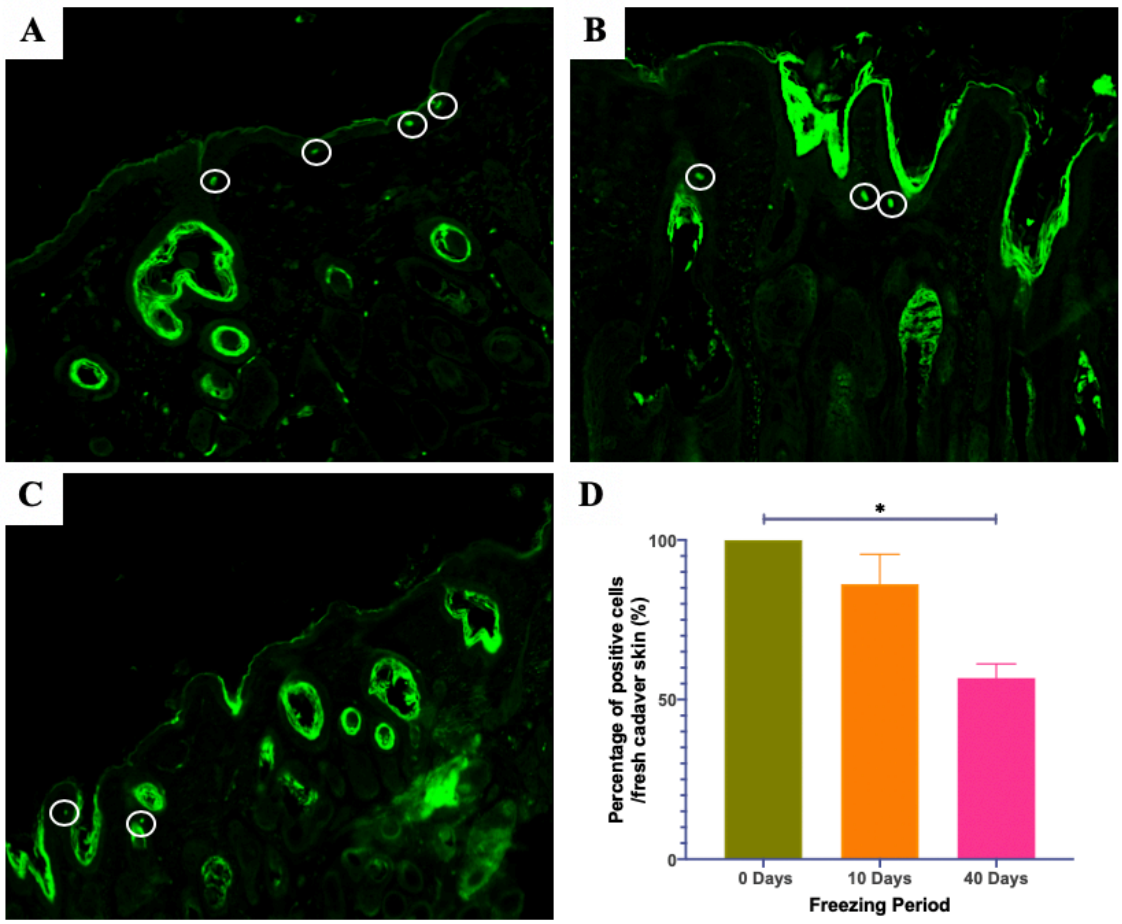

Figure 3.6: Cell proliferation assessment.

Skin samples were incubated in medium containing BrdU for 24 h prior to fixation to test the proliferative capacity of keratinocytes. The distribution of BrdU-positive cells in cadaver skin was detected by immunohistochemical method and the number of positive keratinocytes (White circles) per µm was counted in A) fresh cadaver skin, B) frozen cadaver skin for 10 days, C) frozen cadaver skin for 40 days. Images were taken at a 20x magnification. D) The percentage of BrdU+ cells was calculated by considering day 0 as a 100% and then calculated the percentage of day 10 and 40 as follows= (Number of positive cells/µm2 at day 10 or 40 ÷ Number of positive cells/µm2 at day 0) X 100. Proliferation capacity significantly decreased after 40 days of freezing compared to fresh and cadaver skin frozen for 10 days. No differences were found between fresh cadaver skin and frozen cadaver skin for 10 days. Error bars represent Mean±SEM (Kruskal-Wallis test with Dunn's multiple comparisons test, N=3) (*P<0.03).

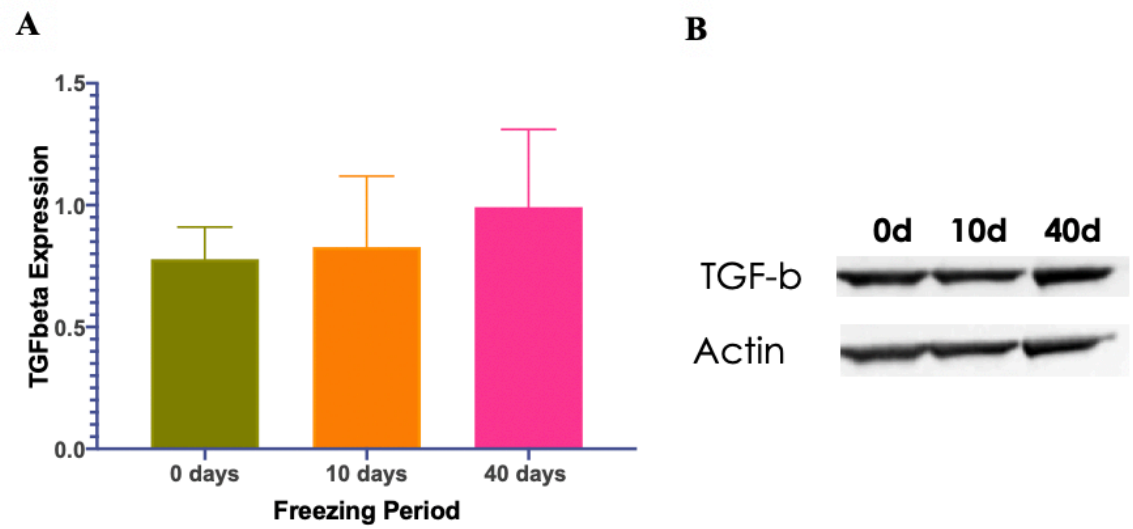

Figure 3.7: TGF-β level in fresh or frozen cadaver skin for 10 or 40 days.

Western blot analysis of anti– TGF-β antibody for fresh or frozen cadaver skin for 10 or 40 days. The TGF-B1 levels were comparable in all types of skin samples, suggesting that the level of TGF-β1 was not affected by the freezing for an extended time period. Error bars represent Mean±SEM (Kruskal-Wallis test with Dunn's multiple comparisons test, N=3).

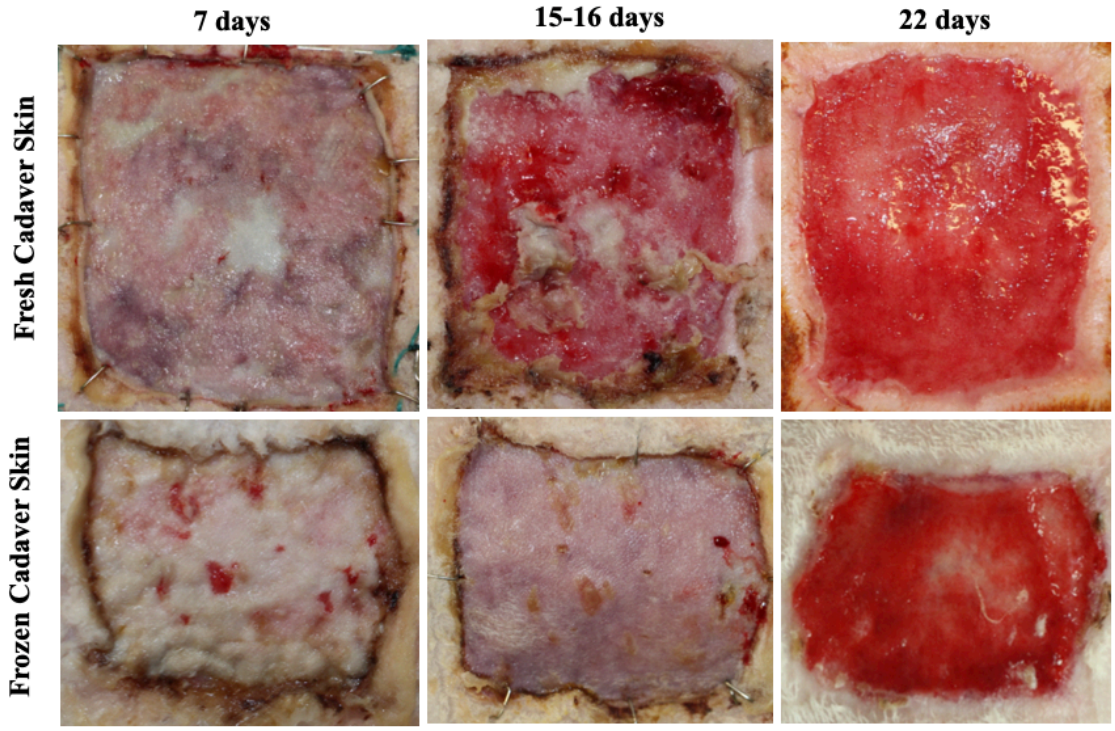

Figure 3.8: Cadaver skin rejection.

The allografts turned to a pink whitish color at 7 days and started to be rejected at day 10. There was a slight delay for frozen cadaver skin rejection compared to fresh skins. However, after 3 weeks, both the fresh and frozen cadaver skins were completely rejected, enabling subsequent grafting.

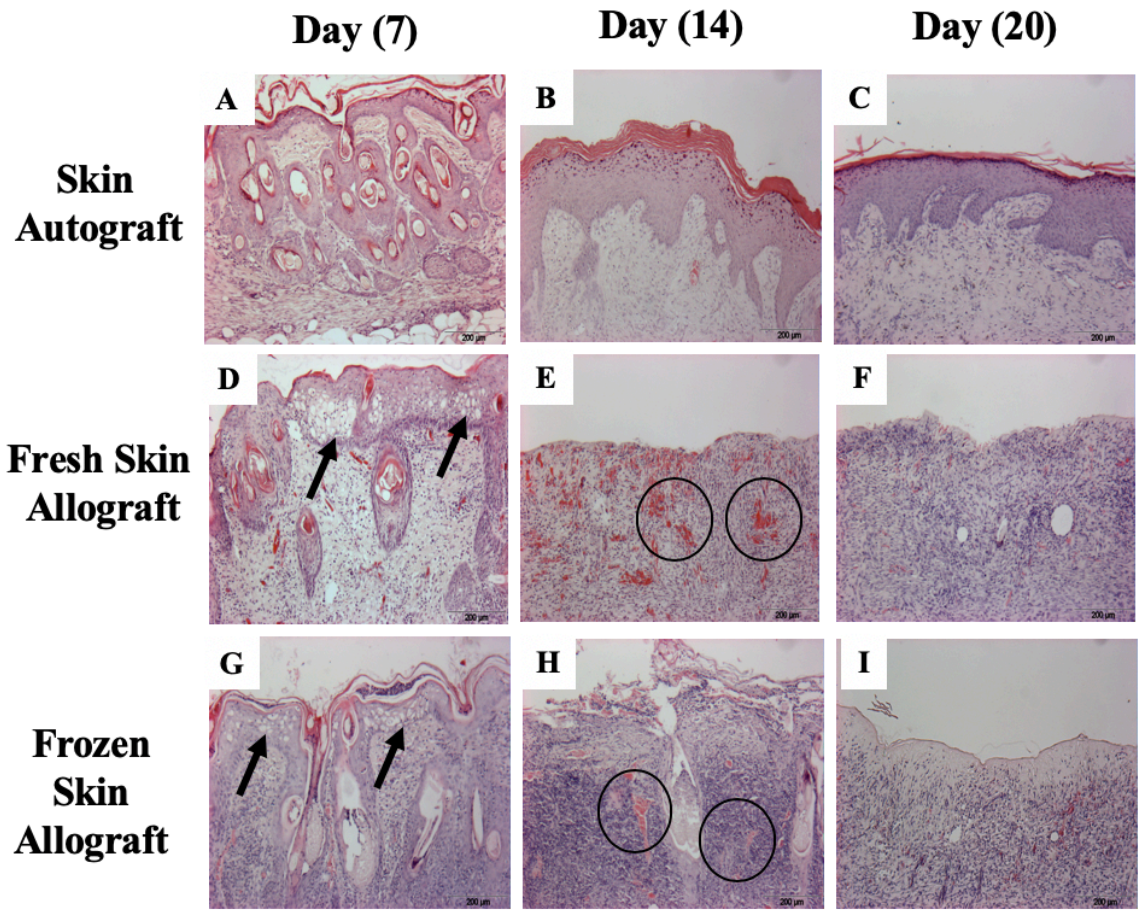

Figure 3.9: Histological evaluation for skin samples collected after 7, 14 and 20 day of autograft, fresh allograft, and frozen allograft.

Histological sections were performed in skin biopsies taken after transplanting of autografts (A-C) , fresh (D-F) or frozen allografts (G-I) to excised wounds after 3rd degree burn at day 7, 14 and 20. Fresh or frozen cadaver skin showed some signs of rejection with presence of vacuoles (arrow) on the epidermis after 7 days of grafting. At day 14, the epidermis was mostly rejected, and the dermis was highly vascularized (circle). After 20 days, 100% epidermis rejection was observed in both types of grafted skins. While there were no signs of rejection found in autografted skin at all at indicated time points.

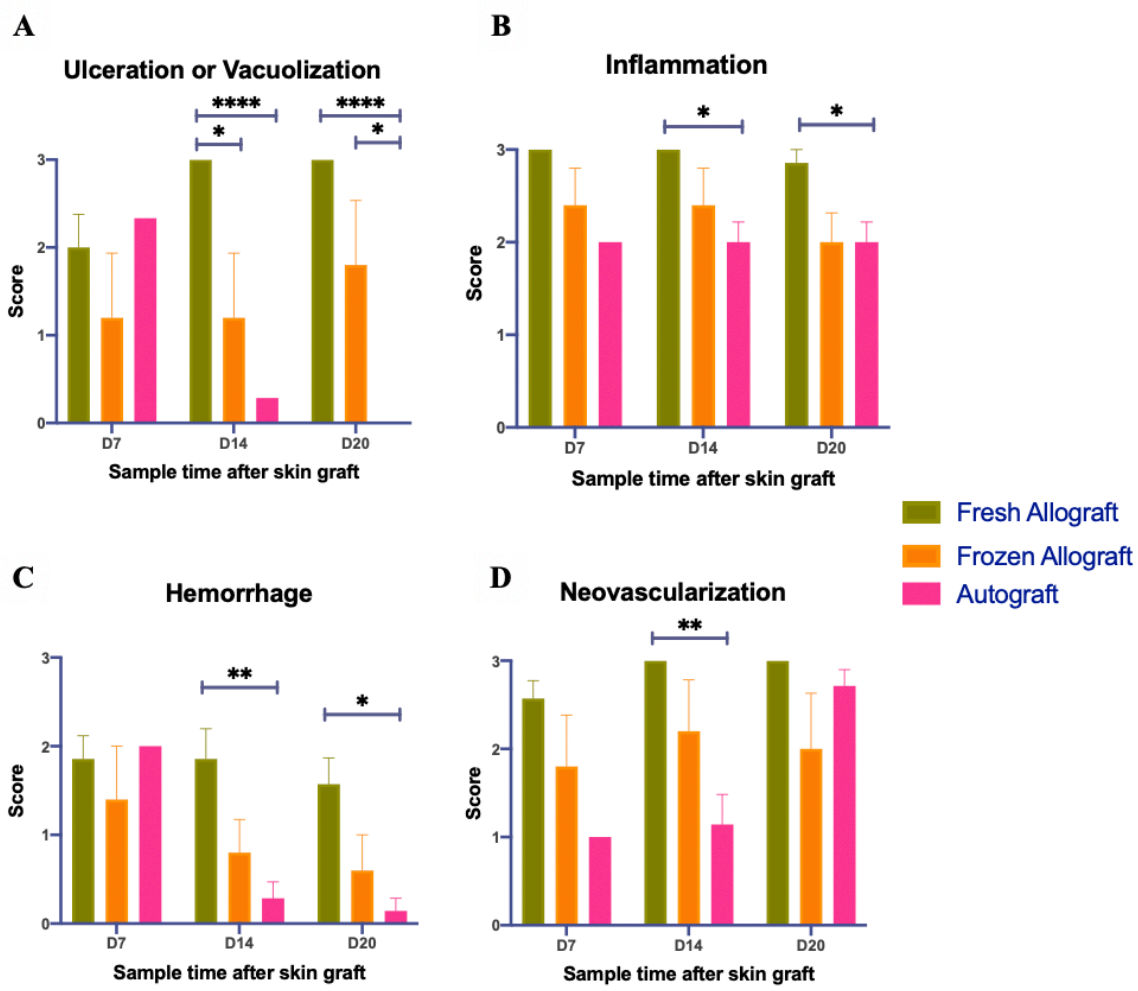

Figure 3.10: Histopathological evaluation of skin samples collected after autograft, fresh allograft, frozen allograft.

Histopathological evaluation for A) ulceration, B) inflammation, C) hemorrhage and D) neovascularization was compared in wounds covered with fresh or frozen cadaver skin vs. autografted wounds. Primary histopathological analysis showed that ulceration, inflammation, and hemorrhage scores were significantly higher in wounds covered with fresh cadaver skin at days 14 and 20 compared to control. Neovascularization rate was significantly higher in wounds grafted with fresh cadaver skin compared to the autograft on day 14, while ulceration was significantly higher at day 20 on wounds grafted with frozen cadaver skin compared to autograft. Error bars represent Mean ± SEM (Two-way ANOVA with Sidak's multiple comparison test, N=3) (*P<0.03; **P<0.002, ****P<0.0001).

	0	1	2	3
Ulceration/ vacuolization (Vac.)	No ulceration/ Vac.	Vac. without separation	Vac. with separation	ulceration
Inflammation	< 10% inflammatory cells	Between 10% - 50%	More than 50%	diffuse inflammation
Hemorrhage	no hemorrhage	small areas of hemorrhage	large areas of hemorrhage	diffuse hemorrhage
Neovascularization (NV)	no NV	up to 5 vessels	Between 5-10 vessels	More than 10 vessels

Table 3.1: Assessment criteria for evaluating skin samples taken after grafting cadaver skin.

Skin samples were fixed, processed, and stained with H&E. Skin biopsies were assessed based on these criteria for ulceration/vacuolization, inflammation, hemorrhage and neovascularization.

CHAPTER 4

Aim 2.1: Examine wound healing efficacy of cultured KSs in healing of burn wounds grafted with cadaver skin

INTRODUCTION

The ultimate outcome of treating burn patients depends on early wound excision and closure. Early wound management is essential for limiting infections and fluid loss, which reduce hospital stay, mortality rate, and hypertrophic scar formation [96, 109, 270]. Using split thickness autologous skin graft is considered to be a gold standard for wound closure after burn wound excision [271]. However, patients with burns exceeding 40% total body surface area (TBSA) suffered from a shortage of donor sites and a delay in wound closure [272]. These limitations have pushed researchers to find alternative methods to substitute autologous skin to achieve rapid healing [271].

One of the alternative methods is using autologous cultured and expanded keratinocytes from a small skin biopsy as cell sheets to replace skin epidermis [96, 107, 273]. This method was introduced over 30 years ago for treatment of burn wounds. Unfortunately, this exciting technology was never translated to clinical practice because of disadvantages, such as inconsistency and unpredictability of engraftment, incidence of infection, spontaneous blistering, and scar contractures [94, 107, 274]. The reason for these negative results is the use of enzyme so called Dispase for detachment of KSs from the culture dishes [115, 119, 275]. The enzymatic treatment using Dispase has been shown to negatively affect cell membrane by cleaving various membrane-associated proteins and extracellular matrix (ECM), thus compromising cell functions [89, 116, 117, 186, 275].

Recently, a new method was introduced by using temperature responsive dishes that do not require any enzymatic treatment for cell detachment [89]. These dishes are coated with polymer that is thermal responsive. At 37°C, the surface is hydrophobic enabling the cells to be attached to that dish surface and proliferate to confluence. With the reduction of temperature to a room temperature (~20°C), the surface becomes hydrophilic which rapidly hydrates the dish surface resulting in a spontaneous KSs detachment without using any enzymes [126, 127]. This approach has been used to fabricate several cell sheets like corneal epithelial [276, 277], oral epithelial [276, 278], esophageal mucosal [279], nasal epithelial cells [280, 281], as well as cardiomyocytes [282], hepatocytes [147], islet cells [283] and thyroid cells [148]. Currently, there are some ongoing clinical trials testing efficacy of certain cell sheets including nasal epithelial sheets and oral mucosal epithelial sheets [140, 152, 281].

In this study we wanted to investigate the efficacy of keratinocyte sheets detached from temperature responsive dishes using temperature reduction on third degree burn wounds and comparing it with wounds grafted with keratinocyte sheets detached by enzymatic treatment using Dispase. We employed our ovine model to enhance the translational aspect of the study. Our goal is to provide evidence to improve the current clinical practice for treating third degree burn wounds using autologous cultured keratinocyte sheets.

MATERIAL AND METHODS

Experimental design

The experiment timeline is shown in Fig. 4.1A. Several full-thickness burn wounds (5x5 cm^2) were induced at the dorsum of the sheep (Day -1) (Fig. 4.1B) (Sup. Fig 4.1A-

C). After 24 hours (Day 0), burned skin was excised to the fascia (Sup. Fig 4.1D). Immediately after the excision of burned skin, a square-shaped metal splint with a 5 cm diameter was centered on the wound injury and fixed to the skin using nylon sutures. Then, wounds were covered with fresh ovine cadaver skin that has been previously prepared using methods similar to that used for preparing human cadaver skin (Described in chapter 3). After the engraftment, the wounds were managed mimicking care provided in burn centers. After three weeks, (Day 19-22) when grafted cadaver allograft epidermis is filly rejected, the wounds were allocated to three different treatments in each sheep as follows (Fig. 4.1B): 1) T-KSs; 2) D-KSs; and 3) control (not grafted with KSs). After applying different treatments (Sup. Fig 4.2A, B), wounds were covered by tight dressing for one week to allow firm attachment of the KSs (Day 26-29) (Sup. Fig 4.2C, D). Then, the dressing was taken off and wounds were monitored for another 7 days. After 14 days of keratinocytes sheet engraftment (Day 33-36), sheep were euthanized, and wound samples were collected for further analysis.

Ovine keratinocytes isolation and sheet formation

Healthy skin samples were harvested (from non-burned areas), during the burn tissue excision and cadaver skin grafting procedure, for keratinocytes isolation and culturing them to form a confluent sheet. The method used for skin harvesting and keratinocyte isolation, culture and sheet formation is fully described in the material and method section of Chapter 2.

Applying KSs over cadaver skin grafted burn wounds

Nitrocellulose membrane was used as a carrier for keratinocyte sheets to overlay onto burn wounds. The edges of membranes were stapled to the wound edges to prevent sheet movement. Control wounds received only carrier without keratinocyte sheet (Sup. Fig 4.3).

Determination of wound epithelialization percentage

For macroscopic evaluation of wound healing, photos were taken of the wounds at day 7 and 14 after grafting KSs. Total wound and epithelized areas were semi-quantified using ImageJ software (NIH, Bethesda, MD, USA) (Sup. Fig 4.4A). The wound epithelialization percentage was measured using the equation:

Wound epithelialization percentage = (Epithelized area / Total wound area) × 100

Microscopic analysis of wound healing

Skin samples were taken at day 14 after grafting the KSs, fixed in formalin and slides prepared for histological analysis. Five-micron-thick sections were prepared for Hematoxylin & Eosin staining. Slides were examined by light microscope (Olympus BX51) and images were taken using 4x magnification. Five images were taken in each section including areas of the edge to the center of the wound. Images were analyzed using ImageJ software (NIH, Bethesda, MD, USA) to determine epidermis thickness using a line grid with 150 μm in distance; whenever the grid touches the section a perpendicular line to the epidermis was measured. An average of 60 measurements were taken in each slide (Sup. Fig 4.4B).

Several histopathological analyses were done on H & E stained slides of wounds samples taken after 14 days of KSs grafting. Serial images of stained sections at 20x magnification were obtained using a BZ-X800 slide scanning microscope (Keyence, Osaka, Japan). Images were stitched together using ImageJ software (Sup. Fig. 4.5). First, the length of any separation between epidermis and dermis was calculated and normalized by epithelization length (Sup. Fig. 4.5). Second, ulceration was calculated by measuring the non-epithelized area and the ulceration percentage, calculated by the equation (ulceration length / dermal-epidermal length) × 100 (Sup. Fig. 4.5). Hemorrhages, ruptured blood vessels, and extravascular red blood cells were determined using a score system: 0 indicates no hemorrhage; 1 indicates scattered erythrocytes; and 2 indicates large areas of hemorrhage. Finally, neutrophils infiltration was evaluated using the criterion: 1 - Neutrophils percentage is < 30% of total white cells, 2 - Neutrophils percentage is between 30 and 50%; and 3 - Neutrophils percentage is > 50%. All specimens were examined by a veterinary pathologist without knowledge of the specimen's group.

Electron microscopy

For ultrastructural analysis in ultrathin sections skin samples were placed in modified Ito's fixative (PFGPA.1) and fixed for at least 1 hr in a mixture of 2.5% formaldehyde prepared from paraformaldehyde powder, and 0.1% glutaraldehyde in 0.05M cacodylate buffer pH 7.3 to which 0.01% picric acid and 0.03% $CaCl_2$ were added. The samples were then washed in 0.1 M cacodylate buffer and post-fixed in 1% OsO_4 in 0.1M cacodylate buffer pH 7.3 for 1 hr. After that they were washed with distilled water, *en bloc* stained with 2% aqueous uranyl acetate for 30 min at 60 ^{o}C and dehydrated in ascending concentrations of ethanol, infiltrated with propylene oxide and embedded in

Poly/Bed 812 (Polysciences, Warrington, PA) epoxy resin. Ultrathin sections 80 nm thick were cut on Leica EM UC7 ultramicrotome (Leica Microsystems, Buffalo Grove, IL), placed on Formvar-carbon coated 200 mesh copper grids, stained with 0.4% lead citrate and examined in a Philips (FEI) CM100 transmission electron microscope (TEM) at 60 kV. Digital images were acquired with a bottom-mounted CCD camera Orius SC200 1 (Gatan, Pleasanton, CA). Some sections were also examined in a JEOL JEM-1400 TEM (JEOL USA, Peabody, MA) at 80 kV and images were acquired on Kodak 4489 EM film (Carestream Health, Rochester, NY).

An average of 690 micrographs per treatment (T-KS and D-KS) from 5 sheep samples were assessed for a number of hemidesmosomes and continuity of lamina densa, using ImageJ software (NIH, Bethesda, MD, USA). In each micrograph, the length of the dermal-epidermal junction and accumulative length of lamina densa were measured (Sup. Fig 4.6A). The lamina densa percentage was calculated using the equation: Lamina Densa Percentage (%) = (Total lamina densa length / Total DEJ length) × 100. Additionally, the number of hemidesmosomes was counted in each micrograph (Sup. Fig 4.6B) and calculated using the equation: Number of hemidesmosomes/µm= Total number of hemidesmosomes / Total DEJ length.

Collagen density

For direct visualization of collagen fibers and histological assessment of collagen deposition, Masson Trichrome (MT) staining was performed using the Masson Trichrome Staining Kit (Thermo Scientific) following the manufacturer instructions. The MT stained slides were examined by light microscope (Olympus BX51) and images were taken using 20x magnification using Stereo Investigator software (Micro Bright Field Inc., Version

2018.2.1). Nine images per section were taken: 3 from top dermis (directly under the epidermis), 3 from mid dermis and 3 from low dermis (above subcutaneous tissues). Analysis was carried out using ImageJ software (version 1.52g) and collagen density was evaluated semi-quantitatively. Any blood vessel areas were eliminated from the total area of the field. The total area of collagen was evaluated by the blue aniline staining in MT slides using a color threshold image adjusting tool from ImageJ software. Collagen density was calculated using equation: Collagen density = (collagen area in the field / total area of field) × 100 (Sup. Fig. 4.7A).

Angiogenesis evaluation

By using the MT slides the vascularization percentage was calculated. The MT stained slides were examined by light microscope (Olympus BX51) and images were taken using 4x magnification with Stereo Investigator software (Micro Bright Field Inc., Version 2018.2.1). Analysis was carried out using ImageJ software (version 1.52g) and vascularization percentage was semi-quantified. The area of the epidermis and normal skin structure from the edge of the wound were eliminated from the total area of the section. The total area of vascularization was evaluated by the red staining in MT slides using a color threshold image adjusting tool from ImageJ software (Sup. Fig. 4.7B). Vascularization percentage was calculated as using equation: Vascularization percentage = (Vascularization area in the field / Total area of field) × 100.

Western blotting

Wound samples not treated (control) and treated with keratinocyte sheets (T-KS, D-KS) were cut into small pieces and extracted in 300 μl T-Per protein extraction reagent

(Thermo Scientific). The samples were processed in a tissue homogenizer (Bullet Blender, Next Advance) with 2 zirconium oxide beads 2.0 mm for 1 min at speed 5 for 2 times with 1 min cooling on ice, followed by gentle shaking for 22 hours at -4°C. Digested samples were centrifuged at 14000 g for 15 min at 4°C. The supernatants were recovered and stored at -80°C for analysis using western blot. To estimate the amount of protein, the supernatant was tested by using a BCA Test (Pierce) which was performed according to the manufacturer's instructions. The samples collected from the sheep after 14-day treatment with keratinocyte sheets were subjected to the measurement of the level of KGF as an indication for the wound healing stage. Actin was used as a loading control. Protein samples (30 μg) were mixed with NuPAGE LDS sample buffer and NuPAGE sample reducing agent (Invetrogen) for reduced condition and heated for 10 min at 70°C for denatured condition, and then separated through NuPAGE™ 4-12% Bis-Tris Protein Gels (Invitrogen). After electrophoresis, proteins were transferred to PVDF membranes by using an iBlot Dry Blotting system (Invitrogen). Membranes were blocked for 1 hr in 5% milk, rinsed and incubated with KGF antibody (diluted at 1:500, ab ab131162) in blocking buffer at 4°C overnight. KGF antibody was then removed by washing in TBS-T thrice and labelled by incubating with HRP-labelled secondary antibodies (1:1000) against rabbits for 1 hr at room temperature. Membrane was washed thrice in TBS-T and visualized using Pierce ECL Western Blotting Substrate (Thermo Scientific) and exposed to the emitted light is captured on CCD camera using G Box imaging system (Syngene) with GeneSnap Software (Syngene, Version 7.09). Results were calculated by imageJ software and expressed as ratio to β-actin protein as the loading control.

Statistical analysis

All data were analyzed using Prism GraphPad version 8.1.0 (GraphPad software, Inc.). All quantitative data were expressed as means ± standard error of the mean. Comparisons between wounds treated with (Control "no treatment", D-KS, and T-KS) were made using the Kruskal Wallis with the Dunn's test for pairwise comparisons. Comparisons between treated wounds at different time points were made using with Two-way ANOVA RM with Sidak's multiple comparison test. Comparisons between D-KS and T-KS treated wounds were made using Unpaired t test with Welch's correction. Quantitative variations were considered significant when the P value was < 0.05.

RESULTS

Burn injury, escharotomy, skin grafting and keratinocyte sheet grafts

We designed the experiment in a way that mimics the clinical situation. The burned skin was excised 24 hrs post injury followed by grafting with sheep cadaver skin. The time of the ovine cadaver skin rejecting in our studies was similar (19-22 days) to that observed in burn patients. Importantly, the formation of KSs was completed within 19-22 days matching the time of grafted cadaver skin rejection thus enabling timely transplantation of KSs to the wounds.

KSs were detached from the culture dishes (temperature sensitive or conventional dishes) using nitrocellulose membrane. However, to apply KSs over the wounds, it is essential to detach the carrier membranes from the cell sheets. In a preliminary study, only 2 out of 6 of the carrier membranes were able to be peeled off from the D-KS. While the carrier membranes were easily peeled off from all 6 T-KSs without any problem (Sup. Fig 4.3A). Therefore, in our future studies, we have decided to overlay both types of KSs onto the wounds with the carrier membranes for adequate comparison purposes (Sup. Fig 4.3B).

Epithelialization percentage

Wound pictorial records from days 7 and 14 showed superior wound healing effects of T-KSs compared to D-KSs (Fig. 4.2A). Planimetric analysis showed that wounds treated with T-KSs had a significantly higher epithelization rate compared to D-KSs and non-treated wounds (Fig. 4.2B). The percentage rate was 29.46 ± 3.59%, 59.10 ± 5.74%, and 95.10 ± 1.32% at day 7 and 61.80 ± 6.20%, 81.12 ± 6.0%, and 98.56 ± 1.36% at day 14 in control, D-KS and T-KS, treated wounds, respectively.

Microscopic analysis of wound samples

Epidermis thickness of wounds was determined with light microscopy 14 days after KSs engraftment. The epidermis thickness was significantly higher in wounds treated with T-KSs or D-KSs compared to control wounds that had no KS graft (Fig. 4.3A). However, there was no significant difference found between T-KSs and D-KSs-treated wounds. The epidermis and dermis separation rate was comparable between the wounds grafted with KSs (Fig. 4.3B). However, wounds treated with T-KS had a lower percentage of ulceration (2.514 ± 2.514 %) compared to control (28.61 ± 7.471) and D-KS-treated (12.38 ± 5.719 %) wounds, respectively (Fig. 4.3C). Wounds treated with T-KS had significantly ($p<0.05$) less hemorrhage scoring compared to control wounds (0.9 ± 0.23 for T-KS, and 1.7 ± 0.21 for control wounds) (Fig. 4.3D). The hemorrhage score was 1.6 ± 0.61 in D-KS-treated wounds ($P>0.05$ vs. T-KSs). Wounds treated with T-KS had a tendency to have lower neutrophils infiltration compared to D-KSs and control wounds. The scores were 0.55 ± 0.28, 1.33 ± 0.26 and 1.1 ± 0.28 for wound treated with T-KS, D-KS and control, respectively (Fig. 4.3E).

Well defined dermal-epidermal junction in wounds treated with T-KS

Transmission electron microscopy (TEM) analysis showed that the basement membrane including the lamina lucida and lamina densa was observed in the wounds with surviving KSs grafts. However, the dermis-epidermis junction (DEJ) of wounds treated with T-KS was firmer than those observed in wounds treated with D-KS (Fig 4.4 A&B). DEJ was assessed by counting numbers of hemidesmosomes and measuring the length of continuous lamina densa. The number of hemidesmosomes (condensations of cellular membrane with attached tonofilaments) per 1μm was significantly higher in wounds treated with T-KS (0.8165 ± 0.01760) compared to wounds treated with D-KS (0.5386 ± 0.01621) (Fig 4.4C).

The lamina densa (formed by laminin and collagen IV polymers) was present in both wound types. However, the percentage of the lamina densa was significantly lower in the D-KS wounds compared to T-KS with 20.76 ± 0.614 % and 42.3 ± 0.84 %, respectively (Fig 4.4D).

Collagen density is comparable between the T-KSs and D-KSs-treated wounds

Regardless of wound type, Masson's trichrome staining showed a clear visible, fine, and coarse collagen deposition in the wounds together with visible signs of angiogenesis. Also, clear skin structure from the edge of the wounds with collagen fibers, adipose tissue, sweat gland, and hair follicle were evidenced. Despite of complete wound epithelization at day 14, the collagen density was lesser (34.84 ± 0.88 %) in T-KSs-treated wounds compared to those in normal skin (64.16 ± 2.26 %). The collagen density in the wounds treated with D-KS (33.94 ± 0.71 %) was comparable to those in T-KS wounds (Fig. 4.5A).

Angiogenesis tend to be higher in wounds treated with T-KS

The MT staining of wound sections showed numbers of capillaries in the T-KSs-treated wound bed tended to be higher at day 14 (1.71 ± 0.2 %) compared to the D-KS wounds (1.29 ± 0.12 %) (Fig 4.5B).

KGF level tend to be lower in wounds treated with T-KS

The effect of enzymatic or temperature reduction treatment for detaching keratinocyte sheets on wound healing was investigated by measuring a marker for wound healing that is highly expressed in early wound healing. We measured keratinocyte growth factor (KGF) in skin samples that was collected after 14 days of treatment with KSs. The level of KGF, (molecular weight is 23 kD) in the wounds treated with D-KS or control wounds (no treatment) was higher compared to wounds treated with T-KSs (Fig. 4.6 A). The KGF expressions after normalization with actin were 0.237 ± 0.026, 0.282 ± 0.03 and 0.34 ± 0.037 in wounds treated with T-KS, D-KS and control, respectively (Fig. 4.6 B).

DISCUSSION

The results of this study indicate that keratinocyte sheets cultured on TRDs and detached by temperature reduction are superior to keratinocyte sheets detached using a conventional method for detachment using enzyme in regards to healing of third-degree grafted skin (cadaver skin) burn wounds. Our data demonstrate that preserving the extracellular matrix proteins was a major contributing factor to salutary effects of T-KSs.

Keratinocyte sheets has been introduced as a wound (including burn) treatment for over 30 years. Woodley *et al*. reported that grafting keratinocytes without any dermal components onto burn wounds, excised to fascia, was not successful because of abnormal adherence and anchoring fibrillin (collagen VII) formation between the dermis and epidermis [284]. However, the following attempt to combine the epidermal and dermal components was not fully successful [222, 285, 286]. In a case report for a 10 year old boy, Desai *et al*. showed that in spite of early success of covering the wounds and replacing the dermis with allogenic fresh cadaver skin, 60% of cultured epithelial autograft areas blistered and sloughed over the following weeks [111]. These observations led to a focus on the critical role of mature dermal and epidermal junction (DEJ) for successful acceptance of epithelial grafts. Takeda *et al*. reported the possibility of promoting a formation of the DEJ by exogenous application of laminin 5 to keratinocyte sheets. Their data showed that laminin 5, collagen IV and collagen VII were strongly stained in the DEJ at 7 days post grafting with KSs preconditioned with laminin 5. Also, early ultrastructural organization of the basement membrane components was noted in laminin 5-preconditioned KSs wounds, resulting in better stability and a higher acceptance rate of the grafts. The results of these studies point out the importance of preserving the ECM in keratinocyte sheets to increase their acceptance.

Investigators faced continued challenges associated with both detaching the cultured KSs from the culture dishes and harvesting the detached KSs using nitrocellulose membrane without compromising the integrity and quality of these sheets. Use of enzyme (Dispase) was suspected as a major contributing factor for these challenges. Treatment with Dispase not only severely digested ECM components of KSs, but it also complicated the

separation of detached KSs from carrier nitrocellulose membrane [116, 117, 186]. The same problem occurred in our present study that we were not able to detach D-KS without the carrier nitrocellulose membrane. Also, Dispase damaged and removed the entire piece of cell membranes from the cell surfaces [287]. Recently, an advanced method for detaching cell sheets without any enzymatic treatment was introduced; importantly, this method preserves extracellular matrix proteins that are crucial for successful sheet grafting and survival. The temperature responsive dishes are covered with polymer [poly(*N*-isopropylacrylamide) (PNIPAAm)] that has reversible temperature-responsive characteristics. At 37°C, the surface is hydrophobic so the cells can adhere to the dish surface, while spreading and proliferating to confluency. By decreasing the temperature to 20°C, the polymer changes its characteristic to the hydrophilic resulting in spontaneous cells sheet detachment because of a rapid hydration surface [89, 117, 128]. Most importantly, this method enables cell sheet detachment with preserved matrix [126]. This method was successfully translated to clinical practice with positive outcomes of grafting a few type of cell sheets, epithelial cell sheets, and oral mucosal epithelium [140, 152, 281]

However, this exciting technology has not been translated yet to the skin burn wound healing research and care. In the past seven years, only a few rodent studies reported use of temperature responsive dishes for wound healing; however, none of them focused on burn wounds. The pathophysiology of burn wounds is differed from other types of skin wound requiring different treatment approaches [288]. In the present study, we demonstrate for first time the efficacy of this novel technology in clinically relevant ovine model of burn wounds mimicking all aspects of burn care (early eschar, excision, temporary cover with cadaver skin, and intermittent wound care).

In an *in vitro* setting, Yamato *et al*. reported the successful culture and detachment of KSs from TRD [117]. The authors demonstrated that this approach preserved the desmosomes between cells, while they were destroyed in KSs detached by Dispase. Moreover, D-KS displayed disruption of E-cadherin and laminin 5 [117]. In another *in vivo* study, Cerqueira *et al.* used three cell types, such as human keratinocytes (hKC), dermal microvascular endothelial cells (hDMEC), and dermal fibroblasts (hDFb) (confluently grown as sheets) for treatment of murine full-thickness wounds. Homotypic and heterotypic three-dimensional (3-D) cell sheets constructs were developed to target wound re-vascularization and re-epithelialization. Both hKC and hDMEC significantly contributed to re-epithelialization by promoting rapid wound closure and early epithelial coverage [133]. In a rodent skin defect model, Osada *et al.* studied the survival and morphology of T-KS vs. D-KS. The T-KS, before grafting, better preserved keratin structure and expressed collagen IV and laminin 5 compared to D-KS. The 7-day survival rate of T-KS after transplantation was higher than that of D-KS, and collagen IV and Laminin 5 expression was stronger in the T-KS transplantation group [118]. The most recent report was done by Matsumine *et al*. where they showed that keratinocyte sheets cultured on temperature-responsive dishes enhanced their survival after *in vivo* grafting on acellular dermal matrices in a rat model [181]. Similarly, our data showed that epithelialization rate and graft acceptance were significantly higher in wounds treated with T-KS compared to wounds treated with D-KS. Taken together the results of previous and present studies, clearly suggested superiority of T-KS over D-KS grafting in healing of grafted skin burn wounds. We report these salutary effects of T-KSs are largely attributed to preserved ECM proteins [118, 133, 181]. Different types of cell sheets that detached

from temperature responsive dishes were used for treating cutaneous wounds like fibroblast [133, 289, 290], adipose-derived stem cells [291-294], and peripheral blood mononuclear cells [289].

As mentioned, in the present study, we aimed to investigate efficacy of T-KSs in a clinically relevant ovine model of grafted burn wounds and demonstrate underlying mechanistic aspects using state-of-art *in vitro* techniques and wound healing models. In our studies, we have prepared the wound bed by grafting with cadaver skin after excision of burned skin, which highly mimics the clinical scenario. Also, a custom-made technique of fixing (by nylon sutures) a square- shaped metal splint on the wound was used to prevent potential wound contraction. Previously, several studies reported advantage of using a silicone splint fixed on the skin of rodents for prevention of wound contraction which enables wound closure by actual epithelialization and granulation tissue formation, but not by contraction [295, 296].

In our study, the wound bed preparation with the initial cadaver skin grafting is crucial for formation of mature dermal components for firm junction of dermis to grafted epidermis. As mentioned, in the previous studies, keratinocyte sheets were directly overlaid onto the wounds excised to the fascia or superficial fascia without proper wound bed formation [118, 133]. The interaction between fibroblast and keratinocytes is critical for proper formation for dermal epidermal junction [297]. Lee *et al.* reported that when culturing keratinocytes in fibroblast-free dermal construct, the expressions of β4 integrin chain, laminin and collagen type IV and VII were present. However, the formation of the dermal-epidermal junction was not established. The culturing the cells on fibroblast populated dermal construct increased the expression of these proteins and the junction was

formed between the epidermis and dermis [298]. Also, the role of the fibroblast in producing new extracellular matrix necessary to support cell growth and blood vessels sprouting is widely acknowledged [50]. Based on previous and present study results, we believe that proper wound bed preparation with cadaver skin grafting, in our studies, resulted in stronger DEJ formation leading to better wound healing in T-KSs. To note, we have also noticed a fairly developed DEJ even in wounds treated with D-KS.

The thickness of epidermis during wound healing process is related to keratinocyte proliferation rate [133]. Changes in cell cycles were monitored at regenerating epidermis after injury, and normal growth homeostasis seems to be gradually reestablished during the second day of regeneration [299]. In our studies, there was a significant difference between T-KS and D-KS sheet thickness before being grafted over burn wounds. Also, no significant differences were found in terms of epidermis thickness after sheet engraftment between the different treatments, suggesting re-establishment of the growth homeostasis in all grafted sites. Our data contradicting the data by Mutsumine *at al.* that significant difference was found in the epidermis thickness between the wounds treated with T-KS vs. D-KS grafted over acellular dermal matrix. This might be due to the difference in sample collection time points for histological analysis between our study and theirs, 14 and 7 days after grafting, respectively. This may also be related to the different wound bed preparation method.

Wound healing consists of the overlapping phases of hemostasis and inflammation, tissue regeneration, and remodeling. During wound hemostasis, which is initiated within minutes after injury, inflammation and platelet activation occur. This stage ends with stable fibrin clot formation and active neutrophil infiltration [39, 159, 300, 301]. Neutrophils are

recruited by several proinflammatory cytokines, such as TNFα and growth factors, such as platelet-derived growth factor (PDGF) and TGF-β [159]. The role of neutrophils on wound healing is the clearance of pathogens, abundant erythrocytes and tissue debris [159, 302]. Also, neutrophils express cytokines that contribute to re-epithelialization and wound closure [303]. Furthermore, stimulated neutrophils secrete VEGF, which may contribute to wound healing by encouraging angiogenesis [304]. However, in germ-free mice, fetuses, and oral mucosa, the wound healing is associated with lower neutrophil infiltration and scar less regeneration. This might explain the benefits of a limited neutrophil involvement [305-307]. Reduced presence of neutrophils in germ-free wounds is correlated with increased levels of IL-10 and VEGF, that is associated with an accelerated wound epithelialization [305]. Neutrophils are phagocyted by macrophages and this is a very strong signal for the macrophage to release TGF-β1. TGF-β1 stimulates differentiation of myofibroblasts, which contribute not only to wound contraction but also to a collagen synthesis [301]. The neutrophils infiltration is generally restricted in the inflammatory phase because of their elimination by macrophages. This process activates the macrophages to secrets TGF- β1, that stimulate the differentiation of myofibroblast that contributes on wound contraction and collagen synthesis [302, 308]. However, the presence of neutrophils can be prolonged by physical trauma or ongoing contamination, which may delay neutrophil clearance and leading to delayed wound healing [309]. In general, neutrophils contribute to bacterial clearance in nonsterile skin wounds; therefore, promoting wound healing. However, the numbers and activity of neutrophils are required to be tightly controlled, which is a challenge in severe wounds. The histopathological evaluation of the wounds, in our study, revealed that the wounds treated with T-KS tend to

have a lower number of neutrophils, compared to D-KS-treated wounds. This confirms the previous finding that treatment with D-KS was associated with secondary wound infections [270, 310].

Briggaman *et al*. studied the formation and origin of basal lamina and anchoring fibrils in adult human skin. They showed that basal lamina, mainly collagen IV and laminin 5, are originated from the epidermis. While anchoring fibrils, and collagen VII are originated from the dermis [311]. This supports our findings explaining better dermal to epidermal junction in wounds treated with T-KS. Previously, after grafting D-KS the detection of well-formed lamina densa with many anchoring fibrils by electron microscopy between 4 to 6 weeks depending on the differences in the graft beds has been reported [312, 313]. Our results showed that the basement membrane was not present on the cultured sheets before grafting (Sup Fig 4.8). However, our TEM results confirmed the presence of the basement membrane structure, on samples collected from wounds at 14 days after engraftment with either T-KS or D-KS. These results indicate that the basement membrane was reassembled after the sheet transplantation. However, the presence of lamina densa and hemidesmosomes was significantly higher in wounds treated with T-KS which proves the importance of preserving the ECM proteins in the proper formation of DEJ.

Histopathological studies are used to assess different stages of wound healing (inflammation, proliferation and remodeling) [39]. By using conventional H&E staining, it is very hard to distinguish between wound healing changes that could lead to misinterpretation for the histopathological observations. By using mason trichrome staining, it is easy to distinguish many of the wound healing features based on colors of keratinocytes, blood vessels (red and pink color) and collagen fibers (blue color) [314].

Number of studies measured collagen fibers and collagen density to evaluate the level of wound healing [315, 316]. Collagen is required in wound healing to restore the anatomical structure of the wounded area [317]. Collagen is oriented in small parallel bundles and is different from the basket-weave collagen in healthy dermis [33]. In our study, the level of collagen density was comparable between the wounds treated with T-KS or D-KS. Both treatments have significantly lower collagen density compared to normal skin collagen density. Similarly, low levels of collagen density on both treatment groups indicate the wounds were still in early stage of healing following treatment with either T-KSs or D-KSs. This is supported by a previous study reporting that total collagen in early wound healing was reduced [318].

The angiogenesis is an essential process in the burned wound healing as it provides the nutrients and oxygen to the granulation tissue, and allows the elimination of the residual products out of the body [261]. Also, immune cells migrate through blood vessels to reach the injury site [261]. Keratinocytes play a vital role in wound healing especially during the proliferative phase during which the epithelialization and restoration of the vascular network occur [174]. This might explain the slight increase in vascularization percentage (using MT staining) on wounds treated with T-KS compared to wounds treated with D-KS; the wounds covered with T-KSs had a higher number of keratinocytes. These results in agreement with a previous report that vascularization rate was temperature gradient-detached adipose derived stem cell sheets compared to control wounds that did not receive sheet transplantation in diabetic rat wound healing model [292].

Epidermal regeneration is a complex process that is regulated with autocrine and paracrine mechanisms that are not fully understood until today [319]. KGF is highly

expressed at wound sites that stimulates the proliferation and migration of epithelial cells [320]. Several studies have shown the successful use of KGF as a treatment for wound healing [321, 322]. In our data, KGF expression tends to be less in late stages in wounds treated with T-KS compared to D-KS or control. This may suggest that T-KS treated wounds were more mature because of completed epithelialization requiring less KGF.

Our studies are associated with several limitations, such as relatively short wound monitoring period (14 days after KSs engraftment) and small wounds sizes (5 cm^2). Nevertheless, our study demonstrated feasibility and efficacy of novel technology using T-KSs in acute phase of grafted burn wound healing which is critically important in reducing morbidity and mortality of burn patients.

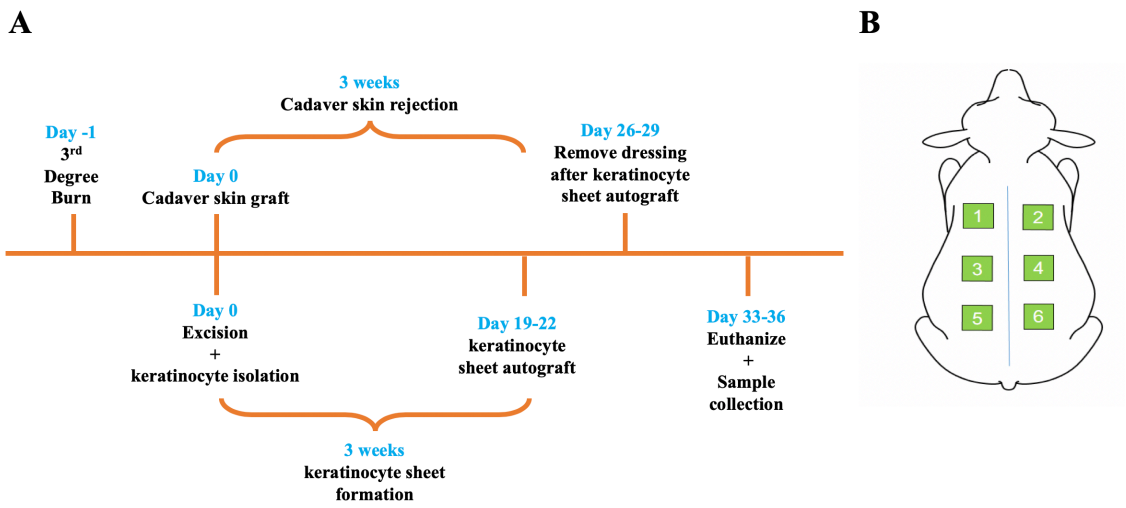

Figure 4.1: Schematic of keratinocyte sheet overlaid onto burn wounds grafted with cadaver skin.

A) The experimental timeline of wound healing procedures. After 24 hrs of burn injury induction, burned skin was excised to the fascia and wounds were covered with fresh ovine cadaver skin. After three weeks, (Day 19-22) when grafted cadaver allograft epidermis was filly rejected, the wounds were allocated to three different treatments groups: 1) overlaid with T-KSs; 2) overlaid with D-KSs; and 3) control (not grafted with KSs). Wounds were covered by tight dressing for one week to allow firm attachment of the KSs (Day 26-29). Then, the dressing was taken off and wounds were monitored for another 7 days (Day 33-36). Sheep were humanely euthanized at 14 days after KSs engraftment and wound samples were collected for further analysis. B) The location of burn wounds. Six full-thickness burn wounds (5x5 cm^2) were induced at the dorsum of the sheep.

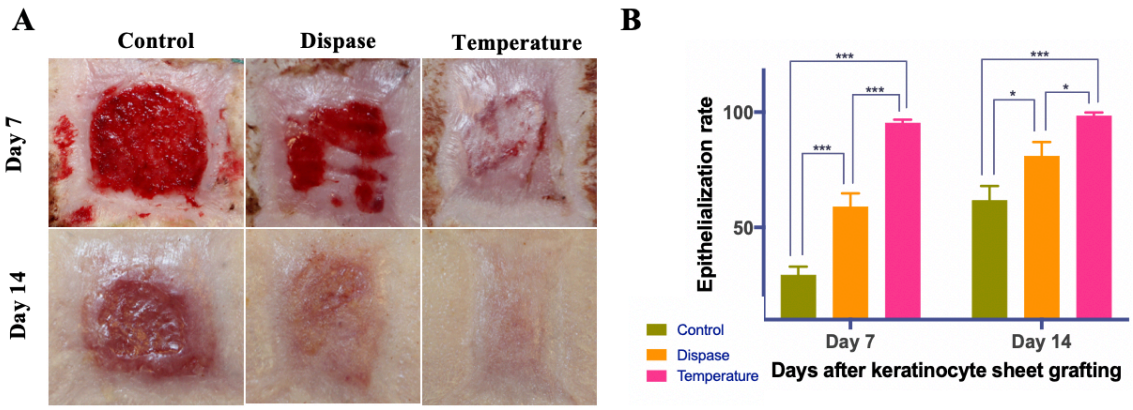

Figure 4.2: Epithelialization percentage after keratinocyte sheet autograft.

A) Pictorial record for grafted burn wounds after 7 and 14 days of grafting keratinocyte sheets. Temperature: wounds covered with T-KSs, Dispase: wounds covered with D-KSs and Control: no treatment. Superior wound healing effect of T-KSs was observed compared to D-KSs. B) Planimetric analysis for the epithelialization percentage showed that wounds treated with T-KSs had a significantly higher epithelialization rate compared to D-KSs and non-treated wounds. Error bars represent Mean±SEM (Two-way ANOVA RM with Sidak's multiple comparison test, N=5) (*P<0.03, ***P<0.0002).

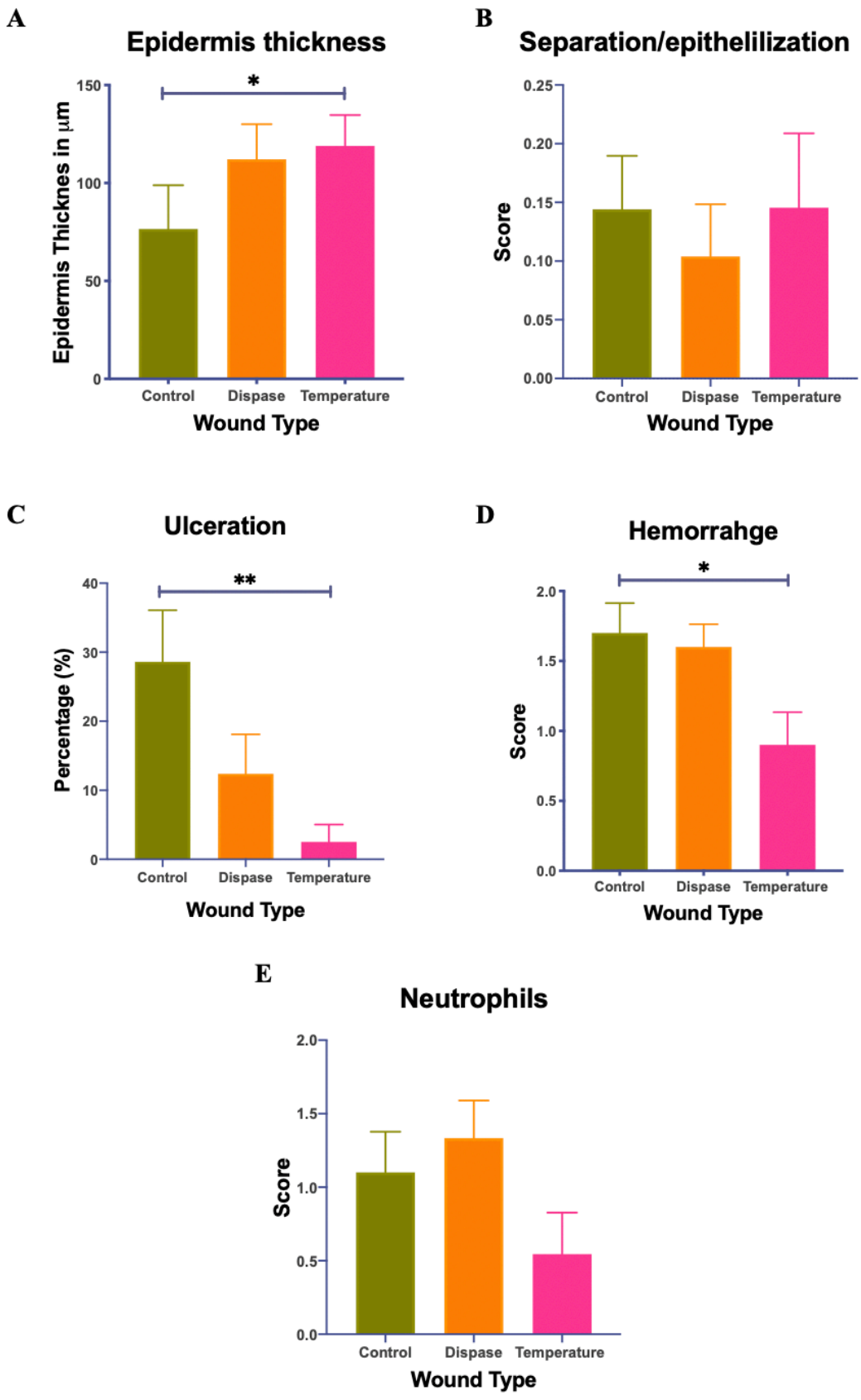
A
Epidermis thickness
Epidermis Thicknes in μm
150
100
50
0
*
Control
Dispase
Temperature
Wound Type
B
Separation/epithelilization
Score
0.25
0.20
0.15
0.10
0.05
0.00
Control
Dispase
Temperature
Wound Type
C
Ulceration
Percentage (%)
40
30
20
10
0
**
Control
Dispase
Temperature
Wound Type
D
Hemorrahge
Score
2.0
1.5
1.0
0.5
0.0
*
Control
Dispase
Temperature
Wound Type
E
Neutrophils
Score
2.0
1.5
1.0
0.5
0.0
Control
Dispase
Temperature
Wound Type

Figure 4.3: Histopathological evaluation of wounds at 14 days after treatment with keratinocyte sheets.

Skin samples were taken at day 14 after KSs grafting. A) Epidermis thickness was analyzed using ImageJ software. The epidermis thickness was significantly higher in wounds treated with T-KSs compared to control wounds that had no KS graft. There was no significant difference found between T-KSs and D-KSs-treated wounds. Error bars represent Mean±SEM (Friedman test with Dunn's multiple comparison test, N=5) (*P<0.03). B) The epidermis and dermis separation rate was comparable between the wounds grafted with T-KSs and D-KSs. Error bars represent Mean±SEM (Kruskal-Wallis test with Dunn's multiple comparisons test, N=5). C) Wounds treated with T-KS had lower percentage of ulceration compared to control and D-KS-treated wounds. Error bars represent Mean±SEM (Kruskal-Wallis test with Dunn's multiple comparisons test, N=5) (**P<0.002). D) Wounds hemorrhage was evaluated scoring for ruptured blood vessels and extravascular red blood cells. 0 indicates no hemorrhage; 1 indicates scattered erythrocytes; and 2 indicates large areas of hemorrhage. Wounds treated with T-KS had significantly less hemorrhage scores compared to control wounds. Error bars represent Mean±SEM (Kruskal-Wallis test with Dunn's multiple comparisons test, N=5) (*P<0.03). E) Neutrophils infiltration was evaluated using the criterion: 1 - Neutrophils percentage is < 30% of total white cells, 2 - Neutrophils percentage is between 30 and 50%; and 3 - Neutrophils percentage is > 50%. Wounds treated with T-KS had tendency to have lower neutrophils infiltration compared to D-KSs and control wounds. Error bars represent Mean±SEM (Kruskal-Wallis test with Dunn's multiple comparisons test, N=5).

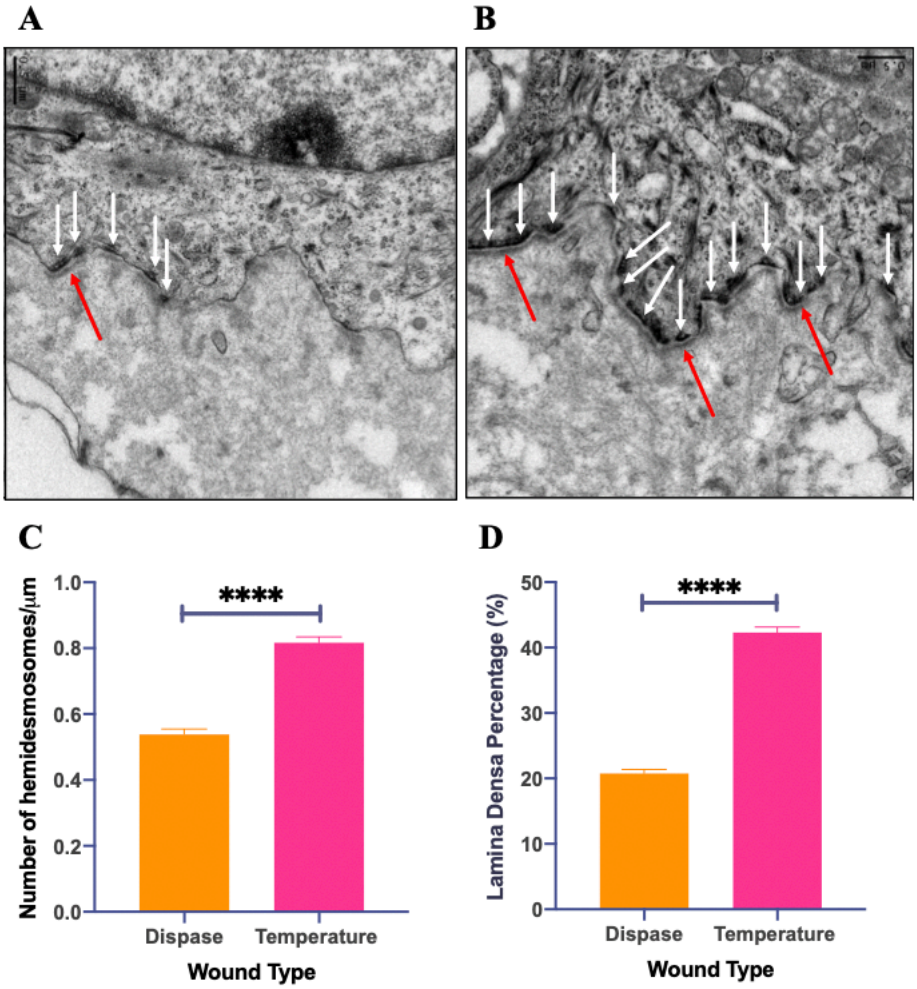

Figure 4.4: Well defined dermal-epidermal junction in wounds treated with T-KS.

Wound samples were fixed and processed for TEM. Analysis showed that the basement membrane including the lamina lucida and lamina densa was present in the wounds with surviving KSs grafts in both groups. However, the DEJ of wounds treated with T-KS (A) was more strongly defined than those observed in wounds treated with D-KS (B). The red arrows indicate lamina densa and white arrows indicate hemidesmosomes. Scale bar 0.5µm. C) The length of the dermal-epidermal junction and accumulative length of lamina densa were measured. The percentage of the lamina densa was significantly lower in the wounds D-KS compared to T-KS. Error bars represent Mean±SEM (Mann Whitney test, N=5) (****P<0.0001). D) The number of hemidesmosomes was counted in each micrograph. The number of hemidesmosomes per 1µm was significantly higher in wounds treated with T-KS compared to wounds treated with D-KS. Error bars represent Mean±SEM (Mann Whitney test, N=5) (****P<0.0001).

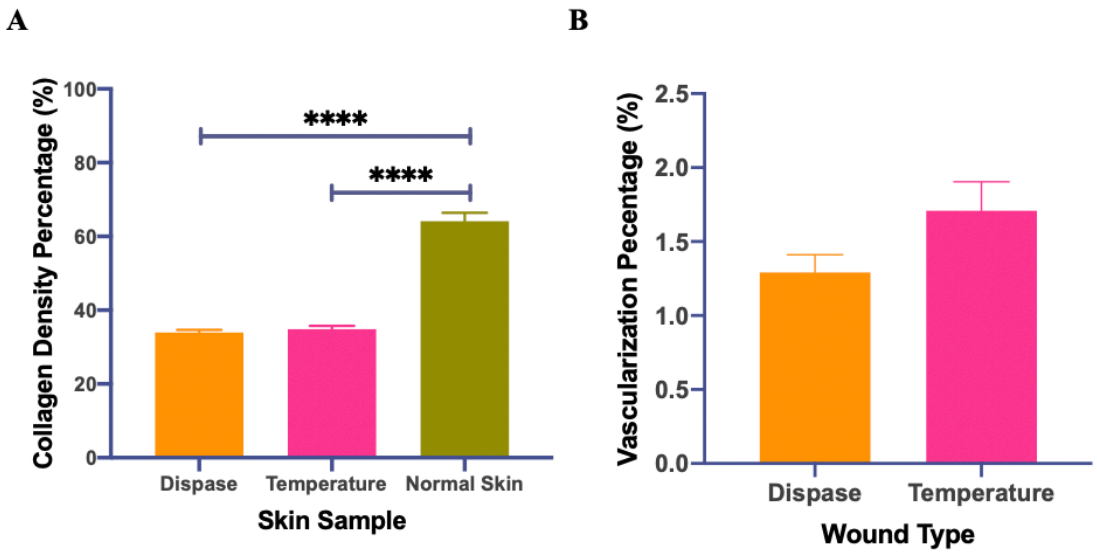

Figure 4.5: Evaluation for collagen and vascularization in wounds after KSs grafting.

A) Collagen density is comparable between the T-KSs and D-KSs-treated wounds**.** Using Masson Trichrome staining, the slides were imaged at 9 different places, and analyzed using ImageJ software. Collagen density was semi-quantitatively evaluated. Despite of complete wound epithelization at day 14, the collagen density was lesser in T-KSs-treated wounds compared to those in normal skin. The collagen density in the wounds treated with D-KS was comparable to those in T-KS wounds. Error bars represent Mean±SEM (Kruskal-Wallis test with Dunn's multiple comparisons test, N=5) (****P<0.0001). B) The vascularization was analyzed using ImageJ software and the percentage was semi-quantified. The MT staining of wound sections showed that number of capillaries in the T-KSs-treated wound bed tended to be higher at day 14 compared to the D-KS wounds. Error bars represent Mean±SEM (Unpaired t test with Welch's correction, N=5).

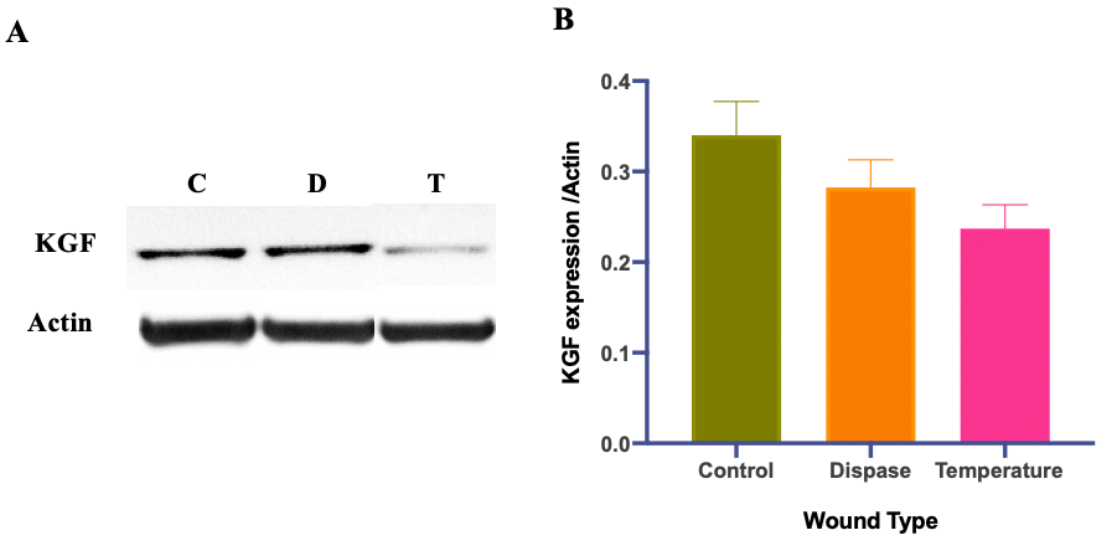

Figure 4.6: KGF level in wounds treated with different types of KSs.

A) Western blot analysis of anti–KGF antibody for skin samples that were collected after 14 days of treatment with T-KS (T), D-KS (D), or control wounds with no KSs graft (C). The level of KGF in the wounds treated with D-KS or control wounds was higher compared to wounds treated with T-KSs. B) KGF expressions (normalized to to β-actin protein as the loading control) tend to be lower in wounds treated with T-KS. Error bars represent Mean±SEM (Kruskal-Wallis test with Dunn's multiple comparisons test, N=5).

CHAPTER 5

Summary, conclusion and future directions

SUMMARY:

Cultured autologous keratinocytes as confluently grown sheets have been proposed for treatments of burn wounds. However, this method has not been successfully translated to clinical practice because of certain limitations, such as inconsistency and unpredictability of engraftment, incidence of infection, spontaneous blistering, and scar contracture. Enzymatic detachment of cultured keratinocyte sheets from culture dishes was attributed to these negative outcomes. To overcome this problem, we are testing a novel technology that allows the detachment of cultured keratinocyte sheets without using any enzymatic treatment. We compared efficacy of keratinocyte sheets cultured on 2 different dishes—temperature responsive (TRD) and conventional. Cells cultured on TRD were detached by temperature reduction (T-KS), whereas the cells cultured on conventional dish were detached by enzyme, dispase (D-KS). We studied efficacy of these sheets (T-KS and D-KS) on both in vitro and in vivo burn wound models and characterized downstream mechanisms underlying differences between these two sheets.

First, we tested overall quality i.e., integrity, fragility of two types KSs (T-KSs and D-KSs) in *in vitro* studies (Chapter 2). In that study, we were able to reveal the numbers of potential differences between these two types of sheets: 1) the T-KS were significantly thicker than D-KS; 2) T-KSs preserved more ECM proteins such as Collagen IV and Laminin 5; 3) The integrity of T-KS, tested using mechanical cell dissociation assay, was still intact, while D-KS was fragmented to multiple pieces; and 4) The number of

disassociated (free floating) cells were significantly higher in D-KS compared to T-KS or T/D-KS. Taken together, above results suggest overall superior quality of T-KSs. These results also suggest that immature sheet integrity and fragility in D-KSs were linked to use of enzyme for detachment of D-KSs that disrupted ECM.

The effect of enzymatic or temperature reduction treatment for detaching keratinocyte sheet on cell cytoskeleton was further investigated by measuring representative of cytoskeleton proteins in keratinocyte sheets such as actin and α-tubulin. Both proteins were detected significantly higher in the sheets detached by temperature reduction treatment compared to D-KS, suggesting that these proteins were negatively impacted by Dispase. This notion was confirmed by the observation that treatment of T-KSs with Dispase (T/D-KS) significantly reduced theses cytoskeleton proteins. Actin and α-tubulin are member of the three major cellular cytoskeleton. The reduction in cytoskeleton proteins were associated with significant shrinkage of D-KS and T/D-KS compared to T-KS, again indicating harmful effects of Dispase treatment.

Second, we created *in vitro* skin wound healing model and tested the efficacy of both types of cultured KSs and investigated their proliferation and cellular mechanisms. To mimic harsh burn environment, we have cultured KSs with burn wound exudate and evaluated survival and proliferation of KSs. We found that T-KS had significantly higher rate of proliferation with or without burn exudate treatment compared to D-KS and T/D-KS.

Next we found that the activation of MAPK, an important pathway for cell survival, was lower in the sheet detached by dispase treatment compared with that detached by temperature reduction. Previous studies demonstrated critical role of MAPK pathway in

cells survival, proliferation and migration [187-190]. These results may suggest treatment with Dispase impaired ECM through inhibiting MAPK activation resulting in poor sheet integrity and survival (proliferation).

Finally, we wanted to compare wound healing efficacy of cultured T-KSs and D-KSs in 3rd degree ovine burn wounds grafted with cadaver skin (Chapter 4). We designed the experiments in such way that closely mimics clinical situation. The burned skin was excised 24 hrs postinjury (mimicking clinical scenario) followed by grafting with sheep cadaver skin. The formation of KSs was completed at the time of grafted cadaver skin rejection, thus enabling timely transplantation of KSs to the wounds. By using Planimetric analysis, we found that wounds treated with T-KSs had a significantly higher epithelization rate compared to D-KSs and non-treated wounds at 14 days of grafting. Although there was no significant difference in epidermis thickness between T-KSs and D-KSs-treated wounds, the dermis-epidermis junction (DEJ) of wounds treated with T-KS was firmer than those observed in wounds treated with D-KS--the number of hemidesmosomes per 1μm and lamina densa percentage was significantly higher in wounds treated with T-KS.

Using various histology examinations, further we found that wounds treated with T-KS had lower percentage of ulceration compared to control and D-KS-treated wounds. Wounds treated with T-KS had significantly less hemorrhage scoring compared to control wounds, while the hemorrhage rate was comparable in D-KSs-treated and control wounds. Wounds treated with T-KS had tendency to have lower neutrophils infiltration compared to D-KSs and control wounds.

Despite comparable total collagen in both treated wounds at day 14, the vascularization rate tended to be higher in in the T-KSs-treated wound beds compared to the D-KS wounds.

Next, we have measured a potent growth factor KGF, which is highly expressed in early wound healing, in skin samples that were collected after 14 days of treatment with KSs. The level of KGF, in the wounds treated with T-KS was tended to be lower reflecting more mature wounds treated with T-KSs.

To more closely mimic clinical practice, we have established the sheep cadaver skin bank (Chapter 3). This was essential for temporary cover of burn wounds until the autologous KSs became available. To my knowledge, this study was the first to establish the ovine cadaver skin preparation method, and there is no study evaluating grafted burn wounds in sheep using cadaver skin.

For this purpose, we followed and modified the same method used for collecting, processing and cryopreserving human cadaver skin. We checked the method used for cryopreserving the cadaver skin us suitable before grafting them over burn wound to assess the rejection pattern. The freezing method used was valid confirmed by preserved skin structure and integrity. Skin cells were viable and able to proliferate in fresh and frozen cadaver skins. After grafting, ovine cadaver skin was started to be rejected within 10 days, which mimics rejection time in humans (~8.4 days). The histological evaluation revealed similar pattern of grafted cadaver skin rejection (timing, ulceration, inflammation, hemorrhage) to human cadaver skin rejection. This model can successfully be used to enhance translational aspects of preclinical wound healing studies.

CONCLUSION:

In this study, we first demonstrated superior effects of KSs detached by non-enzymatic method on ovine grafted burn wound healing compared to KSs detached by enzyme Dispase. We conclude that preserved ECM is attributable to superior effects of T-KSs. This study is associated several advantages: 1) We have used a novel technology of culturing KSs that allows their non-enzymatic detachment; 2) We have characterized cultured KSs using various sophisticated in vitro techniques; and 3) To my knowledge, this is the first study examining the efficacy of T-KSs in a clinically relevant large animal model of grafted burn wound. Our well-characterized ovine model closely mimics all aspects of clinical burn wound care, including early excision of burned tissues, allograft with cadaver skin, debridement of grafted cadaver skin epidermis and intermittent wound dressing changes. Therefore, our studies set the platform for potential clinical trials to test efficacy and safety of T-KS in burn patients.

FUTURE DIRECTIONS

In the present study, we have demonstrated salutary effects of T-KSs in early stage (14 days) of wound healing. Our results warrant fundament for future prolonged studies, to investigate long-term durability of grafted T-KSs. Also, our studies trigger for potential clinical trials testing safety and efficacy of T-KS in burn patients.

Appendix

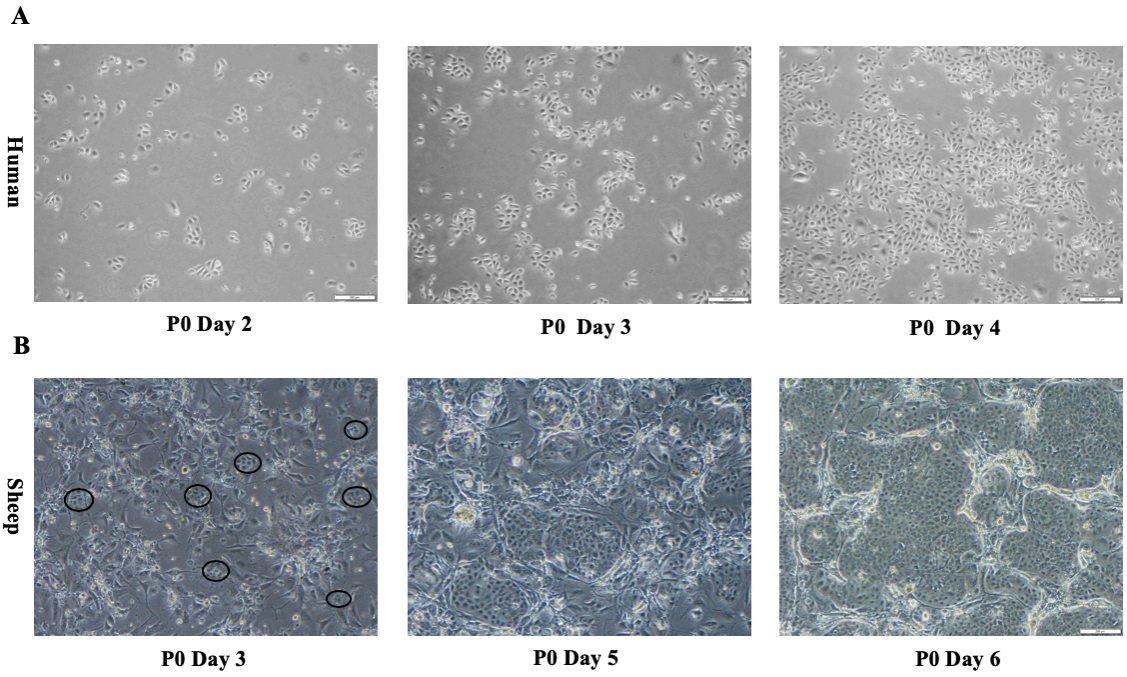

Supplement Figure 2.1: Primary keratinocyte culture.

A) Representative phase contrast images for NHEK cells were cultured on RD in serum-free conditions in Lonza's KGM-Gold media that is supplemented with bovine pituitary extract KGM-Gold media contains low Calcium (Ca^{+2}) that prevent cells to go through differentiation. Images were taken at a 4x magnification. B) Representative images for primary sheep keratinocyte were freshly isolated cells were seeded into a flask prepared with a feeder layer with CKM. Images were taken at a 4x magnification.

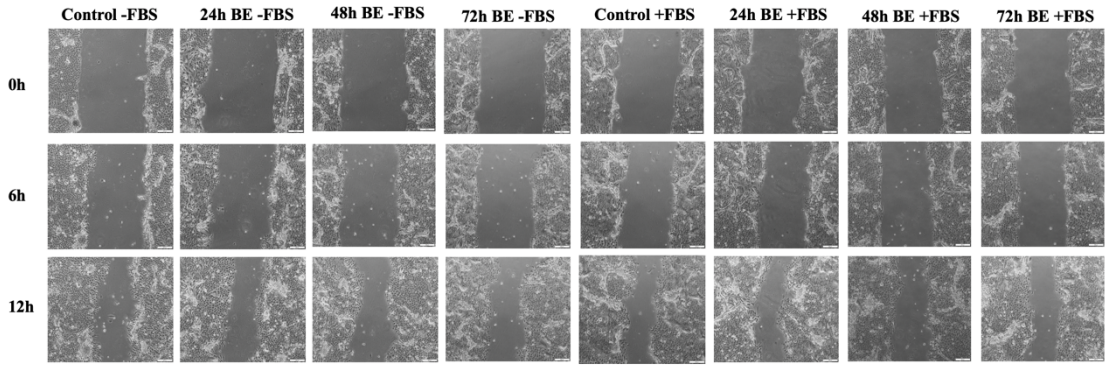

Supplement Figure 2.2: Scratch assay testing the optimal culture condition for the *in vitro* burn wound healing model.

Representative phase contrast images for the scratch assay of Figure 2.8A at time 0h, 6h and 12h for testing the culture conditions (+/- FBS) to create the *in vitro* burn wound healing model. Images were taken at a 4x magnification.

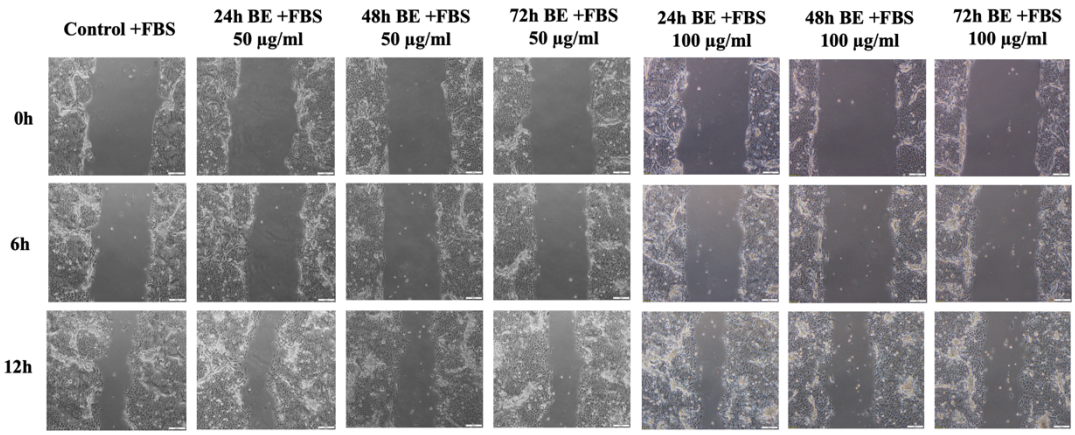

Supplement Figure 2.3: Scratch assay testing the optimal dose and collection time of burn exudate used in the model.

Representative phase contrast images for the scratch assay of Figure 2.8B at time 0h, 6h and 12h for testing the different concentrations of BE to create *in vitro* burn wound healing model. Images were taken at a 4x magnification.

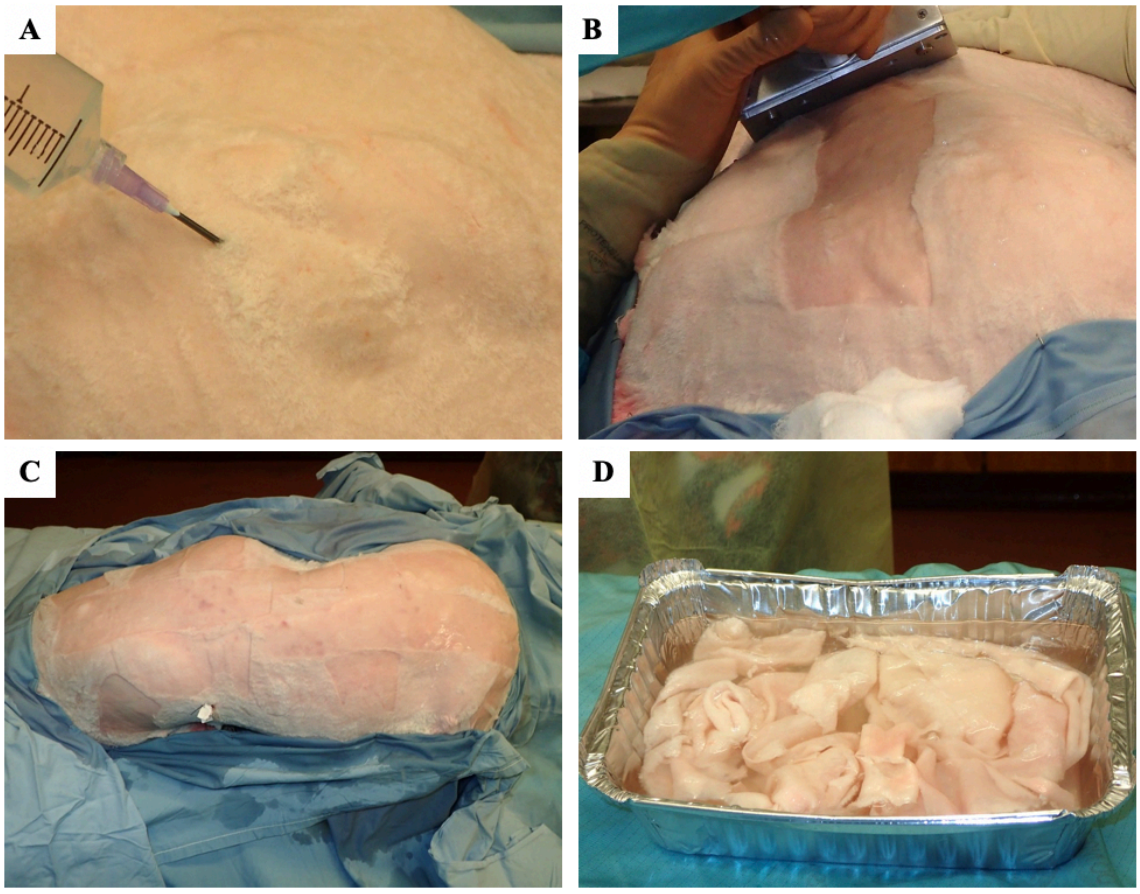

Supplement Figure 3.1: Cadaver skin (allograft) collection.

A) Sterile 0.9% NaCl solution was injected sub-dermally using a 60 ml syringe with a 16G needle to separate the skin from subcutaneous tissue. B) Skin collection was started on the posterior dorsum toward the anterior side using a dermatome set to 3-inch width and 0.02-inch thickness. C) Sheep dorsum side after completing skin collection. D) Skin strips were placed in foil trays with rinse solution (0.9% NaCl sterile solution) before being transferred to sterile jars containing RPMI medium without antibiotics.

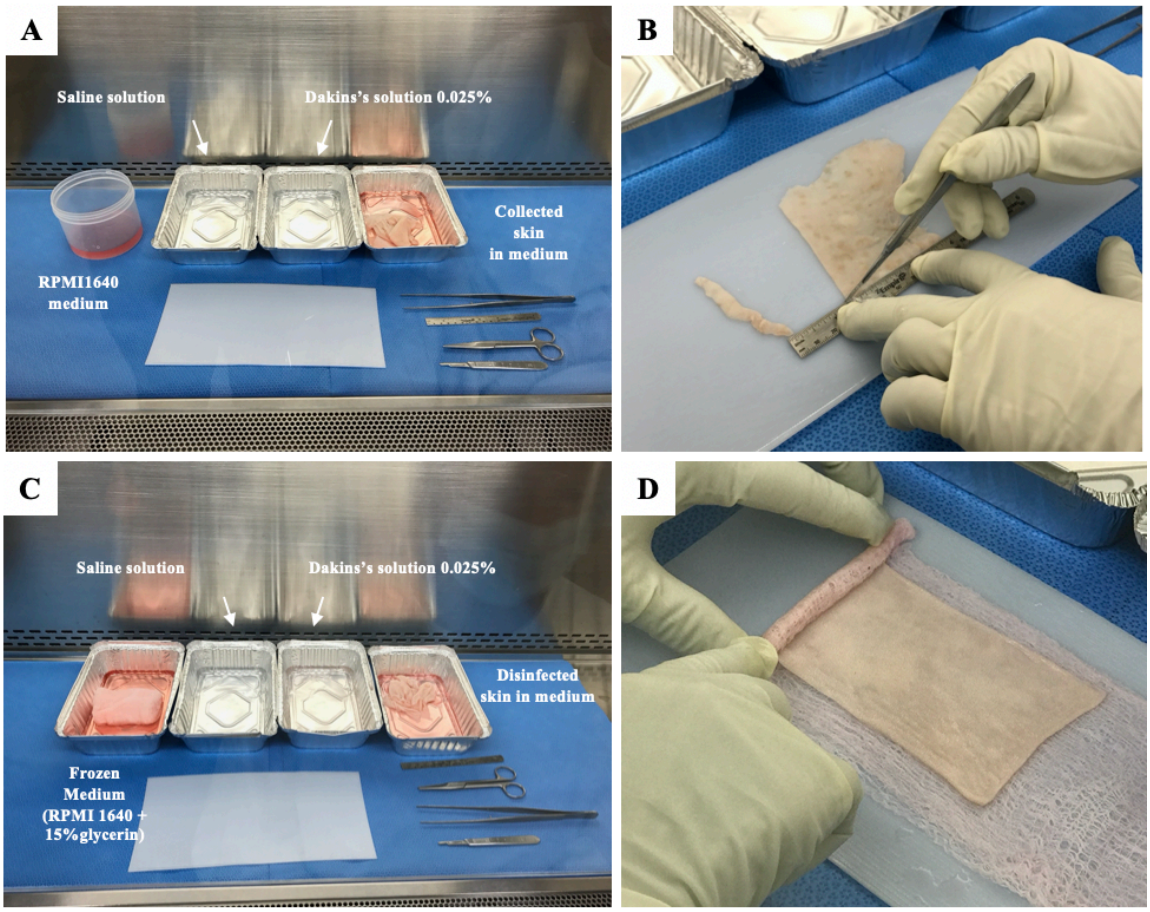

Supplement Figure 3.2: Processing, disinfection and preserving of cadaver skin.

A) Under biological safety cabinets (BSC), three sterile foil container and sterile jars for the tissue were placed in the BSC. Collected cadaver skin was poured into the first sterile foil container then trimmed on cutting board showing in (B). Skin pieces were then transferred to Dakins Solution and soaked for 2 min. Then, skin pieces were transferred rinse solution (0.9 % Sodium Chloride) then placed into sterile jar with RPMI media. B) Skin was placed on a sterile cutting board and skin edges were trimmed and cut into pieces of size ranging from (1.5X2 inches) to (3 x 4 inches) by using scalpel. C) Samples were processed and packaged within 24hrs for storage in frozen condition. The skin samples were undergone a second round of disinfection in the exact same way that was done during first disinfection procedure. Then, skin was soaked in freezing medium (RPMI 1640 with 15% sterile glycerin). D). Prepared skin was placed, dermal side up, on doubled 4 inches wide gauze. Gauze with skin was rolled and returned to the freezing medium until packaging of all skin pieces was completed. Packaged tissues were placed in 50 ml tubes and transferred to Styrofoam box to be stored in -80°C until use.

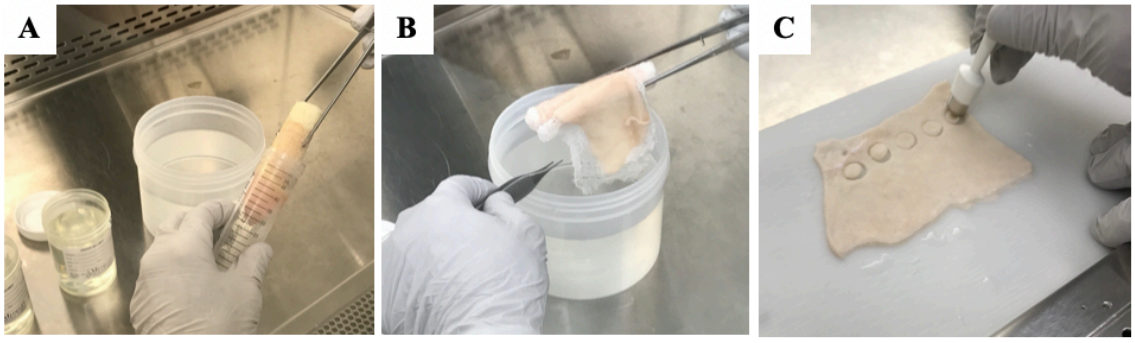

Supplement Figure 3.3: Thawing frozen cadaver skin and sample collection.

A) Frozen cadaver skin was taken from the -80°C freezer and placed in 37°C water bath for 1 min. The slightly thawed rolled skin in gauze was removed from the tube under aseptic technique. B) Skin was completely thawed in pre-warmed to 37°C sterile 0.9% sodium chloride and washed twice from frozen medium. C) For sample collection, skin was placed on a cutting board with epidermis side up and samples were taken using a 10 mm punch biopsy.

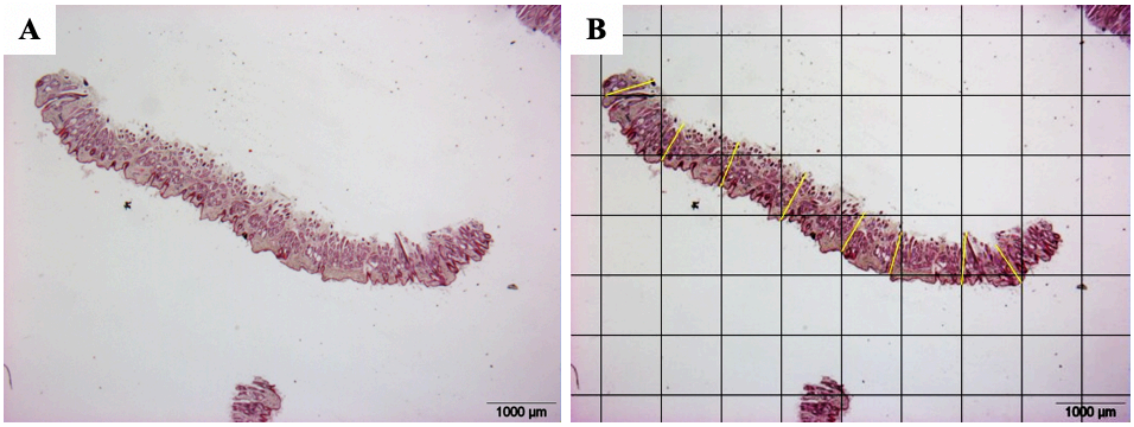

Supplement Figure 3.4: Method used to measure cadaver skin thickness.

A) Samples were processed and embedded on the long axis for cross sectioning all the anatomical layers of the skin and stained with H&E staining. B) Images of the slides were analyzed using ImageJ software using a line grid with 722500 μm^2 area per point; whenever the grid touches the section a perpendicular line to the epidermis was measured.

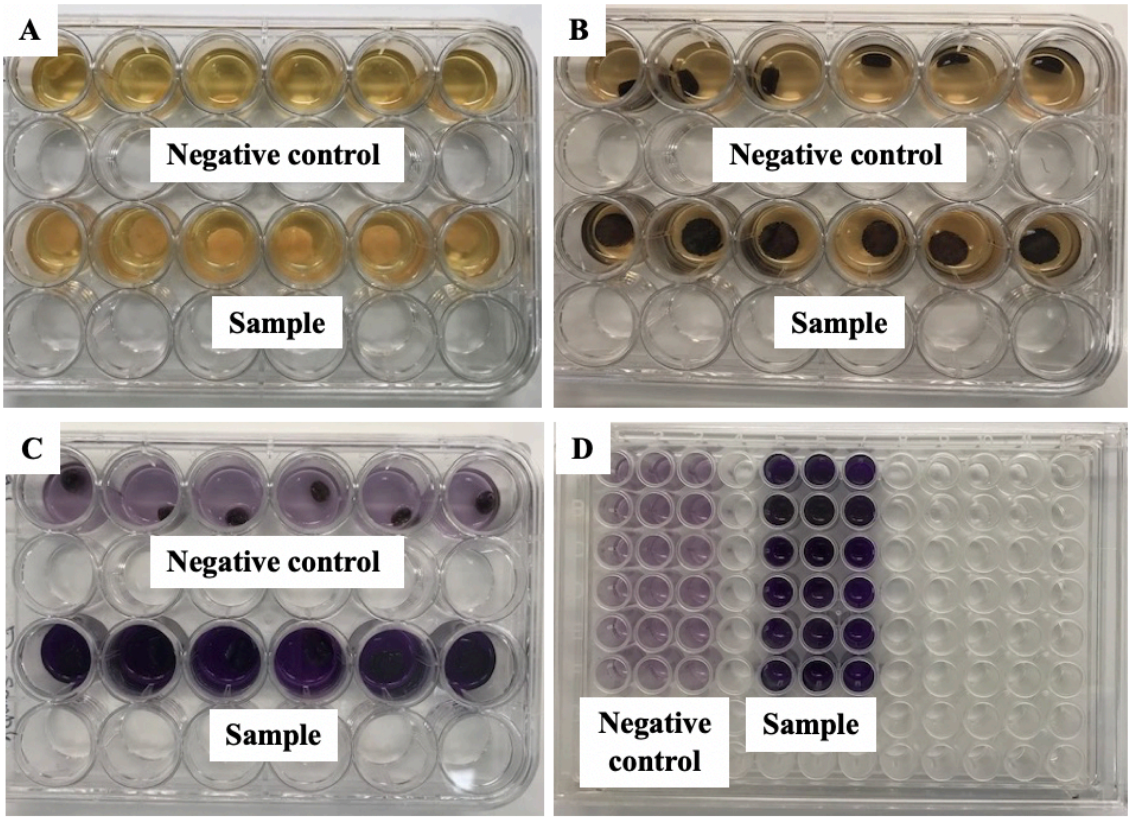

Supplement Figure 3.5: Method used for MTT assay to asses cadaver skin viability.

A) Six punch biopsies were taken from the fresh and frozen cadaver skin for 10 and 40 days and incubated in RPMI 1640 and MTT 1mg/ml for three hours. Negative controls were made by boiling the samples in distilled water for 30 min in the microwave. B) Skin biopsies after incubation already have formed formazan. C) Formazan was extracted in 300 µl isopropanol/skin biopsy at room temperature for 1 hour. D) Dissolved formazan in isopropanol was diluted and the optical density was quantified in a spectrophotometer (OD560).

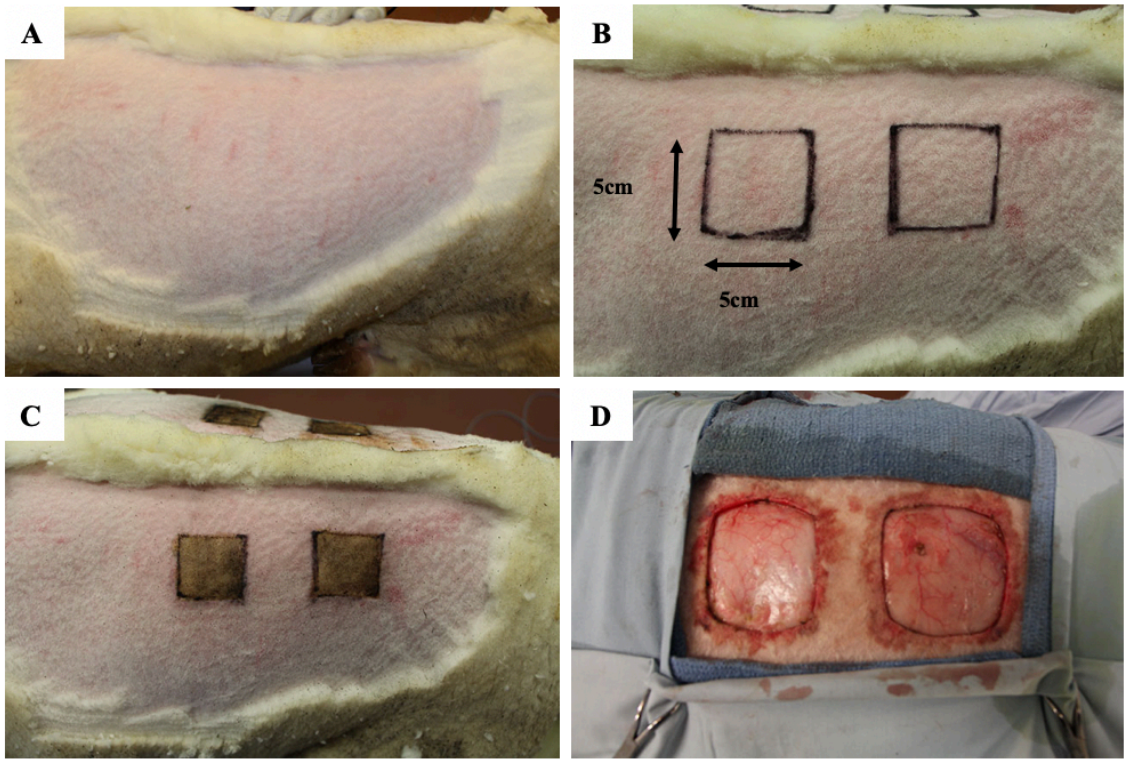

Supplement Figure 4.1: Skin burn wound induction and escharotomy procedure.

A) Sheep's wool was shaved for creating burn wounds. B) Several designs were created to mark the edges of the full-thickness burn wounds (5x5 cm^2). C) Full-thickness burn wounds were induced at the dorsum of the sheep (Day -1). D) After 24 hours (Day 0), burned skin was excised to the fascia.

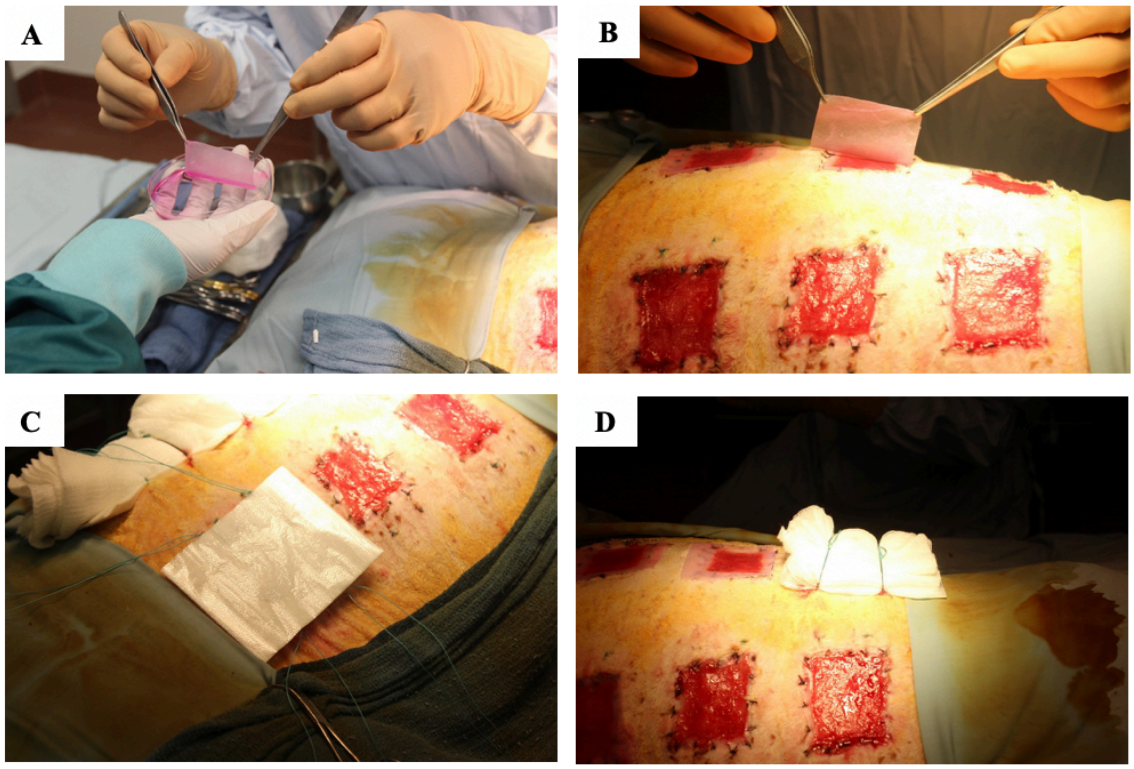

Supplement Figure 4.2: Applying KSs over cadaver skin grafted burn wounds.

A) After three weeks, (Day 19-22) when grafted cadaver allograft epidermis is filly rejected, the wounds were allocated to three different treatments in each sheep as follows: 1) T-KSs; 2) D-KSs; and 3) control (not grafted with KSs). B) KSs was applied to grafted burn wounds using nitrocellulose membranes. C) After applying different treatments, wounds were covered with non-adhesive gauze. D) The tight dressing was applied to the wounds for one week to allow firm attachment of the KSs (Day 26-29).

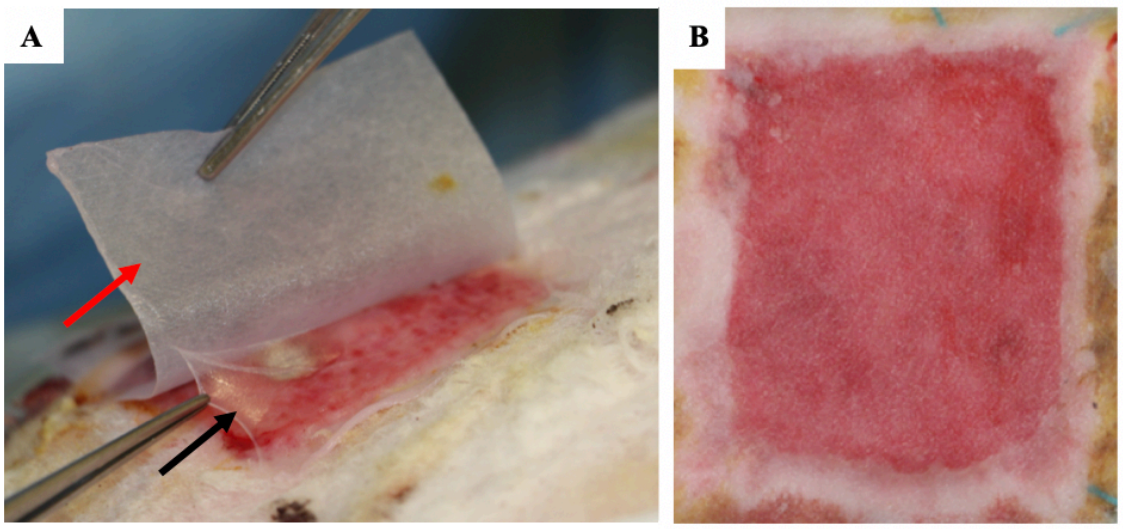

Supplement Figure 4.3: Use of nitrocellulose carrier membrane for applying KSs over cadaver skin grafted burn wounds.

A) Nitrocellulose membrane (red arrow) was used as a carrier for keratinocyte sheets (black arrow) to overlay onto burn wounds. Control wounds received only carrier without keratinocyte sheet. In a preliminary study, only 2 out of 6 of the carrier membranes were successfully peeled off from D-KS. While the carrier membranes were easily peeled off from all 6 T-KSs without any problem. B) Thus, for adequate comparison purposes, the both types of KSs were overlaid with the carrier membranes.

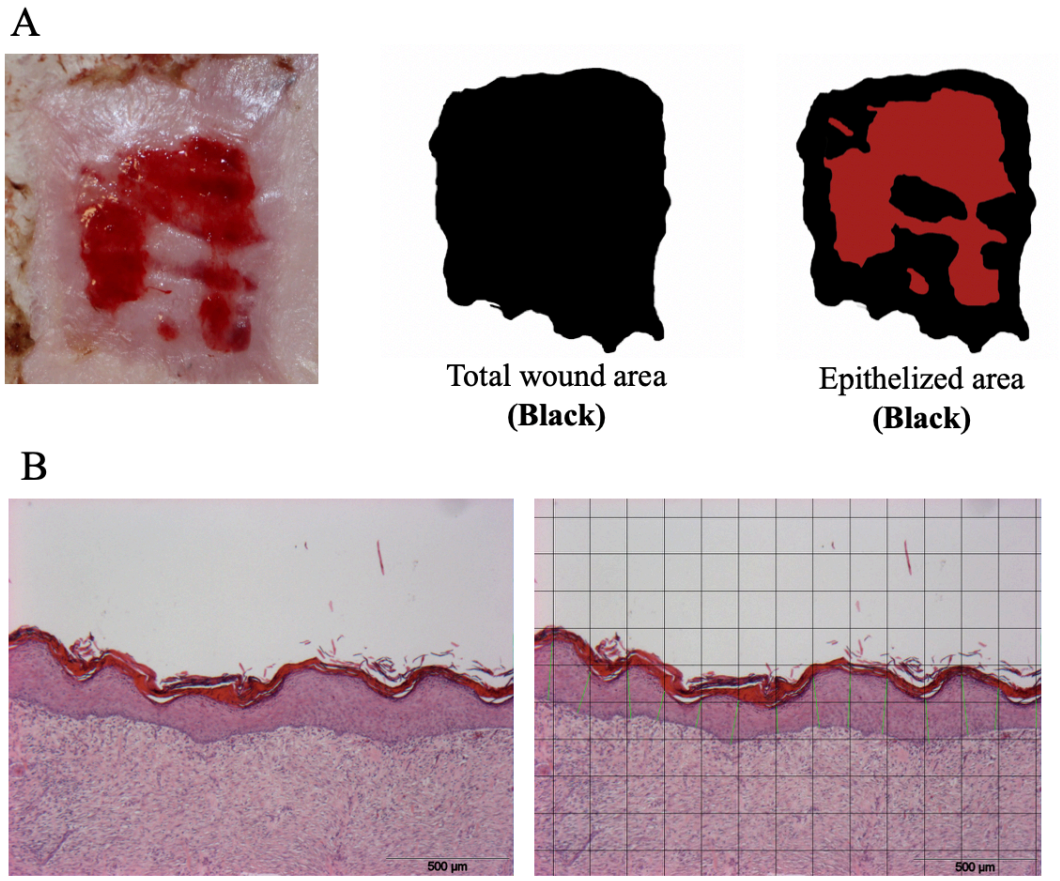

Supplement Figure 4.4: The method used to measure epithelialization percentage and epidermis thickness.

A) Determination of wound epithelialization percentage. The wound photos were taken at days 7 and 14 after grafting KSs. Total wound and epithelized areas were semi-quantified using ImageJ software. The wound epithelialization percentage was determined using the equation: Wound epithelialization percentage = (Epithelized area / Total wound area) × 100. B) Wound images were analyzed by ImageJ software to determine epidermis thickness using a line grid with 150 µm in distance; whenever the grid touches the section a perpendicular line to the epidermis was measured. An average of 60 measurements were taken for each slide.

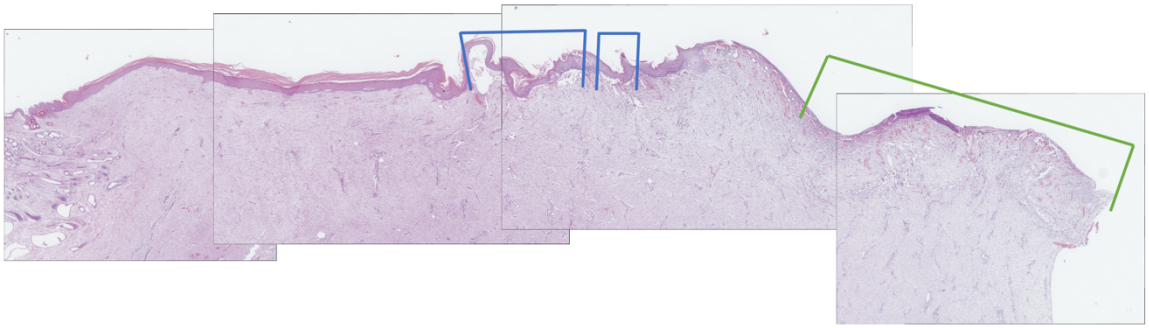

Supplement Figure 4.5: Method used to determine wound ulceration and separation between epidermis and dermis.

Wound ulceration and separation were scored in H & E stained samples taken at 14 days after KSs engraftment. Serial images of stained sections at 20X magnification were obtained and stitched together using ImageJ software. The length of any separation between epidermis and dermis was calculated and normalized by epithelization length (between blue lines). Ulceration was calculated by measuring the non-epithelized area (between green lines) and the ulceration percentage was calculated by the equation (ulceration length / dermal-epidermal length) × 100.

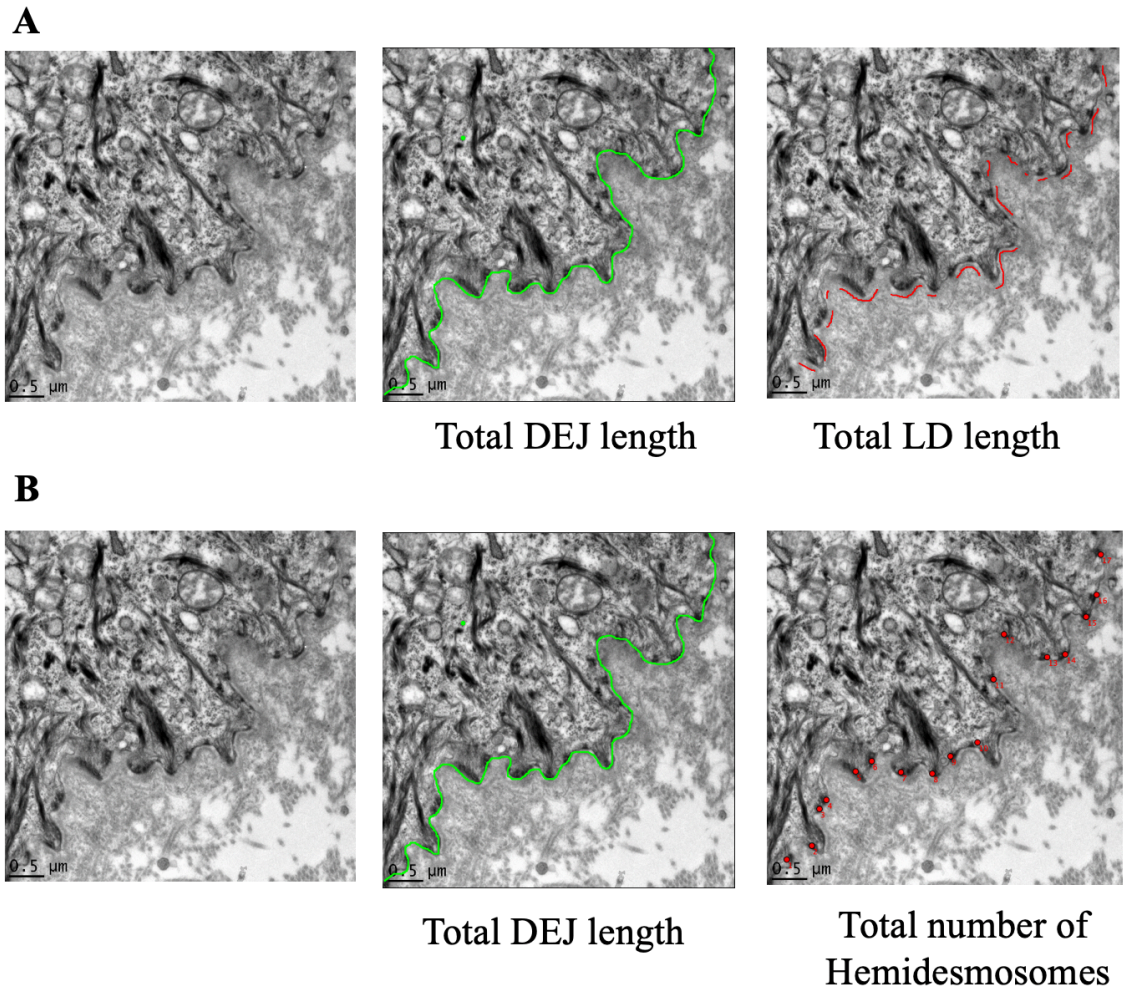

Supplement Figure 4.6: Method used for TEM analysis of wounds samples 14 days after KSs grafting.

A) The length of the dermal-epidermal junction (green line) and accumulative length of lamina densa (red line) were measured. The lamina densa percentage was calculated using the equation: Lamina Densa Percentage (%) = (Total lamina densa length / Total DEJ length) × 100. B) The number of hemidesmosomes (red dots) was counted in each micrograph and calculated using the equation: Number of hemidesmosomes/µm= Total number of hemidesmosomes / Total DEJ length.

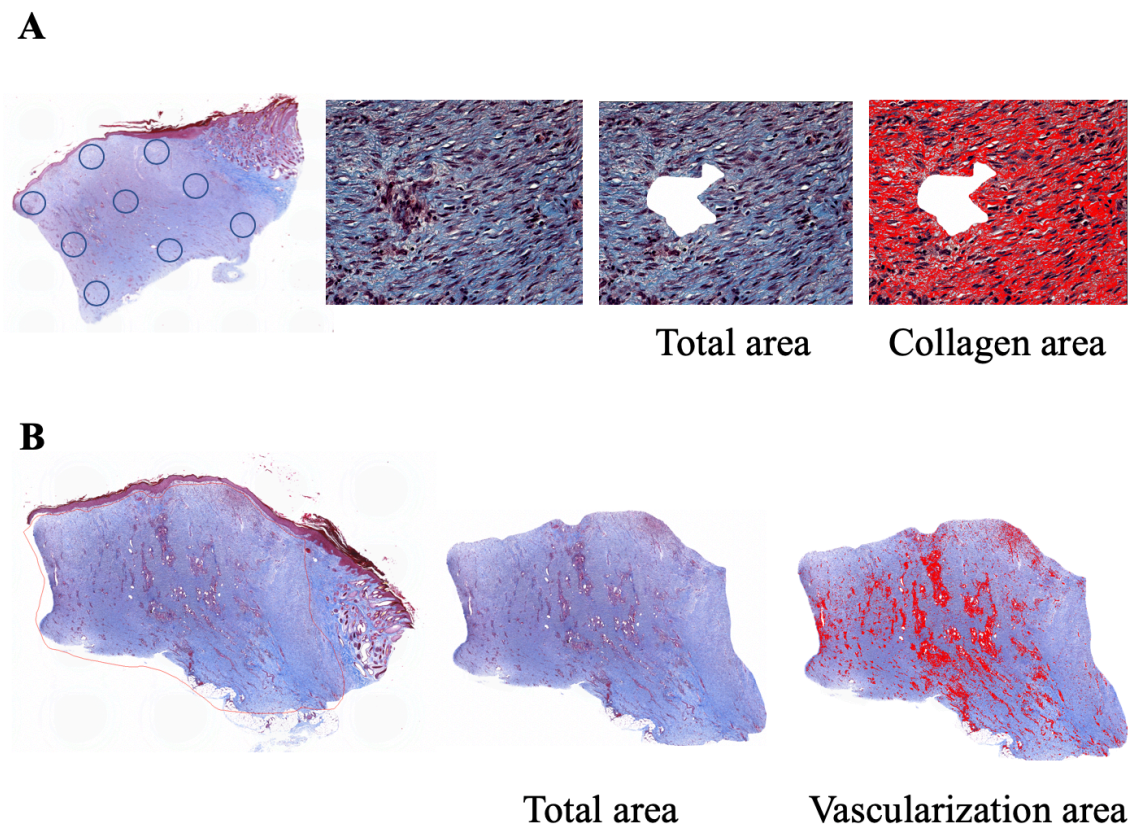

Supplement Figure 4.7: Method used for measuring collagen and vascularization percentage in wound samples 14 days after KSs grafting.

A) Determination of collagen density using MT staining method. Nine images per section were taken; 3 from top dermis (directly under the epidermis), 3 from mid dermis and 3 from low dermis (above subcutaneous tissues). Using ImageJ software, collagen density was evaluated semi-quantitatively. Any blood vessels area was eliminated from the total area of the field. The total area of collagen was evaluated by the blue color staining in MT slides using color threshold image adjusting tool from ImageJ software. Collagen density was calculated using equation: Collagen density = (collagen area in the field / total area of field) × 100. B) Evaluation of angiogenesis using the MT staining method. Vascularization percentage was semi-quantified. The area of the epidermis and normal skin structure from edge of the wound were eliminated from the total area of the section. The total area of vascularization was marked by the red staining in MT slides using color threshold image adjusting tool from ImageJ software. Vascularization percentage was calculated using equation: Vascularization percentage = (Vascularization area in the field / Total area of field) × 100.

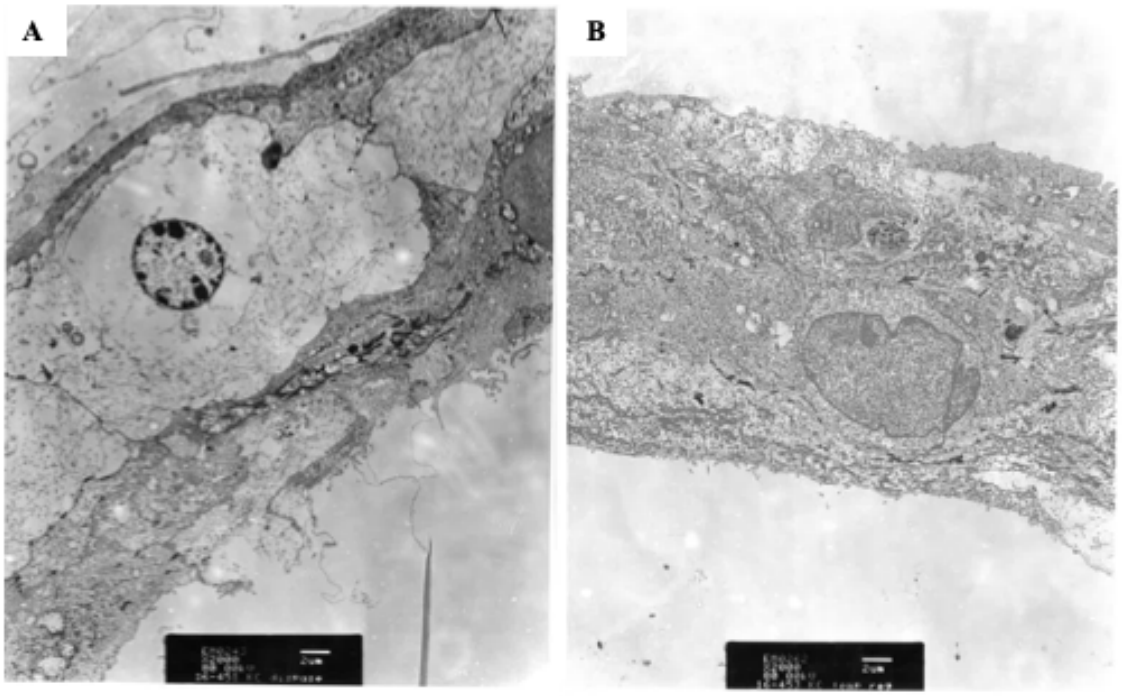

Supplement Figure 4.8: TEM micrographs of keratinocyte sheets before grafting to burn wounds.

No basement membrane components i.e., hemidesmosomes or lamina densa were found in both D-KS (A) or T-KS (B) wounds. Scale bar is 2μm.

Curriculum Vita

NAME: Suzan Alharbi

PRESENT POSITION AND ADDRESS:

Graduate Assistant
The University of Texas Medical Branch at Galveston
Department of Neuroscience, Cell Biology, & Anatomy
Cell Biology Program
Research Support Building
301 University Boulevard
Galveston, Texas 77555-1061
Email: sualharb@utmb.edu

BIOGRAPHICAL:

Date of Birth:	11/23/1984
Birthplace:	Jeddah, Saudi Arabia
Citizenship:	Saudi
Languages:	Arabic (mother language), English
Phone number:	+1(646)327-3318
Address:	1400 El Camino Village Drive Apt 2311 Houston, TX 77058

EDUCATION:

2014 to present **Pre-Doctoral Research Fellow, Current GPA (4.00/4.00)**
Cell Biology Graduate Program
Department of Neuroscience, Cell Biology, & Anatomy
The University of Texas Medical Branch, Galveston, TX

2007 to 2011 **Masters of Science in Biology - Embryology, GPA (4.94/5.00)**
King Abdulaziz University, Jeddah, Saudi Arabia

2002 to 2006 **Bachelors of Science in Biology – Zoology, GPA (4.63/5.00) with Second Honors**
King Abdulaziz University, Jeddah, Saudi Arabia

PROFESSIONAL AND TEACHING EXPERIENCE:

Professional Experience:

10/2015 to present **Predoctoral Research Fellow**, Department of Cell Biology, University of Texas Medical Branch, Galveston, TX
Mentor: Perenlei Enkhbaatar
Project: Preserved extracellular matrix in non-enzymatically detached cultured keratinocyte sheets bolsters the healing effects on grafted burn wounds

Teaching Experience:

2012 to present **Lecturer**
Biological Science Department, King Abdulaziz University, Jeddah, KSA

2009 to 2012 **Teaching Assistant**
Biological Science Department, King Abdulaziz University, Jeddah, KSA
Full responsibility for laboratory in Embryology (BIO355), General Biology (BIO202), Parasitology (BIO451), Invertebrates 1 (BIO351), Mammalian (BIO455)

INVENTION:

Colored embedding medium for small samples Filing No.: 111320609

LEADERSHIP ROLES:

October 15th, 2018 Current Member of the TERMIS-SYIS AM Council - Treasurer

4-7th September 2018 Co-Chair on of the sessions during at TERMIS-WC 2018 conference in Kyoto, Japan "Regenerative medicine in ophthalmological field"

Jul 2017 – June 2018 President of Society of Cell Biology at The University of Texas Medical Branch at Galveston

3-6th December 2017	Co-Chair one of the sessions during at TERMIS-AM conference in Charlotte, NC "Skin regeneration and immunomodulation"

MEMBERSHIPS IN SCIENTIFIC SOCIETIES:

2018 to present	American Society for Investigative Pathology
2018 to Present	Wound Healing Society
2015 to Present	Tissue Engineering and Regenerative Medicine Society
2014 to Present at Galveston	Society of Cell Biology, The University of Texas Medical Branch

HONORS AND AWARDS:

December 17th, 2018	Bohdan Nechay Endowment from the University of Texas Medical Branch in Galveston (1,050.00 $)
December 10th, 2018	State of Mind Award from the National Society of Leadership and Success (1,000.00$)
May 18th, 2018	Selected to Serve as an ambassador for the Cell Biology Program on the day of commencement ceremony
May 9th, 2018	Third place award at T1-T4 in 3 minutes competition held at University of Texas Medical Branch, Galveston (250.00$)
May 1ST, 2018	Outstanding service award for outstanding leadership of Society of Cell Biology in the 5th Annual Cell Biology Student Symposium
May 1ST, 2018	Second place award of overall best presentation of the first oral session in the 5th Annual Cell Biology Student Symposium
April 27th, 2018	The National Engaged Leader Award from The National Society of Leadership and Success

April 18th, 2018	Travel award to attend the WFIRM Regenerative Medicine Essentials Course that will take a place in Wake Forest University, Winston-Salem, North Carolina from Alliance for Regeneration, Rehabilitation, Research and Training "AR3T"
December 14th, 2017	The 2nd place in the podium presentation at the Neuroscience, Cell Biology and Anatomy Departmental Retreat
3-6th December 2017	poster titled "Efficacy of keratinocyte sheet cultured in temperature responsive dish in ovine burn wound healing" presented at TERMIS-AM conference was selected on of the top ten posters for Student and Young Investigators section (SYIS)
3-6th December 2017	Student Scientist Award at TERMIS-AM (Tissue Engineering and Regenerative Medicine International Society - yearly America chapter meeting) conference, Charlotte, NC
November 15th, 2017	Inducted as member in The National Society of Leadership and Success
2017	Selected to join the University of Texas Medical branch chapter of The National Society of Leadership and Success
2012	Granted a fully paid scholarship to pursue PhD in United States of America
2006	B.S. with Second Honors recipient, King Abdulaziz University, Jeddah, KSA

COMMUNITY SERVICE AND ACTIVITIES:

12/2018 to present	Teach a fetal development class, Pregnancy Center, Galveston, TX
03/2018 to present	Organizing committee in the Fetal Membrane Club
10/2018-12/2018	Planning committee, Preterm Birth International Collaborative International conference North America Branch, Galveston, TX
07/2017 to present	Current Graduate School of Biomedical Sciences Cell Biology Representative The University of Texas Medical Branch, TX

05/2017 to present	Department of Cell Biology Curriculum Committee Student Representative The University of Texas Medical Branch, TX
01/2017-05/2017	Planning committee, Preterm Birth International Collaborative International conference, Galveston, TX
04/2017	Oral Session Moderator, TFRS Conference, Baylor University Medical Branch, Houston, TX
01/2017-05/2017	Planning committee, Cell Biology Departmental Symposium, The University of Texas Medical Branch, TX
01/2016-05/2016	Planning committee, Cell Biology Departmental Symposium, The University of Texas Medical Branch, TX

BIBLIOGRAPHY

Publications:

1. Ihara K, Fukuda S, Enkhtaivan B, Trujillo R, Perez-Bello D, Nelson C, Randolph A, Alharbi S, Hanif H, Herndon D, Prough D, Enkhbaatar P. **Adipose-Derived Stem Cells Attenuate Pulmonary Microvascular Hyperpermeability After Smoke Inhalation**. PLoS One, 2017 Oct 5;12(10):e0185937

2. Alharbi S, Elsafadi M, Mobarak M, Alrwili A, Vishnubalaji R, Manikandan M, Al-Qudsi F, Karim S, Al-Nabaheen M, Aldahmash A, Mahmood A. **Ultrastructural characteristics of three undifferentiated mouse embryonic stem cell lines and their differentiated three-dimensional derivatives: a comparative study**. Cell Reprograming, 2014 Apr;16(2):151-65.

Books:

1. Zelai N., Alharbi S. and Al-Yahya H. (2010). Biology II Laboratory Book. *Dar Khawarizm for Academic Publishing and distribution*, Jeddah, ISBN: 978-603-96-7

Scientific Posters:

1. Suzan Alharbi, Yosuke Niimi, Dominique Wiener, Hal Hawkins, Robert Cox, Vsevolod Popov, Atsuyoshi Osada, Hiroyuki Sakurai, David Herndon, Donald Prough, Perenlei Enkhbaatar. **Non-enzymatic detachment for keratinocyte sheets using temperature responsive dishes for treating burn wound.** 31st Annual Meeting for the Wound Healing Society (May 7-10, 2019)

2. Suzan Alharbi, Yosuke Niimi, Hal Hawkins, Robert Cox, Vsevolod Popov, Atsuyoshi Osada, Koji Ihara, Hiroyuki Sakurai, David Herndon, Perenlei Enkhbaatar. **Preserving the extra cellular matrix is critical for improving efficacy of keratinocyte sheets for treatment of burn wounds.** Experimental Biology Annual Meeting (April 6-9, 2019).

3. S. Alharbi, MSc, Y. Niimi, MD, PhD, S. Williamson, MBA, R. Cox, PhD, N. Williams-Bouyer, PhD, C. Andersen, MS, C. Ouellette, BSc, P. Enkhbaatar, MD, PhD. **Establishing Ovine Model of Burn Wounds Grafted with Cadaver Skin.** The 51st Annual Meeting for the American Burn Association. (April 2-5, 2019)

4. Suzan Alharbi, Yosuke Niimi, Hal Hawkins, Robert Cox, Vsevolod Popov, Atsuyoshi Osada, Koji Ihara, Hiroyuki Sakurai, Donald Prough, David Herndon, Perenlei Enkhbaatar. I**mproving the Efficacy of Autologous Keratinocyte Sheets on Ovine Burn Wound Healing Using a Novel Non-enzymatic Detachment Method of Cultured Sheets.** The 5th TERMIS World Congress in Kyoto, Japan (September 3-7, 2018).

5. Suzan Alharbi, Yosuke Niimi, Hal Hawkins, Robert Cox, Vsevolod Popov, Atsuyoshi Osada, Koji Ihara, Hiroyuki Sakurai, David Herndon, Donald Prough, Perenlei Enkhbaatar. **Effects of autologous keratinocyte sheets on ovine burn wound healing.** The 41st Annual Conference on Shock (June 9-12, 2018).

6. Suzan Alharbi, Yosuke Niimi, Robert Cox, Hal Hawkins, Atsuyoshi Osada, Koji Ihara, Hiroyuki Sakurai, Donald Prough, David Herndon, and Perenlei Enkhbaatar. **Efficacy of keratinocyte sheet cultured in temperature responsive dish in ovine burn wound healing.** America Burn Association 50th Annual Meeting (April 10-13, 2018).

7. Suzan Alharbi, Yosuke Niimi, Hal Hawkins, Robert Cox, Atsuyoshi Osada, Koji Ihara, Hiroyuki Sakurai, Perenlei Enkhbaatar. **Efficacy of keratinocyte sheet cultured in temperature responsive dish in ovine burn wound healing**. TERMIS-AM annual meeting (3-6th December 2017).

8. Suzan Alharbi, Yosuke Niimi, Robert Cox, Atsuyoshi Osada, Hiroyuki Sakurai, Perenlei Enkhbaatar. **Efficacy of keratinocyte sheet cultured in temperature responsive dish in ovine burn wound healing**. Advanced in Tissue Engineering course (August 9-12th, 2017).

9. Suzan Alharbi, Yosuke Niimi, Robert Cox, Atsuyoshi Osada, Hiroyuki Sakurai, Perenlei Enkhbaatar. **Efficacy of keratinocyte sheet cultured in temperature responsive dish in ovine burn wound healing.** The 4th Annual Cell Biology Student Symposium (May 25th, 2017).

10. Suzan Alharbi, Atsuyoshi Osada, Koji Ihara, Dannelys Bello-Perez, Perenlei Enkhbaatar. **In Vitro Comparison between Keratinocyte Sheet detachment by Low Temperature vs. Dispase.** The 3rd Annual Cell Biology Student Symposium (May 4th, 2016).

11. S. Alharbi, A. Prasai, A. El Ayadi, D. Herndon, C. Finnerty. **Adipose Derived Stem Cells Alter Fibroblast Extra Cellular Matrix Production.** The 4th TERMIS World Congress (September 8-11, 2015).

12. Michaela Sljivich, Suzan Alharbi, John Roesner, Deborah Boone, Rinat Esenaliev, Donald S. Prough, Maria-Adelaide Micci. **Effect of short laser therapy on svz neurogenesis in a rat model blast-inducaed neurotrauma.**

13. Suzan Alharbi. **Ultrastructural of three mouse embryonic stem cells: comparative study.** Next Gen Stem Cell Conference (May 8th-9th, 2013)

Oral presentations:

1. Will present Suzan Alharbi, Yosuke Niimi, Dominique Wiener, Hal Hawkins, Robert Cox, Vsevolod Popov, Atsuyoshi Osada, Hiroyuki Sakurai, David Herndon, Donald Prough, Perenlei Enkhbaatar**. Improving Third Degree Burn Wound Healing By Using Non-enzymatic Detachment Of Keratinocyte Sheets Cultured On Temperature Responsive Dishes.** TERMIS-AM annual meeting (2-5th December 2019).

2. Suzan Alharbi, Yosuke Niimi, Hal Hawkins, Robert Cox, Vsevolod Popov, Atsuyoshi Osada, Koji Ihara, Hiroyuki Sakurai, David Herndon, Perenlei Enkhbaatar. **Preserving the extra cellular matrix is critical for improving efficacy of keratinocyte sheets for treatment of burn wounds.** Experimental Biology Annual Meeting (April 6-9, 2019).

3. Suzan Alharbi, Yosuke Niimi, Hal Hawkins, Robert Cox, Vsevolod Popov, Atsuyoshi Osada, Koji Ihara, Hiroyuki Sakurai, David Herndon Donald Prough, Perenlei Enkhbaatar. **Novel method for keratinocyte sheet detachment improved their efficacy on ovine burn wound healing**. The 5th Annual Cell Biology Student Symposium, UTMB, Galveston, TX, USA (May 1ST, 2018).

4. Suzan Alharbi, Yosuke Niimi, Hal Hawkins, Robert Cox, Vsevolod L. Popov, Atsuyoshi Osada, Koji Ihara, Hiroyuki Sakurai, Perenlei Enkhbaatar. **Superior effect of temperature reduction detached keratinocyte sheets on ovine burn wound healing**. Neuroscience, Cell Biology and Anatomy Departmental Retreat, UTMB, Galveston, TX, USA (Dec. 14, 2017).

5. Suzan Alharbi. **Ultrastructural of three mouse embryonic stem cells: comparative study.** The second scientific conference of stem cells, King Saud University, Riyadh, Saudi Arabia (November, 2011)**.**

6. Suzan Alharbi. **Strategies of Embryonic Stem Cells Culture.** Summer training course for medical students, Stem Cell Unit, Riyadh, KSA (August, 2011).

PERMANENT ADDRESS: 8000-Villa 1
Almanar district
3607-23456, Jeddah, Saudi Arabia

This dissertation was typed by Suzan Alharbi

References

1. Brigham, P.A. and E. McLoughlin, *Burn incidence and medical care use in the United States: estimates, trends, and data sources.* J Burn Care Rehabil, 1996. **17**(2): p. 95-107.
2. Association, A.B., *National burn repository: report of date from 2006-2015*. 2016.
3. Hop, M.J., et al., *Costs of burn care: a systematic review.* Wound Repair Regen, 2014. **22**(4): p. 436-50.
4. Chu, D.H., *Chapter 7. Development and Structure of Skin*, in *Fitzpatrick's Dermatology in General Medicine, 8e*, L.A. Goldsmith, et al., Editors. 2012, The McGraw-Hill Companies: New York, NY.
5. Freedberg, I.M., et al., *Keratins and the keratinocyte activation cycle.* J Invest Dermatol, 2001. **116**(5): p. 633-40.
6. Fuchs, E., *Keratins and the skin.* Annu Rev Cell Dev Biol, 1995. **11**: p. 123-53.
7. Yin, T. and K.J. Green, *Regulation of desmosome assembly and adhesion.* Semin Cell Dev Biol, 2004. **15**(6): p. 665-77.
8. Schmidt, R., G. Melino, and E. Candi, *The cornified envelope: a model of cell death in the skin.* Nature Reviews Molecular Cell Biology, 2005. **6**(4): p. 328-340.
9. Segre, J.A., *Epidermal barrier formation and recovery in skin disorders.* Journal of Clinical Investigation, 2006. **116**(5): p. 1150-1158.
10. Elias, P.M., *Stratum corneum defensive functions: an integrated view.* J Invest Dermatol, 2005. **125**(2): p. 183-200.
11. Hyldig, K., et al., *Implications of Extracellular Matrix Production by Adipose Tissue-Derived Stem Cells for Development of Wound Healing Therapies.* Int J Mol Sci, 2017. **18**(6).
12. Burgeson, R.E. and M.E. Nimni, *Collagen types. Molecular structure and tissue distribution.* Clin Orthop Relat Res, 1992(282): p. 250-72.
13. Christiano, A.M. and J. Uitto, *Molecular pathology of the elastic fibers.* J Invest Dermatol, 1994. **103**(5 Suppl): p. 53s-57s.
14. Kielty, C.M. and C.A. Shuttleworth, *Microfibrillar elements of the dermal matrix.* Microsc Res Tech, 1997. **38**(4): p. 413-27.
15. Martins, V.L., M. Caley, and E.A. O'Toole, *Matrix metalloproteinases and epidermal wound repair.* Cell Tissue Res, 2013. **351**(2): p. 255-68.
16. Tandara, A.A. and T.A. Mustoe, *MMP- and TIMP-secretion by human cutaneous keratinocytes and fibroblasts – impact of coculture and hydration.* Journal of Plastic, Reconstructive & Aesthetic Surgery, 2011. **64**(1): p. 108-116.
17. Nagase, H., R. Visse, and G. Murphy, *Structure and function of matrix metalloproteinases and TIMPs.* Cardiovascular Research, 2006. **69**(3): p. 562-573.
18. Bruckner-Tuderman, L. and A.S. Payne, *Chapter 53. Epidermal and Epidermal–Dermal Adhesion*, in *Fitzpatrick's Dermatology in General Medicine, 8e*, L.A. Goldsmith, et al., Editors. 2012, The McGraw-Hill Companies: New York, NY.

19. Lowe, J.S., P.G. Anderson, and A. Stevens, *Stevens & Lowe's human histology*. Fourth ed. 2015, Philadelphia, PA: Elsevier/Mosby.
20. Ko, M.S. and M.P. Marinkovich, *Role of dermal-epidermal basement membrane zone in skin, cancer, and developmental disorders.* Dermatol Clin, 2010. **28**(1): p. 1-16.
21. Yurchenco, P.D., P.S. Amenta, and B.L. Patton, *Basement membrane assembly, stability and activities observed through a developmental lens.* Matrix Biol, 2004. **22**(7): p. 521-38.
22. Keene, D.R., M.P. Marinkovich, and L.Y. Sakai, *Immunodissection of the connective tissue matrix in human skin.* Microsc Res Tech, 1997. **38**(4): p. 394-406.
23. Eady, R.A., J.A. McGrath, and J.R. McMillan, *Ultrastructural clues to genetic disorders of skin: the dermal-epidermal junction.* J Invest Dermatol, 1994. **103**(5 Suppl): p. 13s-18s.
24. Palade, G.E. and M.G. Farquhar, *A special fibril of the dermis.* J Cell Biol, 1965. **27**(1): p. 215-24.
25. Keene, D.R., et al., *Type VII collagen forms an extended network of anchoring fibrils.* J Cell Biol, 1987. **104**(3): p. 611-21.
26. Ramirez, F. and L.Y. Sakai, *Biogenesis and function of fibrillin assemblies.* Cell Tissue Res, 2010. **339**(1): p. 71-82.
27. Avram, A.S., M.M. Avram, and W.D. James, *Subcutaneous fat in normal and diseased states: 2. Anatomy and physiology of white and brown adipose tissue.* J Am Acad Dermatol, 2005. **53**(4): p. 671-83.
28. Avram, M.M., A.S. Avram, and W.D. James, *Subcutaneous fat in normal and diseased states 3. Adipogenesis: from stem cell to fat cell.* J Am Acad Dermatol, 2007. **56**(3): p. 472-92.
29. Singer, A.J. and R.A. Clark, *Cutaneous wound healing.* N Engl J Med, 1999. **341**(10): p. 738-46.
30. Strodtbeck, F., *Physiology of wound healing.* Newborn and Infant Nursing Reviews, 2001. **1**(1): p. 43-52.
31. Reinke, J.M. and H. Sorg, *Wound repair and regeneration.* Eur Surg Res, 2012. **49**(1): p. 35-43.
32. Robson, M.C., D.L. Steed, and M.G. Franz, *Wound healing: biologic features and approaches to maximize healing trajectories.* Curr Probl Surg, 2001. **38**(2): p. 72-140.
33. Reinke, J.M. and H. Sorg, *Wound Repair and Regeneration.* European Surgical Research, 2012. **49**(1): p. 35-43.
34. Eming, S.A., T. Krieg, and J.M. Davidson, *Inflammation in wound repair: molecular and cellular mechanisms.* J Invest Dermatol, 2007. **127**(3): p. 514-25.
35. Gurtner, G.C., et al., *Wound repair and regeneration.* Nature, 2008. **453**(7193): p. 314-21.
36. Arnold, F. and D.C. West, *Angiogenesis in wound healing.* Pharmacol Ther, 1991. **52**(3): p. 407-22.
37. Lau, K., et al., *Exploring the role of stem cells in cutaneous wound healing.* Exp Dermatol, 2009. **18**(11): p. 921-33.

38. Miller, S.J., et al., *Re-epithelialization of porcine skin by the sweat apparatus.* J Invest Dermatol, 1998. **110**(1): p. 13-9.
39. Martin, P., *Wound healing--aiming for perfect skin regeneration.* Science, 1997. **276**(5309): p. 75-81.
40. Roh, C. and S. Lyle, *Cutaneous stem cells and wound healing.* Pediatric research, 2006. **59**(4 Pt 2): p. 100R-103R.
41. Shen, T., et al., *Accelerated healing of diabetic wound using artificial dermis constructed with adipose stem cells and poly (L-glutamic acid)/chitosan scaffold.* Chin Med J (Engl), 2013. **126**(8): p. 1498-503.
42. Jacinto, A., A. Martinez-Arias, and P. Martin, *Mechanisms of epithelial fusion and repair.* Nat Cell Biol, 2001. **3**(5): p. E117-23.
43. Goliger, J.A. and D.L. Paul, *Wounding alters epidermal connexin expression and gap junction-mediated intercellular communication.* Mol Biol Cell, 1995. **6**(11): p. 1491-501.
44. Gabbiani, G., C. Chaponnier, and I. Huttner, *Cytoplasmic filaments and gap junctions in epithelial cells and myofibroblasts during wound healing.* J Cell Biol, 1978. **76**(3): p. 561-8.
45. Clark, R.A., et al., *Fibronectin and fibrin provide a provisional matrix for epidermal cell migration during wound reepithelialization.* J Invest Dermatol, 1982. **79**(5): p. 264-9.
46. Liu, Y., et al., *Hypoxia regulates vascular endothelial growth factor gene expression in endothelial cells. Identification of a 5' enhancer.* Circ Res, 1995. **77**(3): p. 638-43.
47. Krafts, K.P., *Tissue repair: The hidden drama.* Organogenesis, 2010. **6**(4): p. 225-33.
48. Enoch, S. and D.J. Leaper, *Basic science of wound healing.* Surgery - Oxford International Edition, 2008. **26**(2): p. 31-37.
49. Nauta, A., G. Gurtner, and M.T. Longaker, *Wound healing and regenerative strategies.* Oral Dis, 2011. **17**(6): p. 541-9.
50. Singer, A.J. and R.A.F. Clark, *Cutaneous Wound Healing.* New England Journal of Medicine, 1999. **341**(10): p. 738-746.
51. Eckes, B., R. Nischt, and T. Krieg, *Cell-matrix interactions in dermal repair and scarring.* Fibrogenesis Tissue Repair, 2010. **3**: p. 4.
52. Barker, T.H., *The role of ECM proteins and protein fragments in guiding cell behavior in regenerative medicine.* Biomaterials, 2011. **32**(18): p. 4211-4.
53. Greenhalgh, D.G., *The role of apoptosis in wound healing.* Int J Biochem Cell Biol, 1998. **30**(9): p. 1019-30.
54. Hinz, B., *Formation and Function of the Myofibroblast during Tissue Repair.* Journal of Investigative Dermatology, 2007. **127**(3): p. 526-537.
55. Madden, J.W. and E.E. Peacock, *Studies on the biology of collagen during wound healing. 3. Dynamic metabolism of scar collagen and remodeling of dermal wounds.* Ann Surg, 1971. **174**(3): p. 511-20.
56. Saarialho-Kere, U.K., *Patterns of matrix metalloproteinase and TIMP expression in chronic ulcers.* Arch Dermatol Res, 1998. **290 Suppl**: p. S47-54.

57. Mignatti, P., et al., *Proteinases and Tissue Remodeling*, in *The Molecular and Cellular Biology of Wound Repair*, R.A.F. Clark, Editor. 1988, Springer US: Boston, MA. p. 427-474.
58. Gurtner, G.C. and G.R. Evans, *Advances in head and neck reconstruction.* Plast Reconstr Surg, 2000. **106**(3): p. 672-82; quiz 683.
59. Tziotzios, C., C. Profyris, and J. Sterling, *Cutaneous scarring: Pathophysiology, molecular mechanisms, and scar reduction therapeutics Part II. Strategies to reduce scar formation after dermatologic procedures.* J Am Acad Dermatol, 2012. **66**(1): p. 13-24; quiz 25-6.
60. Greenhalgh, D.G., *Management of Burns.* New England Journal of Medicine, 2019. **380**(24): p. 2349-2359.
61. Wooldridge, M. and J.A. Surveyer, *Skin Grafting for Full-Thickness Burn Injury.* The American Journal of Nursing, 1980. **80**(11): p. 2000-2004.
62. Sood, R., et al., *Cultured epithelial autografts for coverage of large burn wounds in eighty-eight patients: the Indiana University experience.* J Burn Care Res, 2010. **31**(4): p. 559-68.
63. McHeik, J.N., et al., *Epidermal healing in burns: autologous keratinocyte transplantation as a standard procedure: update and perspective.* Plast Reconstr Surg Glob Open, 2014. **2**(9): p. e218.
64. Herndon, D.N., et al., *A comparison of conservative versus early excision. Therapies in severely burned patients.* Ann Surg, 1989. **209**(5): p. 547-52; discussion 552-3.
65. Burke, J.F., et al., *Temporary skin transplantation and immunosuppression for extensive burns.* N Engl J Med, 1974. **290**(5): p. 269-71.
66. Shevchenko, R.V., S.L. James, and S.E. James, *A review of tissue-engineered skin bioconstructs available for skin reconstruction.* J R Soc Interface, 2010. **7**(43): p. 229-58.
67. *Wound healing and wound infection: Theory and surgical practice*. 1980, New York, NY: Appleton-Century-Crofts.
68. Desai, M.H., et al., *Early burn wound excision significantly reduces blood loss.* Annals of Surgery, 1990. **211**(6): p. 753-762.
69. Saaiq, M., S. Zaib, and S. Ahmad, *Early excision and grafting versus delayed excision and grafting of deep thermal burns up to 40% total body surface area: a comparison of outcome.* Annals of Burns and Fire Disasters, 2012. **25**(3): p. 143-147.
70. Puri, V., et al., *Comparative Analysis of Early Excision and Grafting vs Delayed Grafting in Burn Patients in a Developing Country.* J Burn Care Res, 2016. **37**(5): p. 278-82.
71. Cubison, T.C., S.A. Pape, and N. Parkhouse, *Evidence for the link between healing time and the development of hypertrophic scars (HTS) in paediatric burns due to scald injury.* Burns, 2006. **32**(8): p. 992-9.
72. Rowan, M.P., et al., *Burn wound healing and treatment: review and advancements.* Critical Care (London, England), 2015. **19**(1): p. 243.
73. Stanton, R.A. and D.A. Billmire, *Skin resurfacing for the burned patient.* Clin Plast Surg, 2002. **29**(1): p. 29-51.

74. Akan, M., et al., *An alternative method to minimize pain in the split-thickness skin graft donor site.* Plast Reconstr Surg, 2003. **111**(7): p. 2243-9.
75. Papini, R., *Management of burn injuries of various depths*, in *BMJ*. 2004. p. 158-60.
76. Hermans, M.H., *Preservation methods of allografts and their (lack of) influence on clinical results in partial thickness burns.* Burns, 2011. **37**(5): p. 873-81.
77. Bettman, A.G., *Homogenous thiersch grafting as a life saving measure.* The American Journal of Surgery. **39**(1): p. 156-162.
78. Wood, F.M., M.L. Kolybaba, and P. Allen, *The use of cultured epithelial autograft in the treatment of major burn wounds: eleven years of clinical experience.* Burns, 2006. **32**(5): p. 538-44.
79. Zare, S., et al., *Regenerative Medicine: Novel Approach in Burn Wound Healing.* Journal of Skin and Stem Cell, 2015. **2**(2).
80. Kamel, R.A., et al., *Tissue Engineering of Skin.* Journal of the American College of Surgeons, 2013. **217**(3): p. 533-555.
81. Ehrenreich, M. and Z. Ruszczak, *Tissue-engineered temporary wound coverings. Important options for the clinician.* Acta Dermatovenerol Alp Pannonica Adriat, 2006. **15**(1): p. 5-13.
82. Groeber, F., et al., *Skin tissue engineering--in vivo and in vitro applications.* Adv Drug Deliv Rev, 2011. **63**(4-5): p. 352-66.
83. Mansbridge, J.N., *Tissue-engineered skin substitutes in regenerative medicine.* Curr Opin Biotechnol, 2009. **20**(5): p. 563-7.
84. Catalano, E., et al., *Tissue-engineered skin substitutes: an overview.* J Artif Organs, 2013. **16**(4): p. 397-403.
85. Ehrenreich, M. and Z. Ruszczak, *Update on tissue-engineered biological dressings.* Tissue Eng, 2006. **12**(9): p. 2407-24.
86. Mansbridge, J., *Skin tissue engineering.* J Biomater Sci Polym Ed, 2008. **19**(8): p. 955-68.
87. Jeschke, M.G., et al., *Wound Coverage Technologies in Burn Care: Novel Techniques.* J Burn Care Res, 2013. **34**(6).
88. Supp, D.M. and S.T. Boyce, *Engineered skin substitutes: practices and potentials.* Clin Dermatol, 2005. **23**(4): p. 403-12.
89. Tang, Z. and T. Okano, *Recent development of temperature-responsive surfaces and their application for cell sheet engineering.* Regen Biomater, 2014. **1**(1): p. 91-102.
90. Leclerc, T., et al., *Cell therapy of burns.* Cell Prolif, 2011. **44 Suppl 1**: p. 48-54.
91. Navarro, F.A., et al., *Sprayed keratinocyte suspensions accelerate epidermal coverage in a porcine microwound model.* J Burn Care Rehabil, 2000. **21**(6): p. 513-8.
92. Grant, I., et al., *The co-application of sprayed cultured autologous keratinocytes and autologous fibrin sealant in a porcine wound model.* Br J Plast Surg, 2002. **55**(3): p. 219-27.
93. MacNeil, S., *Progress and opportunities for tissue-engineered skin.* Nature, 2007. **445**(7130): p. 874-880.

94. Ronfard, V., et al., *Long-term regeneration of human epidermis on third degree burns transplanted with autologous cultured epithelium grown on a fibrin matrix.* Transplantation, 2000. **70**(11): p. 1588-98.
95. Gao, Z.R., et al., *Coverage of full skin thickness burns with allograft inoculated with autogenous epithelial cells.* Burns Incl Therm Inj, 1986. **12**(3): p. 220-4.
96. Chester, D.L., D.S. Balderson, and R.P. Papini, *A review of keratinocyte delivery to the wound bed.* J Burn Care Rehabil, 2004. **25**(3): p. 266-75.
97. Billingham, R.E. and J. Reynolds, *Transplantation studies on sheets of pure epidermal epithelium and on epidermal cell suspensions.* Br J Plast Surg, 1952. **5**(1): p. 25-36.
98. Stark, G.B., et al., *Cultured autologous keratinocytes suspended in fibrin glue (KFGS) with allogenic overgraft for definitive burn wound coverage.* European Journal of Plastic Surgery, 1995. **18**(6): p. 267-271.
99. Kaiser, H.W., et al., *Cultured autologous keratinocytes in fibrin glue suspension, exclusively and combined with STS-allograft (preliminary clinical and histological report of a new technique).* Burns, 1994. **20**(1): p. 23-9.
100. Hunyadi, J., et al., *Keratinocyte grafting: covering of skin defects by separated autologous keratinocytes in a fibrin net.* J Invest Dermatol, 1987. **89**(1): p. 119-20.
101. Hernon, C.A., et al., *Clinical experience using cultured epithelial autografts leads to an alternative methodology for transferring skin cells from the laboratory to the patient.* Regen Med, 2006. **1**(6): p. 809-21.
102. Suzuki, K., et al., *Dynamics and mediators of acute graft attrition after myoblast transplantation to the heart.* Faseb j, 2004. **18**(10): p. 1153-5.
103. Hofmann, M., et al., *Monitoring of bone marrow cell homing into the infarcted human myocardium.* Circulation, 2005. **111**(17): p. 2198-202.
104. Hefton, J.M., et al., *Loss of HLA-DR expression by human epidermal cells after growth in culture.* J Invest Dermatol, 1984. **83**(1): p. 48-50.
105. Basham, T.Y., et al., *Recombinant Gamma Interferon Induces HLA-DR Expression on Cultured Human Keratinocytes.* Journal of Investigative Dermatology, 1984. **83**(2): p. 88-90.
106. Madden, M.R., et al., *Grafting of cultured allogeneic epidermis on second- and third-degree burn wounds on 26 patients.* J Trauma, 1986. **26**(11): p. 955-62.
107. *Grafting of burns with cultured epithelium prepared from autologous epidermal cells.* Lancet, 1981. **1**(8211): p. 75-8.
108. Gallico, G.G., 3rd, et al., *Permanent coverage of large burn wounds with autologous cultured human epithelium.* N Engl J Med, 1984. **311**(7): p. 448-51.
109. Atiyeh, B.S. and M. Costagliola, *Cultured epithelial autograft (CEA) in burn treatment: three decades later.* Burns, 2007. **33**(4): p. 405-13.
110. Fang, T., et al., *Clinical application of cultured epithelial autografts on acellular dermal matrices in the treatment of extended burn injuries.* Ann Plast Surg, 2014. **73**(5): p. 509-15.
111. Desai, M.H., et al., *Lack of long-term durability of cultured keratinocyte burn-wound coverage: a case report.* J Burn Care Rehabil, 1991. **12**(6): p. 540-5.

112. Adams, J.C. and F.M. Watt, *Changes in keratinocyte adhesion during terminal differentiation: reduction in fibronectin binding precedes alpha 5 beta 1 integrin loss from the cell surface.* Cell, 1990. **63**(2): p. 425-35.
113. Hotchin, N.A. and F.M. Watt, *Transcriptional and post-translational regulation of beta 1 integrin expression during keratinocyte terminal differentiation.* J Biol Chem, 1992. **267**(21): p. 14852-8.
114. Poumay, Y. and M.R. Pittelkow, *Cell density and culture factors regulate keratinocyte commitment to differentiation and expression of suprabasal K1/K10 keratins.* J Invest Dermatol, 1995. **104**(2): p. 271-6.
115. Green, H., O. Kehinde, and J. Thomas, *Growth of cultured human epidermal cells into multiple epithelia suitable for grafting.* Proc Natl Acad Sci U S A, 1979. **76**(11): p. 5665-8.
116. Stenn, K.S., et al., *Dispase, a neutral protease from Bacillus polymyxa, is a powerful fibronectinase and type IV collagenase.* J Invest Dermatol, 1989. **93**(2): p. 287-90.
117. Yamato, M., et al., *Thermo-responsive culture dishes allow the intact harvest of multilayered keratinocyte sheets without dispase by reducing temperature.* Tissue Eng, 2001. **7**(4): p. 473-80.
118. Osada, A., et al., *Harvesting epithelial keratinocyte sheets from temperature-responsive dishes preserves basement membrane proteins and improves cell survival in a skin defect model.* J Tissue Eng Regen Med, 2016.
119. Poumay, Y., et al., *Specific internalization of basal membrane domains containing the integrin alpha 6 beta 4 in dispase-detached cultured human keratinocytes.* Eur J Cell Biol, 1993. **60**(1): p. 12-20.
120. Schaefer, B.M., et al., *Dispase-mediated basal detachment of cultured keratinocytes induces urokinase-type plasminogen activator (uPA) and its receptor (uPA-R, CD87).* Exp Cell Res, 1996. **228**(2): p. 246-53.
121. Reinartz, J., et al., *The receptor for urokinase-type plasminogen activator of a human keratinocyte line (HaCaT).* Exp Cell Res, 1994. **214**(2): p. 486-98.
122. Wei, Q., et al., *Keratinocyte cytoskeletal roles in cell sheet engineering.* BMC Biotechnol, 2013. **13**: p. 17.
123. Takeda, A., et al., *Pretreatment of human keratinocyte sheets with laminin 5 improves their grafting efficiency.* J Invest Dermatol, 1999. **113**(1): p. 38-42.
124. Carver, N., et al., *Restoration of basement membrane structure in pigs following keratinocyte autografting.* Br J Plast Surg, 1993. **46**(5): p. 384-92.
125. Putland, M., et al., *Histologic comparison of cultured epithelial autograft and meshed expanded split-thickness skin graft.* J Burn Care Rehabil, 1995. **16**(6): p. 627-40.
126. Okano, T., et al., *A novel recovery system for cultured cells using plasma-treated polystyrene dishes grafted with poly(N-isopropylacrylamide).* J Biomed Mater Res, 1993. **27**(10): p. 1243-51.
127. Yamada, N., et al., *Thermo-responsive polymeric surfaces; control of attachment and detachment of cultured cells.* Die Makromolekulare Chemie, Rapid Communications, 1990. **11**(11): p. 571-576.

128. Yamato, M., et al., *Temperature-responsive cell culture surfaces for regenerative medicine with cell sheet engineering.* Progress in Polymer Science, 2007. **32**(8): p. 1123-1133.
129. Forte, G., et al., *Cardiac Muscle Engineering: Strategies to Deliver Stem Cells to the Damaged Site*, in *Tissue Engineering for Tissue and Organ Regeneration*, D. Eberli, Editor. 2011, InTech: Rijeka. p. Ch. 02.
130. Waymouth, C., *To disaggregate or not to disaggregate injury and cell disaggregation, transient or permanent?* In Vitro, 1974. **10**: p. 97-111.
131. Revel, J.P., P. Hoch, and D. Ho, *Adhesion of culture cells to their substratum.* Exp Cell Res, 1974. **84**(1): p. 207-18.
132. Osunkoya, B.O., et al., *Synthesis and fate of immunological surface receptors on cultured burkitt lymphoma cells.* International Journal of Cancer, 2017. **4**(2): p. 159-165.
133. Cerqueira, M.T., et al., *Cell sheet technology-driven re-epithelialization and neovascularization of skin wounds.* Acta Biomater, 2014. **10**(7): p. 3145-55.
134. Kushida, A., et al., *Decrease in culture temperature releases monolayer endothelial cell sheets together with deposited fibronectin matrix from temperature-responsive culture surfaces.* J Biomed Mater Res, 1999. **45**(4): p. 355-62.
135. Yamato, M., et al., *Signal transduction and cytoskeletal reorganization are required for cell detachment from cell culture surfaces grafted with a temperature-responsive polymer.* J Biomed Mater Res, 1999. **44**(1): p. 44-52.
136. Ebara, M., et al., *Temperature-responsive cell culture surfaces enable "on-off" affinity control between cell integrins and RGDS ligands.* Biomacromolecules, 2004. **5**(2): p. 505-10.
137. Kobayashi, J., et al., *Surface design of antibody-immobilized thermoresponsive cell culture dishes for recovering intact cells by low-temperature treatment.* J Biomed Mater Res A, 2014. **102**(11): p. 3883-93.
138. Arisaka, Y., et al., *Switching of cell growth/detachment on heparin-functionalized thermoresponsive surface for rapid cell sheet fabrication and manipulation.* Biomaterials, 2013. **34**(17): p. 4214-22.
139. Nishida, K., et al., *Functional bioengineered corneal epithelial sheet grafts from corneal stem cells expanded ex vivo on a temperature-responsive cell culture surface.* Transplantation, 2004. **77**(3): p. 379-85.
140. Nishida, K., et al., *Corneal reconstruction with tissue-engineered cell sheets composed of autologous oral mucosal epithelium.* N Engl J Med, 2004. **351**(12): p. 1187-96.
141. Kushida, A., et al., *A noninvasive transfer system for polarized renal tubule epithelial cell sheets using temperature-responsive culture dishes.* Eur Cell Mater, 2005. **10**: p. 23-30; discussion 23-30.
142. Akizuki, T., et al., *Application of periodontal ligament cell sheet for periodontal regeneration: a pilot study in beagle dogs.* J Periodontal Res, 2005. **40**(3): p. 245-51.
143. Hasegawa, M., et al., *Human periodontal ligament cell sheets can regenerate periodontal ligament tissue in an athymic rat model.* Tissue Eng, 2005. **11**(3-4): p. 469-78.

144. Ebihara, G., et al., *Cartilage repair in transplanted scaffold-free chondrocyte sheets using a minipig model.* Biomaterials, 2012. **33**(15): p. 3846-51.
145. Yaguchi, Y., et al., *Middle ear mucosal regeneration with three-dimensionally tissue-engineered autologous middle ear cell sheets in rabbit model.* J Tissue Eng Regen Med, 2016. **10**(3): p. E188-94.
146. Shimizu, H., et al., *Topographical Arrangement of α- and β-Cells Within Neo-islet Tissues Engineered by Islet Cell Sheet Transplantation in Mice.* Transplantation Proceedings. **45**(5): p. 1881-1884.
147. Ohashi, K., et al., *Engineering functional two- and three-dimensional liver systems in vivo using hepatic tissue sheets.* Nat Med, 2007. **13**(7): p. 880-5.
148. Arauchi, A., et al., *Tissue-engineered thyroid cell sheet rescued hypothyroidism in rat models after receiving total thyroidectomy comparing with nontransplantation models.* Tissue Eng Part A, 2009. **15**(12): p. 3943-9.
149. Shimizu, T., et al., *Long-term survival and growth of pulsatile myocardial tissue grafts engineered by the layering of cardiomyocyte sheets.* Tissue Eng, 2006. **12**(3): p. 499-507.
150. Miyahara, Y., et al., *Monolayered mesenchymal stem cells repair scarred myocardium after myocardial infarction.* Nat Med, 2006. **12**(4): p. 459-65.
151. Burillon, C., et al., *Cultured autologous oral mucosal epithelial cell sheet (CAOMECS) transplantation for the treatment of corneal limbal epithelial stem cell deficiency.* Invest Ophthalmol Vis Sci, 2012. **53**(3): p. 1325-31.
152. Ohki, T., et al., *Prevention of esophageal stricture after endoscopic submucosal dissection using tissue-engineered cell sheets.* Gastroenterology, 2012. **143**(3): p. 582-588.e2.
153. Sawa, Y., et al., *Tissue engineered myoblast sheets improved cardiac function sufficiently to discontinue LVAS in a patient with DCM: report of a case.* Surg Today, 2012. **42**(2): p. 181-4.
154. Iwata, T., et al., *Cell sheet engineering and its application for periodontal regeneration.* J Tissue Eng Regen Med, 2015. **9**(4): p. 343-56.
155. Abdullahi, A., S. Amini-Nik, and M. Jeschke, *Animal Models in Burn Research.* Cell Mol Life Sci, 2014. **71**(17): p. 3241-55.
156. Dahiya, P., *Burns as a model of SIRS.* Front Biosci (Landmark Ed), 2009. **14**: p. 4962-7.
157. Wong, V.W., et al., *Surgical approaches to create murine models of human wound healing.* J Biomed Biotechnol, 2011. **2011**: p. 969618.
158. Dorsett-Martin, W.A., *Rat models of skin wound healing: a review.* Wound Repair Regen, 2004. **12**(6): p. 591-9.
159. Li, J., J. Chen, and R. Kirsner, *Pathophysiology of acute wound healing.* Clin Dermatol, 2007. **25**(1): p. 9-18.
160. Sullivan, T.P., et al., *The pig as a model for human wound healing.* Wound Repair Regen, 2001. **9**(2): p. 66-76.
161. Abdullahi, A., S. Amini-Nik, and M.G. Jeschke, *Animal Models in Burn Research.* Cell Mol Life Sci, 2014. **71**(17): p. 3241-55.
162. Traber, D.L., R.E. Barrow, and D.N. Herndon, *31 - Animal Models of Burn Injury A2 - Souba, Wiley W*, in *Surgical Research*, D.W. Wilmore, Editor. 2001, Academic Press: San Diego. p. 367-377.

163. Tokyay, R., et al., *Effects of hypertonic saline dextran resuscitation on oxygen delivery, oxygen consumption, and lipid peroxidation after burn injury.* J Trauma, 1992. **32**(6): p. 704-12; discussion 712-3.
164. Horne, R.S., et al., *Wound healing in foetal sheep: a histological and electron microscope study.* Br J Plast Surg, 1992. **45**(5): p. 333-44.
165. Ito, H., et al., *Healing efficacy of sea buckthorn (Hippophae rhamnoides L.) seed oil in an ovine burn wound model.* Burns, 2014. **40**(3): p. 511-9.
166. Jonkam, C.C., et al., *Effects of the bradykinin B2 receptor antagonist icatibant on microvascular permeability after thermal injury in sheep.* Shock, 2007. **28**(6): p. 704-9.
167. Lange, M., et al., *Combined neuronal and inducible nitric oxide synthase inhibition in ovine acute lung injury.* Crit Care Med, 2009. **37**(1): p. 223-9.
168. Enkhbaatar, P., et al., *Inhibition of neuronal nitric oxide synthase by 7-nitroindazole attenuates acute lung injury in an ovine model.* Am J Physiol Regul Integr Comp Physiol, 2003. **285**(2): p. R366-72.
169. Alpard, S.K., et al., *New clinically relevant sheep model of severe respiratory failure secondary to combined smoke inhalation/cutaneous flame burn injury.* Crit Care Med, 2000. **28**(5): p. 1469-76.
170. Enkhbaatar, P., et al., *The inducible nitric oxide synthase inhibitor BBS-2 prevents acute lung injury in sheep after burn and smoke inhalation injury.* Am J Respir Crit Care Med, 2003. **167**(7): p. 1021-6.
171. Enkhbaatar, P., et al., *Novel ovine model of methicillin-resistant Staphylococcus aureus-induced pneumonia and sepsis.* Shock, 2008. **29**(5): p. 642-9.
172. Scully, C.G., et al., *Effect of hemorrhage rate on early hemodynamic responses in conscious sheep.* Physiol Rep, 2016. **4**(7).
173. Proksch, E. and J.-M. Jensen, *Chapter 47. Skin as an Organ of Protection*, in *Fitzpatrick's Dermatology in General Medicine, 8e*, L.A. Goldsmith, et al., Editors. 2012, The McGraw-Hill Companies: New York, NY.
174. Ter Horst, B., et al., *Advances in keratinocyte delivery in burn wound care.* Adv Drug Deliv Rev, 2018. **123**: p. 18-32.
175. Wood, F.M., M.L. Kolybaba, and P. Allen, *The use of cultured epithelial autograft in the treatment of major burn injuries: a critical review of the literature.* Burns, 2006. **32**(4): p. 395-401.
176. Boudreau, N.J. and P.L. Jones, *Extracellular matrix and integrin signalling: the shape of things to come.* The Biochemical journal, 1999. **339 (Pt 3)**(Pt 3): p. 481-488.
177. Hynes, R.O., *Integrins: Bidirectional, Allosteric Signaling Machines.* Cell, 2002. **110**(6): p. 673-687.
178. Giancotti, F.G. and E. Ruoslahti, *Integrin Signaling.* Science, 1999. **285**(5430): p. 1028.
179. Schulze, A., et al., *Analysis of the transcriptional program induced by Raf in epithelial cells.* Genes & Development, 2001. **15**(8): p. 981-994.
180. Yin, T., et al., *Mechanisms of plakoglobin-dependent adhesion: desmosome-specific functions in assembly and regulation by epidermal growth factor receptor.* J Biol Chem, 2005. **280**(48): p. 40355-63.

181. Matsumine, H., et al., *Keratinocyte sheets prepared with temperature-responsive dishes show enhanced survival after in vivo grafting on acellular dermal matrices in a rat model of staged bi-layered skin reconstruction.* Regenerative Therapy, 2019. **11**: p. 167-175.
182. Hamill, K.J., et al., *Fibronectin expression determines skin cell motile behavior.* The Journal of investigative dermatology, 2012. **132**(2): p. 448-457.
183. Wilke, M.S. and L.T. Furcht, *Human Keratinocytes Adhere to a Unique Heparin-Binding Peptide Sequence Within the Triple Helical Region of Type IV Collagen.* Journal of Investigative Dermatology, 1990. **95**(3): p. 264-270.
184. Woodley, D.T., K.C. Wynn, and E.J. O'Keefe, *Type IV Collagen and Fibronectin Enhance Human Keratinocyte Thymidine Incorporation and Spreading in the Absence of Soluble Growth Factors.* Journal of Investigative Dermatology, 1990. **94**(1): p. 139-143.
185. Tjin, M.S., et al., *Human Epidermal Keratinocyte Cell Response on Integrin-Specific Artificial Extracellular Matrix Proteins.* Macromolecular Bioscience, 2014. **14**(8): p. 1125-1134.
186. Lim, L.S., et al., *Effect of dispase denudation on amniotic membrane.* Molecular vision, 2009. **15**: p. 1962-1970.
187. Fujisaki, H., E. Adachi, and S. Hattori, *Keratinocyte Differentiation and Proliferation are Regulated by Adhesion to the Three-Dimensional Meshwork Structure of Type IV Collagen.* Connective Tissue Research, 2008. **49**(6): p. 426-436.
188. Manohar, A., et al., *α3β1 integrin promotes keratinocyte cell survival through activation of a MEK/ERK signaling pathway.* Journal of Cell Science, 2004. **117**(18): p. 4043.
189. Gonzales, M., et al., *A Cell Signal Pathway Involving Laminin-5, α3β1 Integrin, and Mitogen-activated Protein Kinase Can Regulate Epithelial Cell Proliferation.* Molecular Biology of the Cell, 1999. **10**(2): p. 259-270.
190. Matsubayashi, Y., et al., *ERK Activation Propagates in Epithelial Cell Sheets and Regulates Their Migration during Wound Healing.* Current Biology, 2004. **14**(8): p. 731-735.
191. Frixione, E. and M. Hernández, *1.26 - Structural Organization of Cells – The Cytoskeleton*, in *Comprehensive Biotechnology (Second Edition)*, M. Moo-Young, Editor. 2011, Academic Press: Burlington. p. 367-381.
192. Mooney, D.J., R. Langer, and D.E. Ingber, *Cytoskeletal filament assembly and the control of cell spreading and function by extracellular matrix.* Journal of Cell Science, 1995. **108**(6): p. 2311.
193. Wang, N., J.P. Butler, and D.E. Ingber, *Mechanotransduction across the cell surface and through the cytoskeleton.* Science, 1993. **260**(5111): p. 1124.
194. Ananthakrishnan, R. and A. Ehrlicher, *The forces behind cell movement.* International journal of biological sciences, 2007. **3**(5): p. 303-317.
195. Schoenwaelder, S.M. and K. Burridge, *Bidirectional signaling between the cytoskeleton and integrins.* Current Opinion in Cell Biology, 1999. **11**(2): p. 274-286.
196. Wei, Q., V. Hariharan, and H. Huang, *Cell-Cell Contact Preserves Cell Viability via Plakoglobin.* PLOS ONE, 2011. **6**(10): p. e27064.

197. Muniandy, K., et al., *In Vitro Wound Healing Potential of Stem Extract of Alternanthera sessilis.* Evidence-based complementary and alternative medicine : eCAM, 2018. **2018**: p. 3142073-3142073.
198. Moulin, V., et al., *In vitro models to study wound healing fibroblasts.* Burns, 1996. **22**(5): p. 359-362.
199. Coolen, N.A., et al., *Development of an in vitro burn wound model.* Wound Repair and Regeneration, 2008. **16**(4): p. 559-567.
200. Emanuelsson, P. and G. Kratz, *Characterization of a new in vitro burn wound model.* Burns, 1997. **23**(1): p. 32-36.
201. Baudoin, J., et al., *Topical Negative Pressure on Burns: An Innovative Method for Wound Exudate Collection.* Plastic and reconstructive surgery. Global open, 2016. **4**(11): p. e1117-e1117.
202. Widgerow, A.D., et al., *The burn wound exudate—An under-utilized resource.* Burns, 2015. **41**(1): p. 11-17.
203. Pan, S.-C., et al., *Deep partial thickness burn blister fluid promotes neovascularization in the early stage of burn wound healing.* Wound Repair and Regeneration, 2010. **18**(3): p. 311-318.
204. Wilson, A.M., et al., *The effect of burn blister fluid on fibroblast contraction.* Burns, 1997. **23**(4): p. 306-312.
205. Berger, M.M., et al., *Cutaneous copper and zinc losses in burns.* Burns, 1992. **18**(5): p. 373-380.
206. Grinnell, F. and M. Zhu, *Fibronectin Degradation in Chronic Wounds Depends on the Relative Levels of Elastase, α1-Proteinase Inhibitor, and α2-Macroglobulin.* Journal of Investigative Dermatology, 1996. **106**(2): p. 335-341.
207. Klopfer, M., et al., *A fluid collection system for dermal wounds in clinical investigations.* Biomicrofluidics, 2016. **10**(2): p. 024113-024113.
208. Inoue, M., et al., *Effects of cytokines in burn blister fluids on fibroblast proliferation and their inhibition with the use of neutralizing antibodies.* Wound Repair and Regeneration, 1996. **4**(4): p. 426-432.
209. Croft, C.B. and D. Tarin, *Ultrastructural studies of wound healing in mouse skin. I. Epithelial behaviour.* Journal of anatomy, 1970. **106**(Pt 1): p. 63-77.
210. Kainulainen, T., et al., *Laminin-5 Expression Is Independent of the Injury and the Microenvironment During Reepithelialization of Wounds.* Journal of Histochemistry & Cytochemistry, 1998. **46**(3): p. 353-360.
211. Laplante, A.F., et al., *Mechanisms of wound reepithelialization: hints from a tissue-engineered reconstructed skin to long-standing questions.* The FASEB Journal, 2001. **15**(13): p. 2377-2389.
212. Iorio, V., L.D. Troughton, and K.J. Hamill, *Laminins: Roles and Utility in Wound Repair.* Advances in wound care, 2015. **4**(4): p. 250-263.
213. Kurpakus, M.A., E.L. Stock, and J.C. Jones, *Analysis of wound healing in an in vitro model: early appearance of laminin and a 125 × 10(3) Mr polypeptide during adhesion complex formation.* Journal of Cell Science, 1990. **96**(4): p. 651.
214. Betz, P., et al., *The time-dependent rearrangement of the epithelial basement membrane in human skin wounds —immunohistochemical localization of Collagen IV and VII.* International Journal of Legal Medicine, 1992. **105**(2): p. 93-97.

215. Wolfe, R.A., et al., *Mortality differences and speed of wound closure among specialized burn care facilities.* Jama, 1983. **250**(6): p. 763-6.
216. Halim, A.S., T.L. Khoo, and S.J. Mohd. Yussof, *Biologic and synthetic skin substitutes: An overview*, in *Indian J Plast Surg*. 2010. p. S23-8.
217. Naoum, J.J., et al., *The use of homograft compared to topical antimicrobial therapy in the treatment of second-degree burns of more than 40% total body surface area.* Burns, 2004. **30**(6): p. 548-551.
218. See, P., et al., *Our Clinical Experience using Cryopreserved Cadaveric Allograft for the Management of Severe Burns.* Cell and Tissue Banking, 2001. **2**(2): p. 113-117.
219. Liu, H.-F., F. Zhang, and W.C. Lineaweaver, *History and Advancement of Burn Treatments.* Annals of Plastic Surgery, 2017. **78**(2).
220. Kreis, R.W., et al., *Historical appraisal of the use of skin allografts in the treatment of extensive full skin thickness burns at the Red Cross Hospital Burns centre, Beverwijk, The Netherlands.* Burns, 1992. **18**: p. S19-S22.
221. Vig, K., et al., *Advances in Skin Regeneration Using Tissue Engineering.* International journal of molecular sciences, 2017. **18**(4): p. 789.
222. Cuono, C.B., et al., *Composite Autologous-Allogeneic Skin Replacement: Development and Clinical Application.* Plastic and Reconstructive Surgery, 1987. **80**(4).
223. Fabre, J.W., *Epidermal allografts.* Immunology Letters, 1991. **29**(1): p. 161-165.
224. Gaucher, S., et al., *Viability of cryopreserved human skin allografts: effects of transport media and cryoprotectant.* Cell and Tissue Banking, 2012. **13**(1): p. 147-155.
225. Boekema, B.K.H.L., B. Boekestijn, and R.S. Breederveld, *Evaluation of saline, RPMI and DMEM/F12 for storage of split-thickness skin grafts.* Burns, 2015. **41**(4): p. 848-852.
226. Franchini, M., et al., *Evaluation of cryopreserved donor skin viability: the experience of the regional tissue bank of Verona.* Blood Transfus, 2009. **7**(2): p. 100-5.
227. Hautier, A., et al., *Assessment of organ culture for the conservation of human skin allografts.* Cell and Tissue Banking, 2008. **9**(1): p. 19-29.
228. DeBono, R., G.S. Rao, and R.B. Berry, *The Survival of Human Skin Stored by Refrigeration at 4°C in McCoy's 5A Medium: Does Oxygenation of the Medium Improve Storage Time?* Plastic and Reconstructive Surgery, 1998. **102**(1).
229. Fahmy, F.S., et al., *Skin graft storage and keratinocyte viability.* British Journal of Plastic Surgery, 1993. **46**(4): p. 292-295.
230. Leon-Villapalos, J., M. Eldardiri, and P. Dziewulski, *The use of human deceased donor skin allograft in burn care.* Cell and Tissue Banking, 2010. **11**(1): p. 99-104.
231. de Backere, A.C.J., *Euro skin bank: large scale skin-banking in Europe based on glycerol-preservation of donor skin.* Burns, 1994. **20**: p. S4-S9.
232. van Baare, J., et al., *Virucidal effect of glycerol as used in donor skin preservation.* Burns, 1994. **20**: p. S77-S80.

233. Khoo, T.L., et al., *The application of glycerol-preserved skin allograft in the treatment of burn injuries: An analysis based on indications.* Burns, 2010. **36**(6): p. 897-904.
234. Hussmann, J., et al., *Use of glycerolized human allografts as temporary (and permanent) cover in adults and children.* Burns, 1994. **20**: p. S61-S66.
235. Yun, S.-Y., et al., *Synergistic immunosuppressive effects of rosmarinic acid and rapamycin in vitro and in vivo1.* Transplantation, 2003. **75**(10).
236. Borel, J.F., et al., *Biological effects of cyclosporin A: A new antilymphocytic agent.* Agents and Actions, 1976. **6**(4): p. 468-475.
237. Lagodzinski, Z., A. Górski, and M. Wasik, *Effect of FK506 and cyclosporine on primary and secondary skin allograft survival in mice.* Immunology, 1990. **71**(1): p. 148-150.
238. *Quantitative assessment of mouse skin transplant rejection using digital photography.* Laboratory Animals, 2005. **39**(2): p. 209-214.
239. Pakyari, M., et al., *A new method for skin grafting in murine model.* Wound Repair and Regeneration, 2016. **24**(4): p. 695-704.
240. Racki, W.J., et al., *NOD-scid IL2rgamma(null) mouse model of human skin transplantation and allograft rejection.* Transplantation, 2010. **89**(5): p. 527-36.
241. Kirkiles-Smith, N.C., et al., *Human TNF Can Induce Nonspecific Inflammatory and Human Immune-Mediated Microvascular Injury of Pig Skin Xenografts in Immunodeficient Mouse Hosts.* The Journal of Immunology, 2000. **164**(12): p. 6601.
242. Rosenberg, A.S. and A. Singer, *Cellular Basis of Skin Allograft Rejection: An In Vivo Model of Immune-Mediated Tissue Destruction.* Annual Review of Immunology, 1992. **10**(1): p. 333-360.
243. Zhai, Q., et al., *An immune-competent rat split thickness skin graft model: useful tools to develop new therapies to improve skin graft survival.* American journal of translational research, 2018. **10**(6): p. 1600-1610.
244. Cheng, C.-H., et al., *Murine Full-thickness Skin Transplantation.* Journal of visualized experiments : JoVE, 2017(119): p. 55105.
245. Yoon, C., et al., *Comparison between cryopreserved and glycerol-preserved allografts in a partial-thickness porcine wound model.* Cell and Tissue Banking, 2016. **17**(1): p. 21-31.
246. Wachtel, T.L., et al., *Viability of frozen allografts.* The American Journal of Surgery, 1979. **138**(6): p. 783-787.
247. Castagnoli, C., et al., *Evaluation of donor skin viability: fresh and cryopreserved skin using tetrazolioum salt assay.* Burns, 2003. **29**(8): p. 759-767.
248. Wood, J.M.B., et al., *The biomechanical and histological sequelae of common skin banking methods.* Journal of Biomechanics, 2014. **47**(5): p. 1215-1219.
249. Haarstad, A.C., et al., *Isolation of bacterial skin flora of healthy sheep, with comparison between frequent and minimal human handling.* Veterinary Dermatology, 2014. **25**(3): p. 215-e56.
250. Kearney, J.N., *Guidelines on processing and clinical use of skin allografts.* Clinics in Dermatology, 2005. **23**(4): p. 357-364.
251. Britton-Byrd, B.W., et al., *Early Use of Allograft Skin: Are 3-Day Microbiologic Cultures Safe?* Journal of Trauma and Acute Care Surgery, 2008. **64**(3).

252. Pirnay, J.-P., et al., *Evaluation of a microbiological screening and acceptance procedure for cryopreserved skin allografts based on 14 day cultures.* Cell and tissue banking, 2012. **13**(2): p. 287-295.
253. Kua, E.H.J., et al., *Comparing the use of glycerol preserved and cryopreserved allogenic skin for the treatment of severe burns: differences in clinical outcomes and in vitro tissue viability.* Cell and Tissue Banking, 2012. **13**(2): p. 269-279.
254. Cleland, H., et al., *Clinical application and viability of cryopreserved cadaveric skin allografts in severe burn: A retrospective analysis.* Burns, 2014. **40**(1): p. 61-66.
255. Pianigiani, E., et al., *Assessment of cryopreserved donor skin viability: the experience of the regional tissue bank of Siena.* Cell Tissue Bank, 2016. **17**(2): p. 241-53.
256. Schiozer, W.A., et al., *An outcome analysis and long-term viability of cryopreserved cultured epidermal allografts: assessment of the conservation of transplantable human skin allografts.* Acta Cirurgica Brasileira, 2013. **28**: p. 824-832.
257. Saffle, J.R., *Closure of the excised burn wound: temporary skin substitutes.* Clin Plast Surg, 2009. **36**(4): p. 627-41.
258. Olszewski, W.L., M. Moscicka, and D. Zolich, *Human skin preserved in anhydric sodium chloride for months can be successfully transplanted.* Ann Transplant, 2004. **9**(4): p. 37-9.
259. Olszewski, W.L., M. Moscicka, and D. Zolich, *Human skin preserved long-term in anhydric pulverized sodium chloride retains cell molecular structure and resumes function after transplantation.* Transplantation, 2006. **81**(11): p. 1583-8.
260. Boekema, B.K., B. Boekestijn, and R.S. Breederveld, *Evaluation of saline, RPMI and DMEM/F12 for storage of split-thickness skin grafts.* Burns, 2015. **41**(4): p. 848-52.
261. Li, J., Y.-P. Zhang, and R.S. Kirsner, *Angiogenesis in wound repair: Angiogenic growth factors and the extracellular matrix.* Microscopy Research and Technique, 2003. **60**(1): p. 107-114.
262. Merwin, J.R., et al., *Transforming growth factor beta1 modulates extracellular matrix organization and cell-cell junctional complex formation during in vitro angiogenesis.* Journal of Cellular Physiology, 1990. **142**(1): p. 117-128.
263. Gaucher, S., et al., *Viability and efficacy of coverage of cryopreserved human skin allografts in mice.* Int J Low Extrem Wounds, 2010. **9**(3): p. 132-40.
264. Cinamon, U., et al., *A Simplified Testing System to Evaluate Performance After Transplantation of Human Skin Preserved in Glycerol or in Liquid Nitrogen.* Journal of Burn Care & Research, 1993. **14**(4): p. 435-439.
265. Ben-Bassat, H., et al., *How long can cryopreserved skin be stored to maintain adequate graft performance?* Burns, 2001. **27**(5): p. 425-431.
266. Tesar, B.M., et al., *Direct Antigen Presentation by a Xenograft Induces Immunity Independently of Secondary Lymphoid Organs.* The Journal of Immunology, 2004. **173**(7): p. 4377.
267. Larsen, C.P., et al., *Migration and maturation of Langerhans cells in skin transplants and explants.* The Journal of experimental medicine, 1990. **172**(5): p. 1483-1493.

268. Achauer, B., et al., *LONG-TERM SKIN ALLOGRAFT SURVIVAL AFTER SHORT-TERM CYCLOSPORIN TREATMENT IN A PATIENT WITH MASSIVE BURNS.* The Lancet, 1986. **327**(8471): p. 14-15.
269. Wendt, J.R., T. Ulich, and P.N. Rao, *Long-Term Survival of Human Skin Allografts in Patients with Immunosuppression.* Plastic and Reconstructive Surgery, 2004. **113**(5).
270. Paddle-Ledinek, J.E., D.G. Cruickshank, and J.P. Masterton, *Skin replacement by cultured keratinocyte grafts: an Australian experience.* Burns, 1997. **23**(3): p. 204-211.
271. Atiyeh, B.S., S.N. Hayek, and S.W. Gunn, *New technologies for burn wound closure and healing—Review of the literature.* Burns, 2005. **31**(8): p. 944-956.
272. Lo, C.H., et al., *A systematic review: Current trends and take rates of cultured epithelial autografts in the treatment of patients with burn injuries.* Wound Repair and Regeneration, 2019. **0**(0).
273. Pye, R.J., *Cultured keratinocytes as biological wound dressings.* Eye (Basingstoke), 1988. **2**(2): p. 172-178.
274. Nguyen, T.T., et al., *Current treatment of severely burned patients.* Annals of Surgery, 1996. **223**(1): p. 14-25.
275. Poumay, Y., et al., *Basal Detachment of the Epidermis Using Dispase: Tissue Spatial Organization and Fate of Integrin α6β4 and Hemidesmosomes.* Journal of Investigative Dermatology, 1994. **102**(1): p. 111-117.
276. Nakajima, R., et al., *Fabrication of transplantable corneal epithelial and oral mucosal epithelial cell sheets using a novel temperature-responsive closed culture device.* Journal of Tissue Engineering and Regenerative Medicine, 2015. **9**(5): p. 637-640.
277. Kobayashi, T., et al., *Corneal regeneration by transplantation of corneal epithelial cell sheets fabricated with automated cell culture system in rabbit model.* Biomaterials, 2013. **34**(36): p. 9010-9017.
278. Morino, T., et al., *Explant culture of oral mucosal epithelial cells for fabricating transplantable epithelial cell sheet.* Regenerative therapy, 2018. **10**: p. 36-45.
279. Kanai, N., M. Yamato, and T. Okano, *Cell sheets engineering for esophageal regenerative medicine.* Annals of translational medicine, 2014. **2**(3): p. 28-28.
280. Yamamoto, K., et al., *The effect of transplantation of nasal mucosal epithelial cell sheets after middle ear surgery in a rabbit model.* Biomaterials, 2015. **42**: p. 87-93.
281. Hama, T., et al., *Autologous human nasal epithelial cell sheet using temperature-responsive culture insert for transplantation after middle ear surgery.* Journal of Tissue Engineering and Regenerative Medicine, 2017. **11**(4): p. 1089-1096.
282. Shimizu, T., et al., *Fabrication of Pulsatile Cardiac Tissue Grafts Using a Novel 3-Dimensional Cell Sheet Manipulation Technique and Temperature-Responsive Cell Culture Surfaces.* Circulation Research, 2002. **90**(3): p. e40-e48.
283. Shimizu, H., et al., *Bioengineering of a functional sheet of islet cells for the treatment of diabetes mellitus.* Biomaterials, 2009. **30**(30): p. 5943-5949.
284. Woodley, D.T., et al., *Burn Wounds Resurfaced by Cultured Epidermal Autografts Show Abnormal Reconstitution of Anchoring Fibrils.* JAMA, 1988. **259**(17): p. 2566-2571.

285. Kumagai, N., et al., *Clinical Application of Autologous Cultured Epithelia for the Treatment of Burn Wounds and Burn Scars.* Plastic and Reconstructive Surgery, 1988. **82**(1).
286. Boyce, S.T., D.J. Christianson, and J.F. Hansbrough, *Structure of a collagen-GAG dermal skin substitute optimized for cultured human epidermal keratinocytes.* Journal of Biomedical Materials Research, 1988. **22**(10): p. 939-957.
287. Merrick, P., et al., *Scanning electron microscopy of cultured human keratinocytes.* The Journal of burn care & rehabilitation, 1990. **11**(3): p. 228-236.
288. Tiwari, V.K., *Burn wound: How it differs from other wounds?* Indian journal of plastic surgery : official publication of the Association of Plastic Surgeons of India, 2012. **45**(2): p. 364.
289. Mizoguchi, T., et al., *Treatment of Cutaneous Ulcers with Multilayered Mixed Sheets of Autologous Fibroblasts and Peripheral Blood Mononuclear Cells.* Cellular Physiology and Biochemistry, 2018. **47**(1): p. 201-211.
290. Benchaprathanphorn, K., et al. *Preparation and characterization of skin cell sheets for treatment of burn wounds*. in *2015 8th Biomedical Engineering International Conference (BMEiCON)*. 2015.
291. Lin, Y.-C., et al., *Evaluation of a multi-layer adipose-derived stem cell sheet in a full-thickness wound healing model.* Acta Biomaterialia, 2013. **9**(2): p. 5243-5250.
292. Kato, Y., et al., *Allogeneic Transplantation of an Adipose-Derived Stem Cell Sheet Combined With Artificial Skin Accelerates Wound Healing in a Rat Wound Model of Type 2 Diabetes and Obesity.* Diabetes, 2015. **64**(8): p. 2723.
293. Hamada, M., et al., *Xenogeneic transplantation of human adipose-derived stem cell sheets accelerate angiogenesis and the healing of skin wounds in a Zucker Diabetic Fatty rat model of obese diabetes.* Regenerative Therapy, 2017. **6**: p. 65-73.
294. Kato, Y., et al., *Creation and Transplantation of an Adipose-derived Stem Cell (ASC) Sheet in a Diabetic Wound-healing Model.* Journal of visualized experiments : JoVE, 2017(126): p. 54539.
295. Nie, C., et al., *Locally Administered Adipose-Derived Stem Cells Accelerate Wound Healing through Differentiation and Vasculogenesis.* Cell Transplantation, 2011. **20**(2): p. 205-216.
296. Galiano, R.D., et al., *Quantitative and reproducible murine model of excisional wound healing.* Wound Repair and Regeneration, 2004. **12**(4): p. 485-492.
297. Smola, H., et al., *Dynamics of Basement Membrane Formation by Keratinocyte–Fibroblast Interactions in Organotypic Skin Culture.* Experimental Cell Research, 1998. **239**(2): p. 399-410.
298. Lee, D.-Y. and K.-H. Cho, *The effects of epidermal keratinocytes and dermal fibroblasts on the formation of cutaneous basement membrane in three-dimensional culture systems.* Archives of Dermatological Research, 2005. **296**(7): p. 296-302.
299. Clausen, O.P.F., B. Kirkhus, and A.R. Schjølberg, *Cell Cycle Progression Kinetics of Regenerating Mouse Epidermal Cells: An In Vivo Study Combining DNA Flow Cytometry, Cell Sorting, and [3H]dThd Autoradiography.* Journal of Investigative Dermatology, 1986. **86**(4): p. 402-405.

300. Park, J.E. and A. Barbul, *Understanding the role of immune regulation in wound healing.* The American Journal of Surgery, 2004. **187**(5, Supplement 1): p. S11-S16.
301. Sinno, H. and S. Prakash, *Complements and the wound healing cascade: an updated review.* Plast Surg Int, 2013. **2013**: p. 146764.
302. Kovtun, A., et al., *Neutrophils in Tissue Trauma of the Skin, Bone, and Lung: Two Sides of the Same Coin.* Journal of immunology research, 2018. **2018**: p. 8173983-8173983.
303. Feiken, E., et al., *Neutrophils express tumor necrosis factor-α during mouse skin wound healing.* Journal of investigative dermatology, 1995. **105**(1): p. 120-123.
304. McCourt, M., et al., *Proinflammatory Mediators Stimulate Neutrophil-Directed Angiogenesis.* JAMA Surgery, 1999. **134**(12): p. 1325-1331.
305. Canesso, M.C.C., et al., *Skin Wound Healing Is Accelerated and Scarless in the Absence of Commensal Microbiota.* The Journal of Immunology, 2014. **193**(10): p. 5171.
306. Hopkinson-Woolley, J., et al., *Macrophage recruitment during limb development and wound healing in the embryonic and foetal mouse.* Journal of Cell Science, 1994. **107**(5): p. 1159.
307. Liechty, K.W., et al., *Fetal wound repair results in scar formation in interleukin-10-deficient mice in a syngeneic murine model of scarless fetal wound repair.* J Pediatr Surg, 2000. **35**(6): p. 866-72; discussion 872-3.
308. Desmoulière, A., et al., *Transforming growth factor-beta 1 induces alpha-smooth muscle actin expression in granulation tissue myofibroblasts and in quiescent and growing cultured fibroblasts.* The Journal of Cell Biology, 1993. **122**(1): p. 103.
309. de Oliveira, S., E.E. Rosowski, and A. Huttenlocher, *Neutrophil migration in infection and wound repair: going forward in reverse.* Nature Reviews Immunology, 2016. **16**: p. 378+.
310. Meuli, M. and M. Raghunath, *Tops and flops using cultured epithelial autografts in children.* Pediatric Surgery International, 1997. **12**(7): p. 471-477.
311. Briggaman, R.A., F.G. Dalldorf, and C.E. Wheeler, Jr., *Formation and origin of basal lamina and anchoring fibrils in adult human skin.* The Journal of cell biology, 1971. **51**(21): p. 384-395.
312. Mommaas, A.M., et al., *Ontogenesis of the Basement Membrane Zone After Grafting Cultured Human Epithelium: A Morphologic and Immunoelectron Microscopic Study.* Journal of Investigative Dermatology, 1992. **99**(1): p. 71-77.
313. Aihara, M., *Ultrastructural study of grafted autologous cultured human epithelium.* British Journal of Plastic Surgery, 1989. **42**(1): p. 35-42.
314. SUVIK, A. and A.W.M. EFFENDY, *THE USE OF MODIFIED MASSON'S TRICHROME ST AINING IN COLLAGEN E V ALUA TION IN WOUND HEALING STUDY.* M al aysi an J ournal of V eterinary r esearch, 2012. **3**(1).
315. Caetano, G.F., et al., *Comparison of collagen content in skin wounds evaluated by biochemical assay and by computer-aided histomorphometric analysis.* Pharmaceutical Biology, 2016. **54**(11): p. 2555-2559.
316. Aijaz, A., et al., *Hydrogel Microencapsulated Insulin-Secreting Cells Increase Keratinocyte Migration, Epidermal Thickness, Collagen Fiber Density, and*

Wound Closure in a Diabetic Mouse Model of Wound Healing. Tissue Engineering Part A, 2015. **21**(21-22): p. 2723-2732.
317. Chattopadhyay, S. and R.T. Raines, *Review collagen-based biomaterials for wound healing.* Biopolymers, 2014. **101**(8): p. 821-833.
318. Harris, E. and A. Sjoerdsma, *COLLAGEN PROFILE IN VARIOUS CLINICAL CONDITIONS.* The Lancet, 1966. **288**(7466): p. 707-711.
319. Pessa, M.E., K.I. Bland, and E.M. Copeland, *Growth factors and determinants of wound repair.* Journal of Surgical Research, 1987. **42**(2): p. 207-217.
320. Latkowski, J.A.M., I.M. Freedberg, and M. Blumenberg, *Keratinocyte growth factor and keratin gene regulation.* Journal of Dermatological Science, 1995. **9**(1): p. 36-44.
321. Staiano-Coico, L., et al., *Human keratinocyte growth factor effects in a porcine model of epidermal wound healing.* The Journal of experimental medicine, 1993. **178**(3): p. 865-878.
322. Kopp, J., et al., *Accelerated Wound Healing by In vivo Application of Keratinocytes Overexpressing KGF.* Molecular Therapy, 2004. **10**(1): p. 86-96.